



# **D1 design, short model manufacturing and tests**

**Michinaka Sugano**

**KEK**

**On behalf of CERN-KEK Collaboration for  
D1 development for HL-LHC**

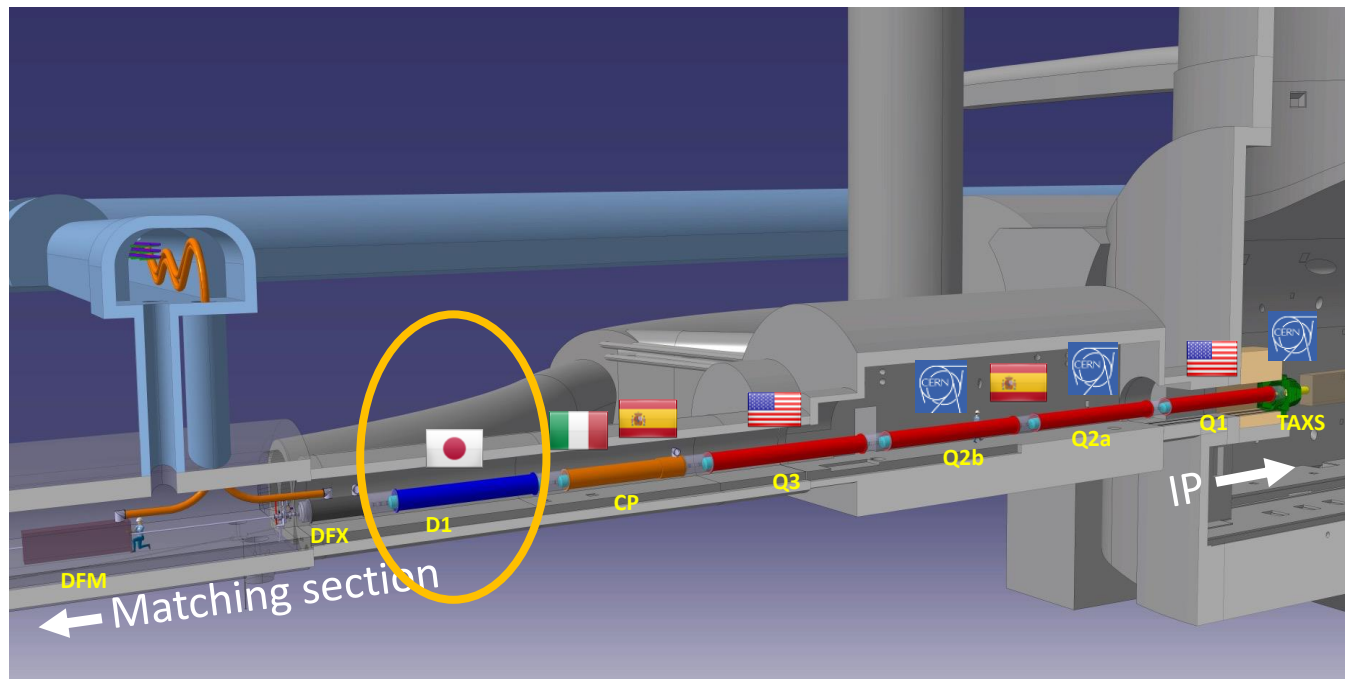
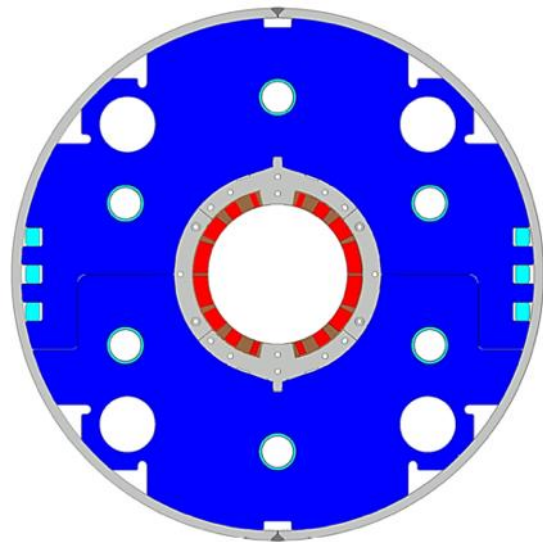
International review on D1 Superconducting  
magnets for HL-LHC, 11-13 March, 2019

# Outline

- **D1 magnet for HL-LHC**
- **Design update in the second 2 m model magnet (MBXFS2)**
- **Test result of MBXFS2**
- **Status of MBXFS3**
- **Prospect for prototype**

# D1 magnet for HL-LHC

# Japanese Contribution to HL-LHC: D1 magnets



- Beam separation dipole (D1) by KEK
  - Design study of D1 for HL-LHC within the framework of the CERN-KEK collaboration since 2011.
  - 150 mm single aperture, 35 Tm (5.6 T x 6.3 m), Nb-Ti technology.
  - [Development 2-m long model magnets \(3 units\) at KEK](#)
- Deliverables for HL-LHC
  - 1 full-scale prototype cold mass (MBXFP)
  - 6 series cold masses (MBXF1-6)

# Design Requirements, Constraints

- Coil aperture: **150 mm**
- **35 Tm** w/ nominal field 5.6 T at 12 kA
  - Upper limit of P/C: < 15 kA
- Field quality: <  $10^{-4}$  at  $R_{ref}=50$  mm
- Mechanical magnet length: < 7.0 m
  - limit of the vertical cryostat at KEK.
- Magnet outer diameter: **570 mm** (same as LHC MB)
  - limited passage space in the LHC tunnel.
- Radiation and energy deposition w/ Tangsten shield
  - Total heat load: **135 W** at ultimate
  - Peak dose in lifetime: **25 MGy**
  - Peak energy deposition :  **$\sim 2$  mW/cm<sup>3</sup>** @  $5 \times 10^{34}$  cm<sup>-2</sup>sec<sup>-1</sup>
- Helium cooling
  - **4 x  $\phi 61$  mm** holes (for 2 x HX) in line with the MQXF
  - Free area in cross section: **>100 cm<sup>2</sup>**
  - Radial gap of 4 % to HX holes

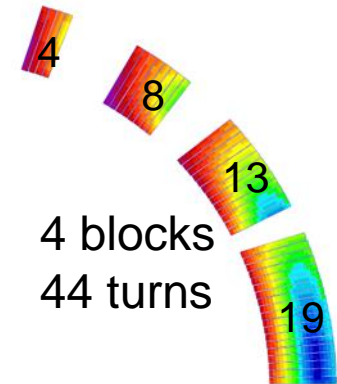
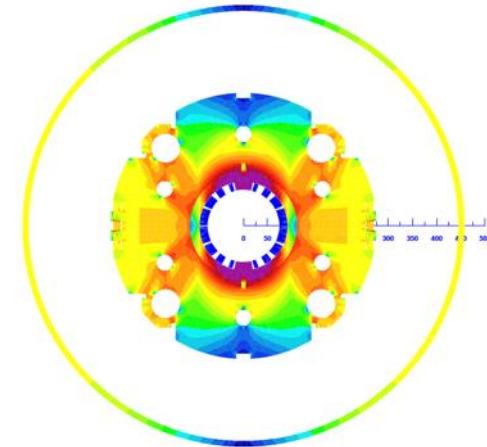
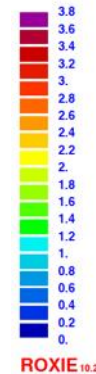
# Design Guidelines

- Use of spare unit lengths of the LHC Nb-Ti superconducting cable from the main dipole (MB) outer layer, wrapped with the polyimide insulation.
- Operational temperature of 1.9 K by superfluid helium cooling while operating around 75 % of short sample current (i.e. 25 % margin on the load-line).
- A single layer coil for better cooling capability and to leave more space to the iron yoke for reducing the fringe field.
- Enhancement of the amount of iron yoke in the cross section accomplished by “a collared yoke structure” like RHIC magnets and LHC MQXA quadrupoles.
- A yoke outer diameter of 550 mm, same as J-PARC SCFM , enabling reuse of the assembly tooling and relevant facilities at KEK.
- Use of radiation resistant materials for the coil parts: wedges, end spacers.

# Design overview from MBXFS2

A series production (7m) MBXFS2 (2 m)

IBI flux density (T)



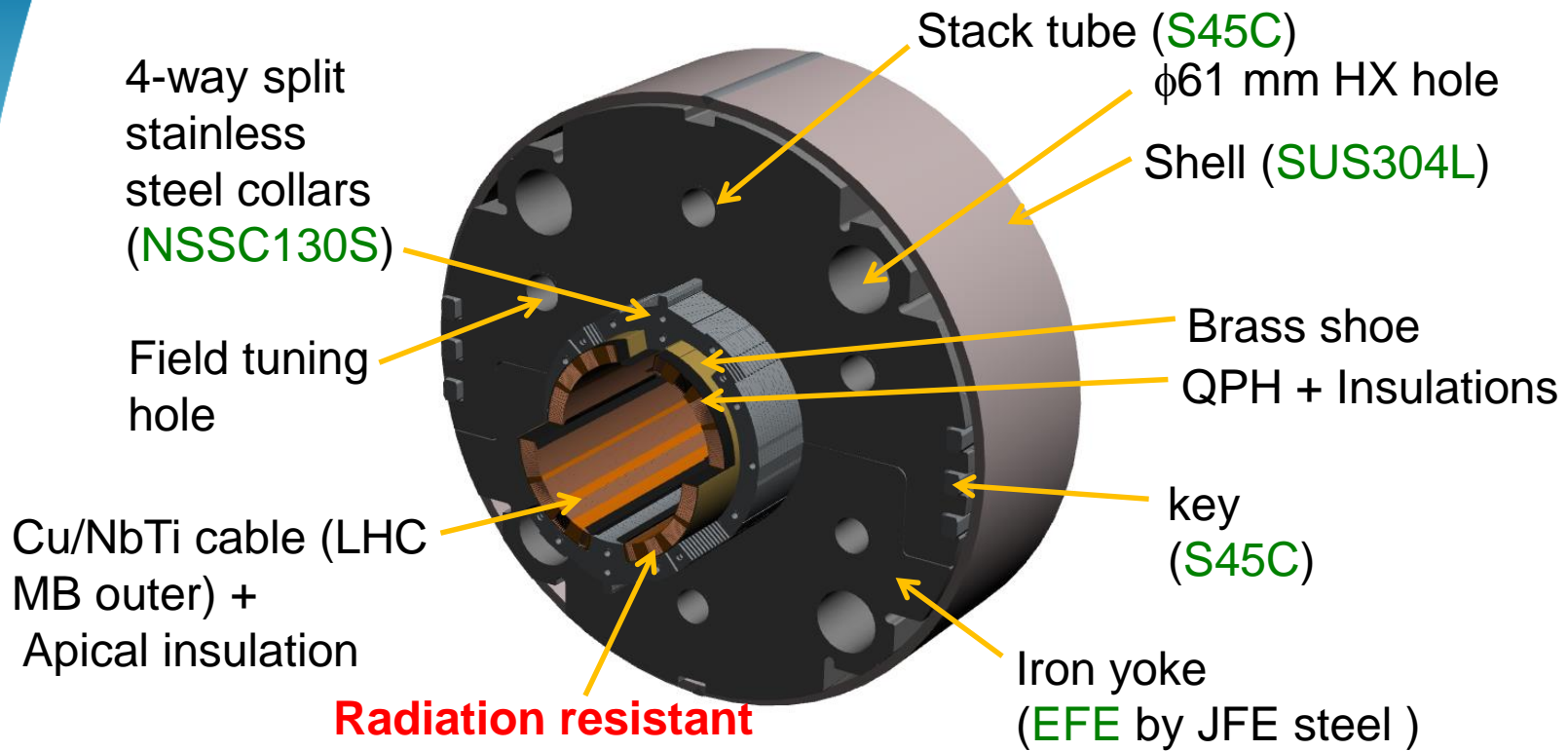
4 blocks  
44 turns

Coil aperture	<b>150 mm</b>	
Field integral	<b>35 T m</b>	9.5 T m
Field (3D)	<b>Nominal: 5.60 T, Ultimate: 6.04 T</b>	
Peak field (3D)	<b>Nominal: 6.58 T, Ultimate: 71.4 T</b>	
Current	Nominal : 12.047 kA, Ultimate 13.280 kA	
Operating temperature	1.9 K	
Field quality	$<10^{-4}$ w.r.t $B_1$ ( $R_{ref}=50$ mm)	
Load line ratio (3D)	<b>Nominal: 76.5%, Ultimate: 83.1% at 1.9 K</b>	
Differential inductance	Nominal: 4.0 mH/m	
Conductor	Nb-Ti: LHC-MB outer cable	
Stored energy	Nominal: 340 kJ/m	
Magnetic length	6.26 m	1.67 m
Coil mech. length	6.58 m	2.00 m
Magnet mech. length	6.73 m	2.15 m
Heat load	<b>135 W (Magnet total)</b> <b>2 mW/cm<sup>3</sup> (Coil peak)</b>	
Radiation dose	<b>&gt; 25 MGy</b>	

## Technical challenges

- **Large aperture**: Management of coil size and pre-stress.
- **Radiation resistance**: Radiation resistant material for coil parts. Cooling capability.
- **Iron saturation**: Good field quality from injection to nominal current

# Cross section of D1



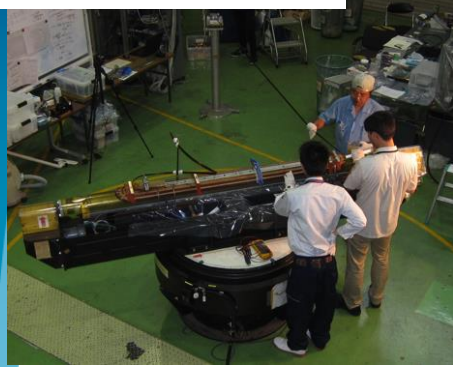
**Radiation resistant GFRP wedge for dose of 25 MGy (S2 glass fiber + Bismaleimide-Triazine (BT) resin)**

- **Nb-Ti/Cu cable** with APICAL and PIXEO insulations, same as MB outer cable.
- Wedges and end spacers made of **radiation resistant GFRP**
- **Radiation resistant resin to bond cable and spacer (40% cyanate ester+60% epoxy + silica filler)**
- **Collared yoke structure** to increase amount of iron yoke.
- Design features for better cooling
  - **A single layer coil.**
  - **Packing factor of collar and yoke less than 100% for superfluid He passage**



# Fabrication steps

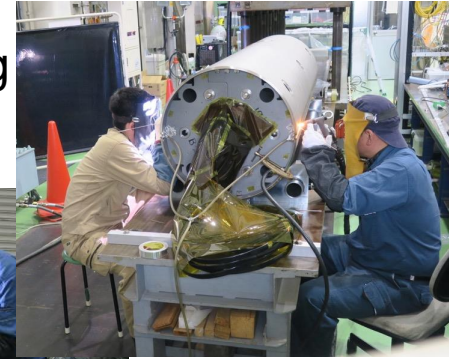
1. Coil winding



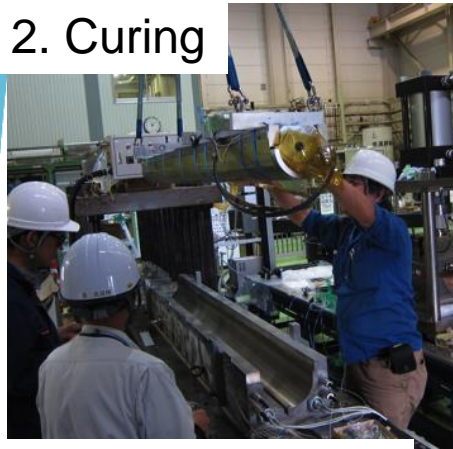
4. QPH, insulation wrapping



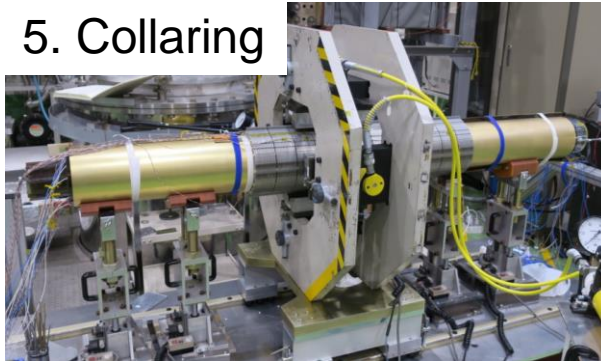
7. Shell, end-ring welding



2. Curing



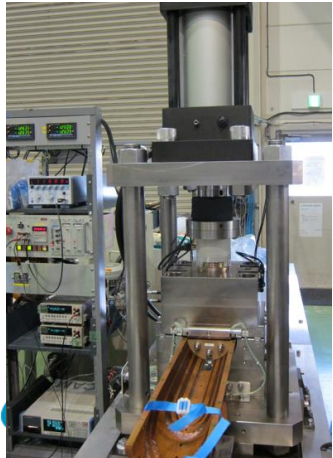
5. Collaring



8. Axial pre-loading



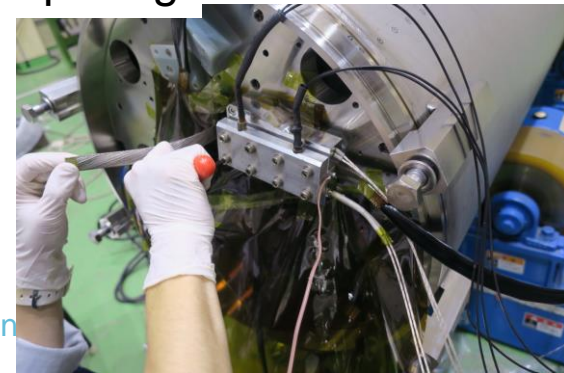
3. Coil size meas.



6. Yoking



9. Splicing

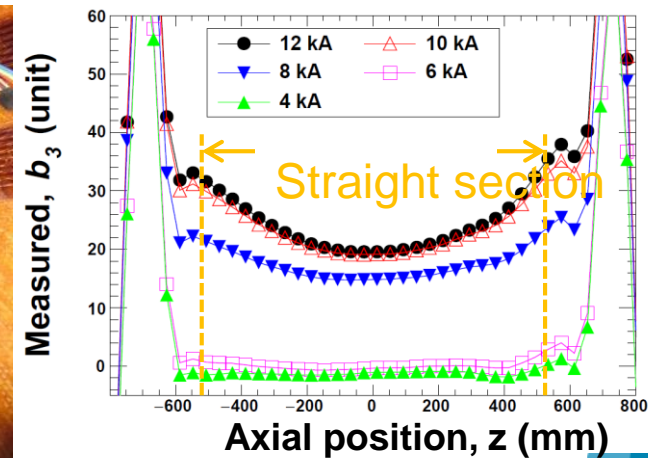
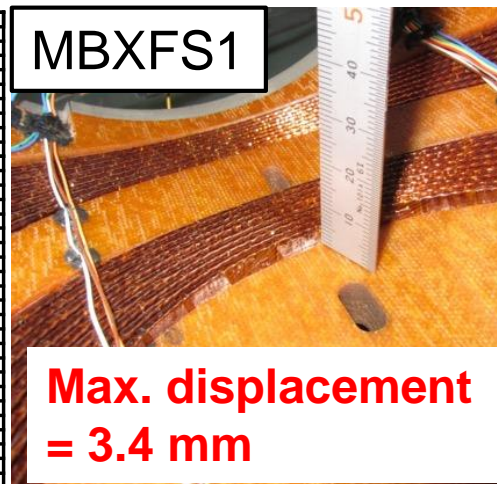
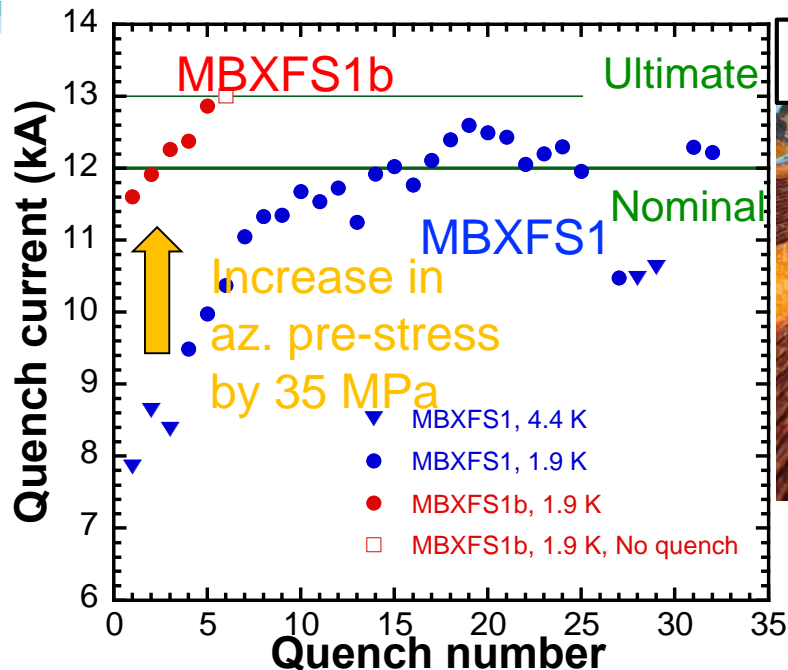


# Brief summary of test result of MBXFS1 and 1b

**MBXFS1:** fabricated in Sep, 2015-Apr, 2016, tested Apr-Jun, 2016

**MBXFS1b:** re-assembled in Nov, 2016-Feb, 2017, tested in Feb-Apr, 2017

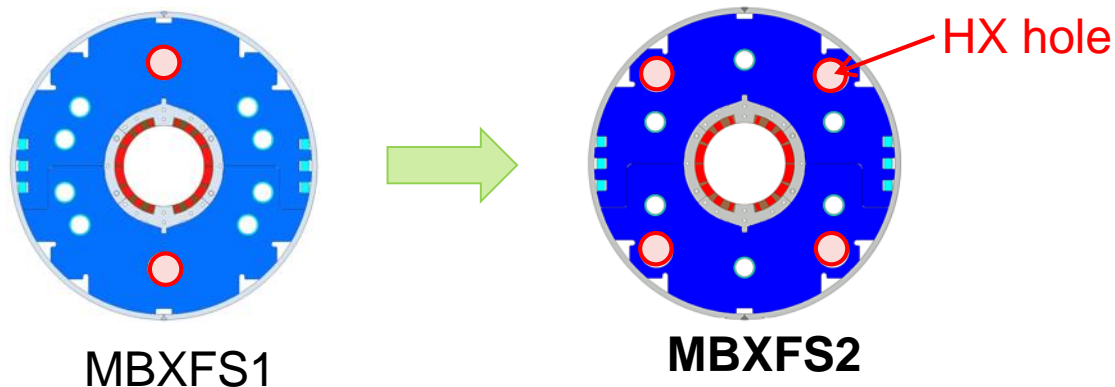
- Training performance
  - Achieved ultimate of 13 kA after increasing azimuthal coil pre-stress in MBXFS1b
  - Azimuthal coil pre-stress in SS remained up to nominal, but was released at ultimate.
  - Cable displacement at coil end
- Field quality
  - Not yet evaluated up to nominal current due to limited training performance
  - Significant coil end effect on field quality even at magnet center
- Quench protection
  - Required new QPH to reduce MIITs (maximum hot spot temperature)



# Design update in MBXFS2

# Updates from MBXFS1/1b to MBXFS2

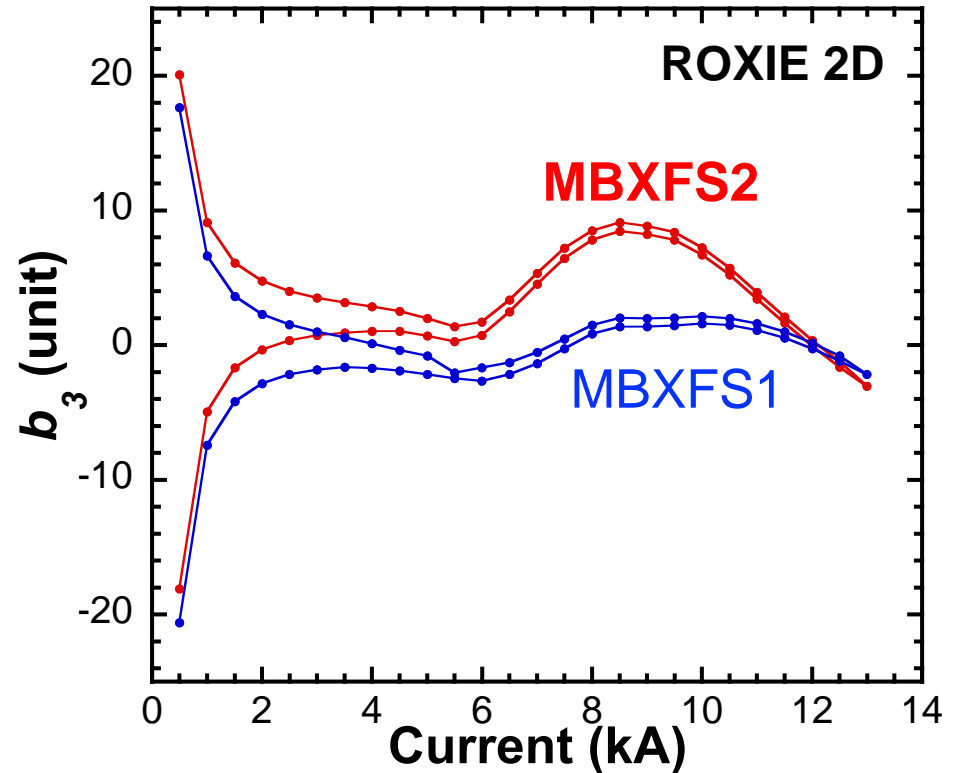
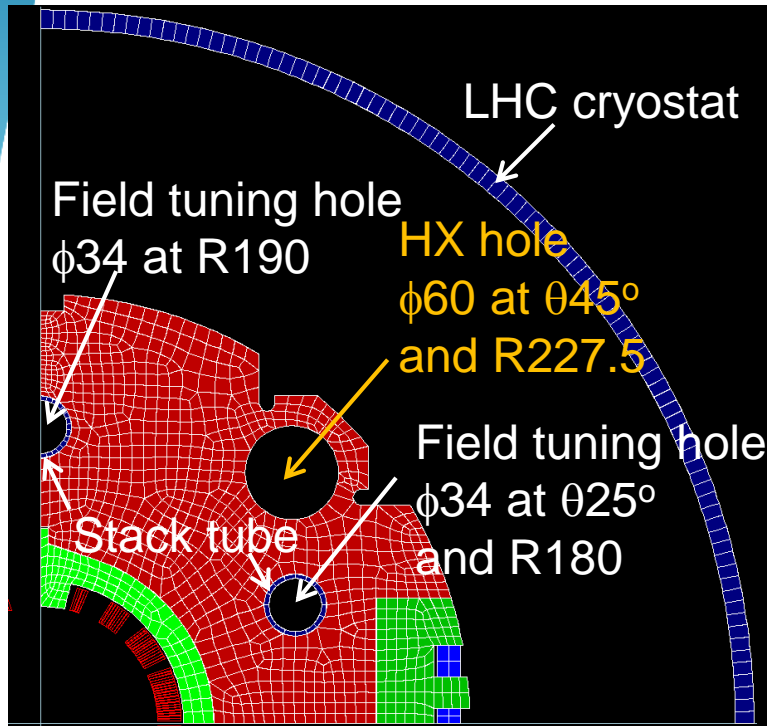
- **Four HX holes** instead of two in yoke: **REQUEST** from CERN.
  - Yoke cross-section and coil block arrangement were modified
- Enhancement of mechanical support of coil blocks
  - Azimuthal pre-stress in SS: **Total target pre-stress = 115 MPa** (MBXFS1b:100 MPa)
  - Countermeasures to cable displacement at coil end
    - **Wet-winding** with epoxy-blended cyanate ester at coil end
    - Increase in axial pre-load
- Modification of coil end shape: Subdividing one coil end block
- **Newly designed QPH for reducing MIITs (max T)**



MBXFS1

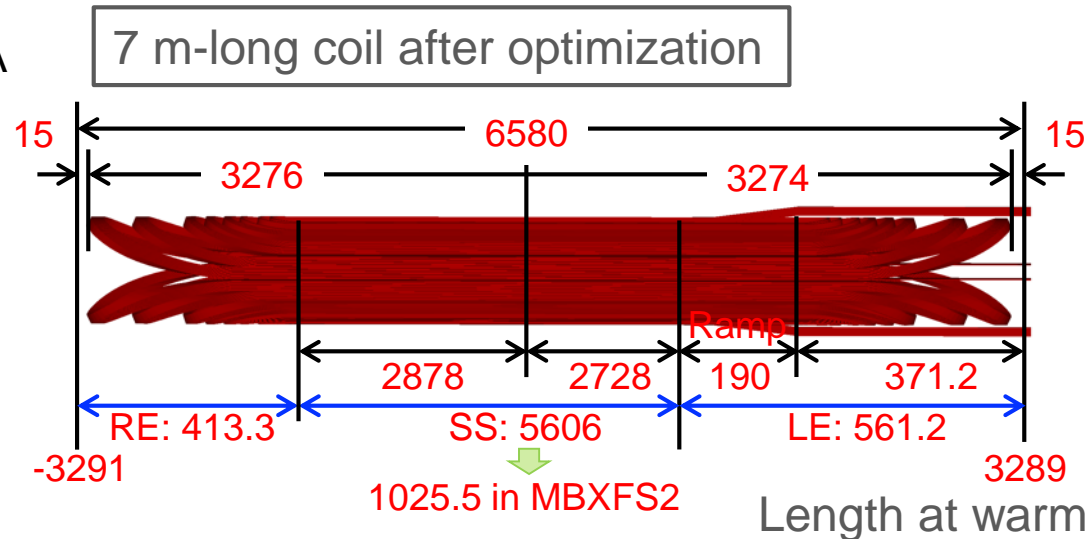
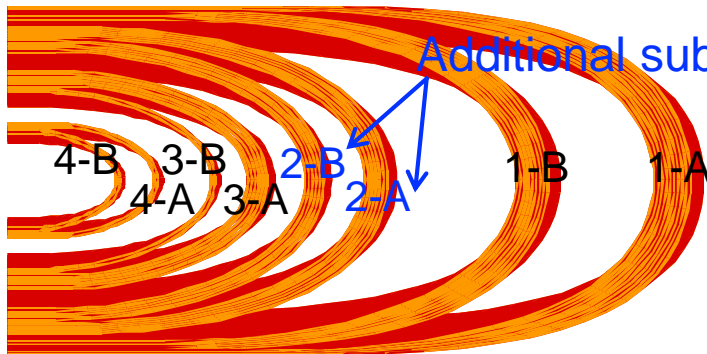
MBXFS2

# 2D cross-section and coil end shape



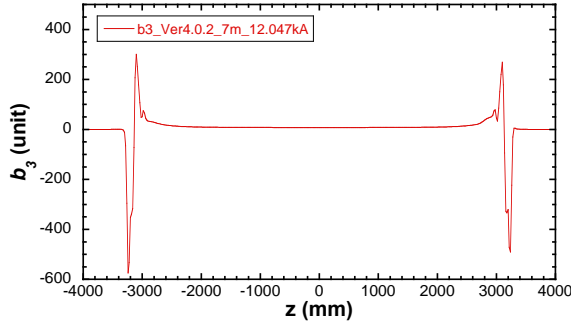
- For new HX hole condition (four holes with  $\phi 60$  at  $\theta=45$  and  $R=227.5$ )
  - Field tuning hole conditions were optimized to keep variation of multipoles with current as low as possible.  $\rightarrow$  Maximum  $b_3$  of 8.5 units at 8.5 kA
  - Optimization of coil block arrangement to minimize multipoles at nominal
  - ✓ Note:  $b_3$  in ROXIE 2D is much different from ROXIE 3D due to end-effects.

# Modified coil end shape

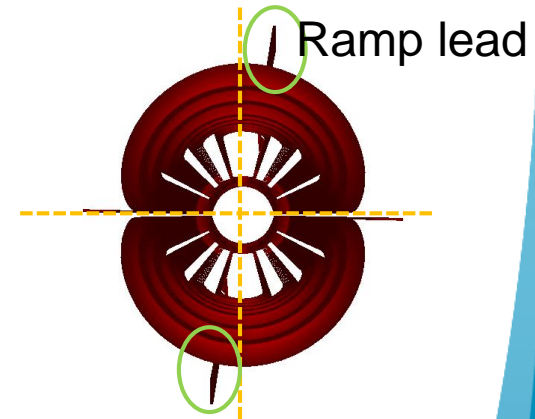
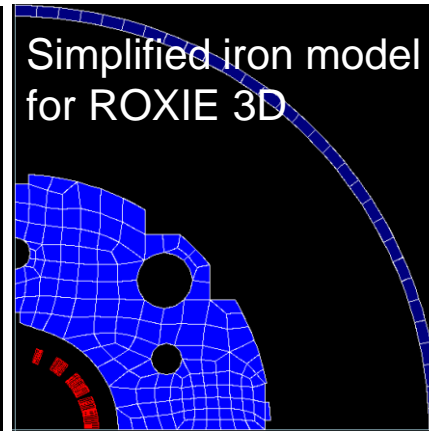
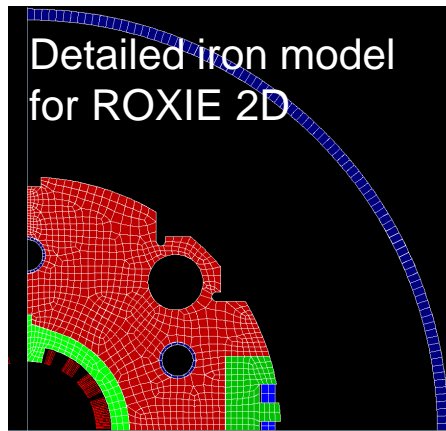
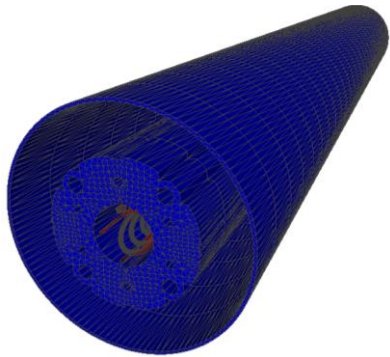


- Coil end block 2 was subdivided into 7+6 turns
- Minimizing multipole components **integrated over 7 m-long magnet** with LHC cryostat by adjusting axial position of coil end blocks
- MBXFS2 has the same cross-section and coil ends, but straight section is shortened.

# Field integral in 7 m magnet by ROXIE 3D

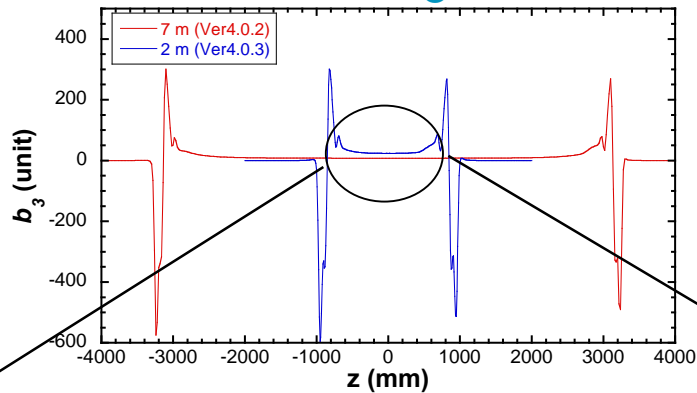


	RE (unit)	SS (unit)	LE (unit)	Total (unit)	2D (unit)	2D with 3D iron (unit)	Expected (unit)
z (mm)	-4000 ~ -2870	-2870 ~ 2720	2720 ~ 4000	-4000 ~ 4000			
BL (Tm)	1.422	31.343	2.262	35.027			35.027
b3 (unit)	-3.600	8.824	-2.128	3.096	-0.028	3.057	0.011
b5 (unit)	-0.280	0.049	0.300	0.069	-0.045	-0.228	0.251
b7 (unit)	-0.287	0.010	-0.059	-0.336	-0.054	-0.228	-0.162
b9 (unit)	-0.269	0.087	-0.167	-0.349	0.139	0.109	-0.320
b11 (unit)	-0.119	0.166	-0.087	-0.040	0.176	0.188	-0.052
b13 (unit)	-0.055	-0.620	-0.054	-0.729	-0.695	-0.696	-0.728
b15 (unit)	-0.035	-1.030	-0.060	-1.124	-1.157	-1.154	-1.127
b17 (unit)	-0.011	-0.726	-0.027	-0.764	-0.815	-0.814	-0.765
b19 (unit)	0.006	0.359	0.015	0.380	0.402	0.401	0.380
a1 (unit)	0.001	0.152	-5.532	-5.379	0.000	0.000	-5.379
a3 (unit)	0.000	0.039	1.808	1.847	0.000	0.000	1.847

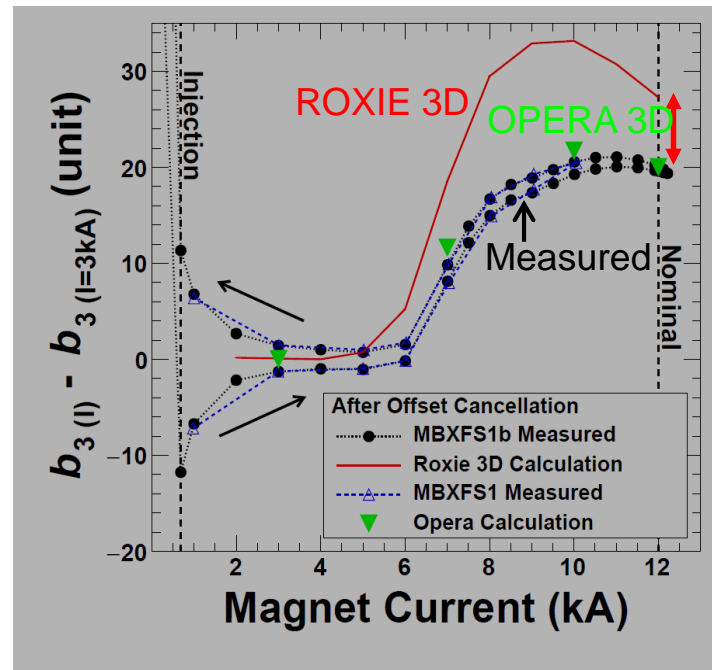
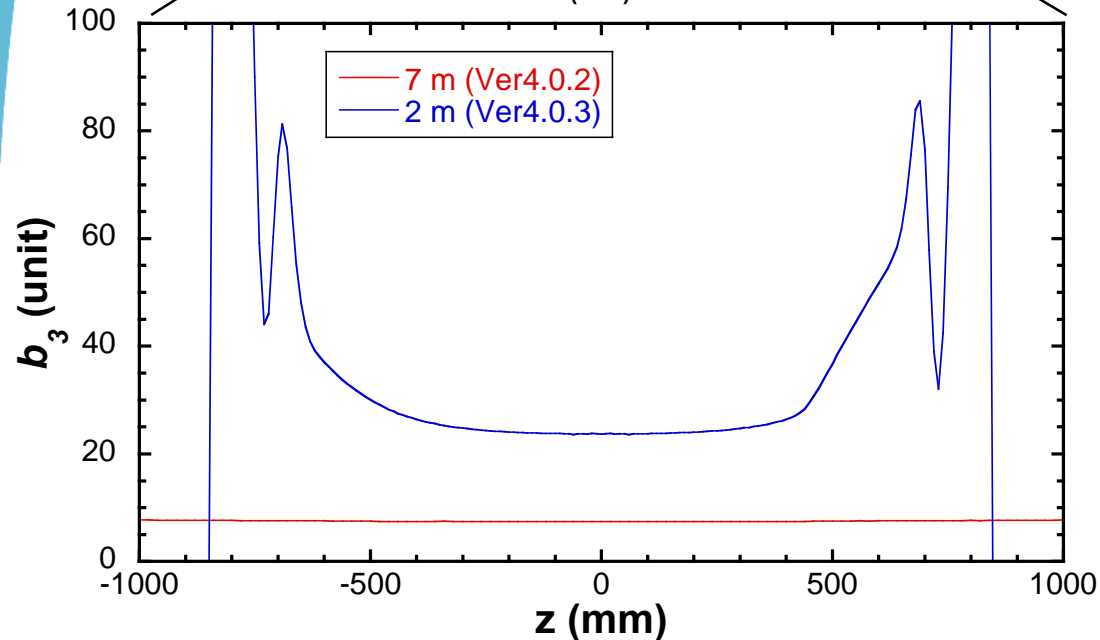


- Target multipole coefficient in 3D optimization is taken into account the different iron models in 2D and 3D calculations.
  - ✓  $b_3 \sim b_9$  can be controlled within 0.5 unit with respect to the target values.
  - ✓ Intrinsic  $a_1$  and  $a_3$  due to rotational symmetry.

# Difference of $b_3$ between 2-m model and prototype



- $b_3$  at magnet center ( $z=0$  in ROXIE)
  - 7 m magnet: 7.4 unit
  - 2 m magnet (MBXFS2): 23.7 unit



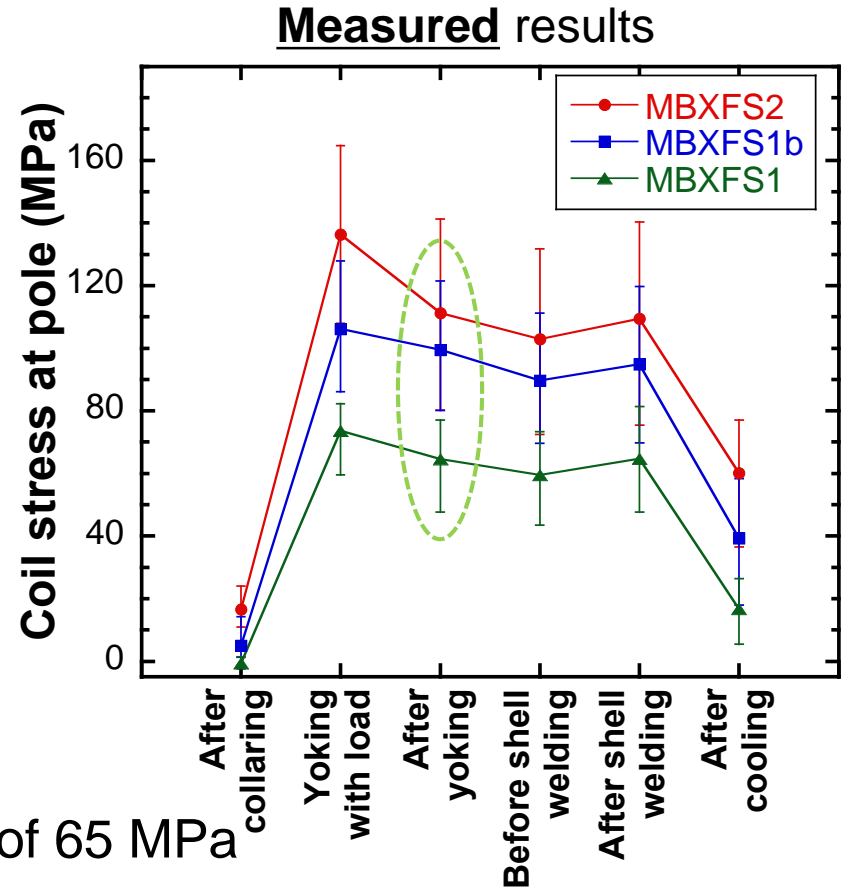
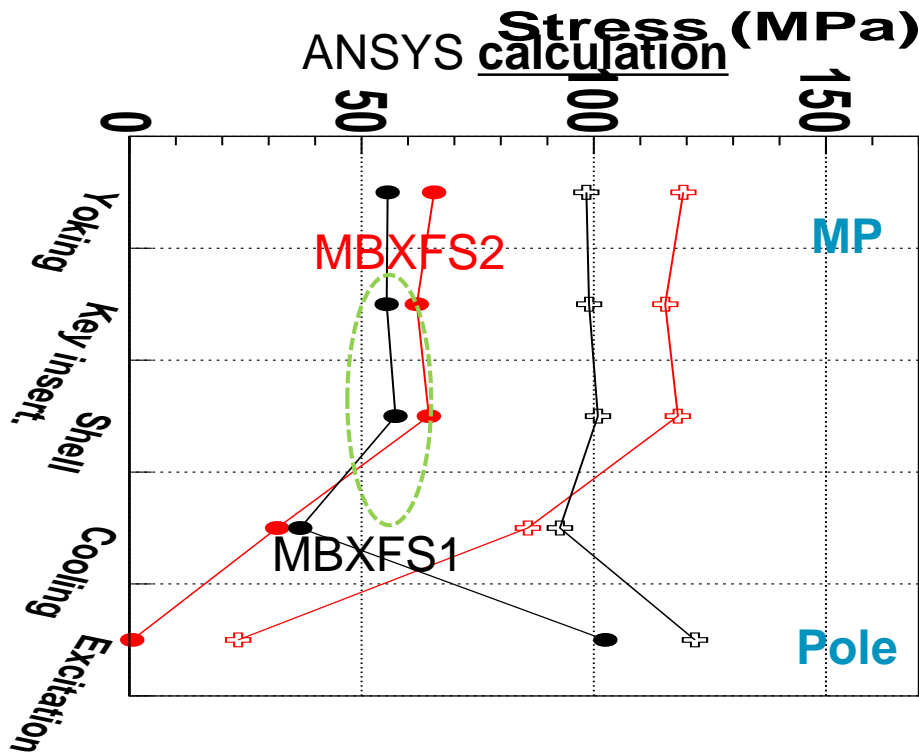
$b_3$  of MBXFS1b w/  
ROXIE 3D & OPERA 3D

For prototype and series, initial engineering design will be mainly performed by ROXIE3D, but final tuning of a coil geometry would be performed by using **OPERA3D output**. (ref. P53 in appendix)



# Mechanical design

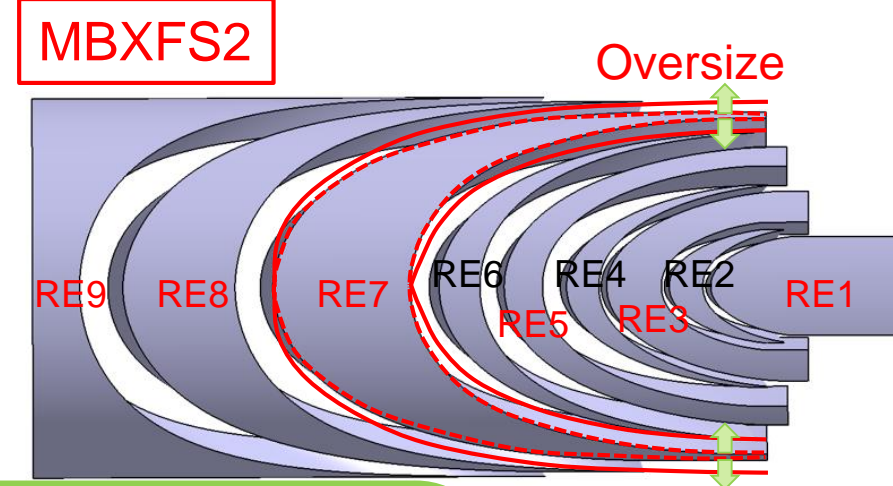
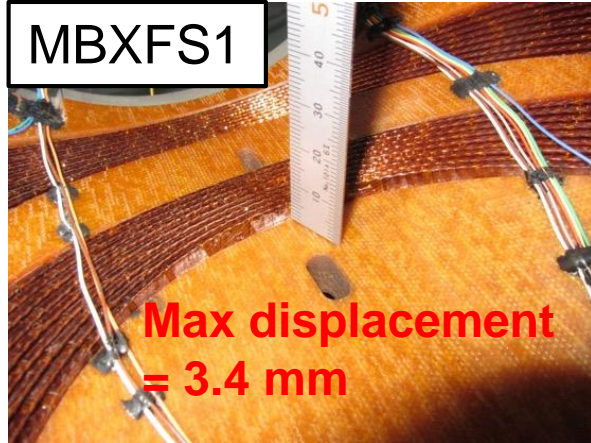
## Azimuthal coil pre-stress in SS



- MBXFS1: azimuthal stress at pole of 65 MPa
- MBXFS1b: 100 MPa with 0.8mm additional shim at MP
- MBXFS2: target of 115 MPa by oversize wedge (0.8 + 0.34 mm)
  - Larger coil size before assembly than MBXFS1/1b
- Measured azimuthal coil pre-stress after yoking in MBXFS2=111 MPa (Target = 115 MPa)

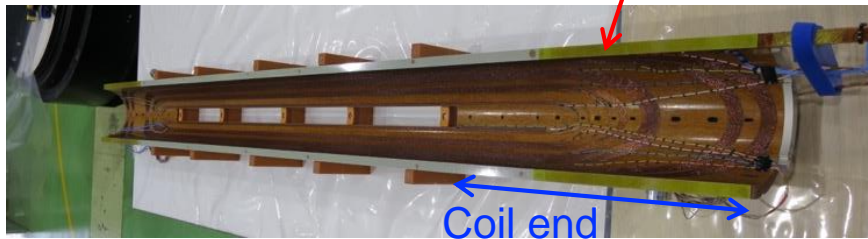
# Countermeasure to cable displacement at coil end 1

## Increase in coil pre-stress (azimuthal and axial)



MBXFS1b

G10 shim + Polyimide tapes = 0.9 mm



Max displacement = 2.5 mm



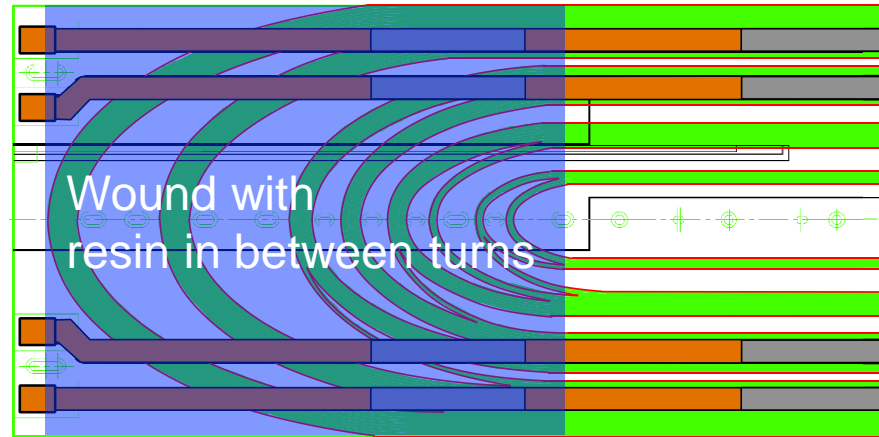
- The reason of cable displacement has not been fully understood, but we are attempting to solve this issue by **enhancing mechanical support of cable**.
- **End spacers were oversized in the azimuthal direction** by the same amount as wedges. (0.24 mm thicker per quadrant than 1b)
- Axial pre-loading: MBXFS1/1b = 12 Nm → MBXFS2 = 20 Nm (30~43 kN per coil)

Measured pre-load

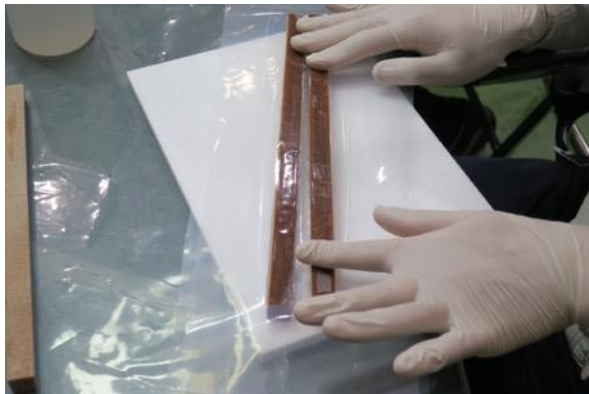
# Countermeasure to cable displacement at coil end 2

## Wet-winding

### Cable surface



### Wedges



### End spacers



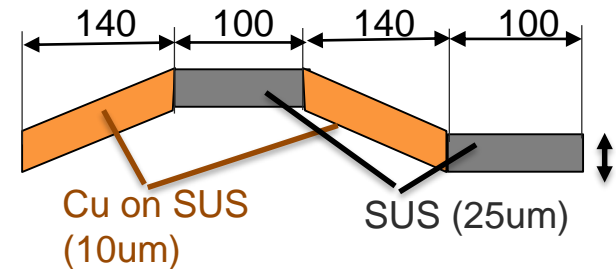
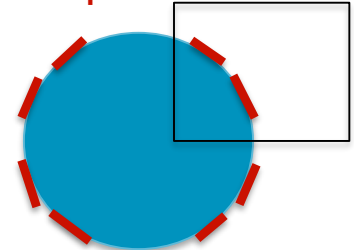
Coil after curing

- Coil-winding with resin only at coil end to enhance turn-to-turn bonding
- Radiation resistant resin: 60% epoxy + 40% cyanate ester + 7% Silica filler
- Minimum amount of resin was applied for easy release and keeping coil surface smooth
- Curing condition: 120°C x 4h + 150°C x 4h

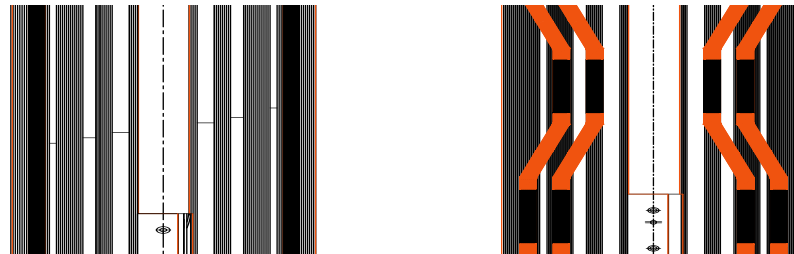
# Quench simulation for new QPH design

- QPH was designed for 7 m-long magnet using our standalone quench simulation program based on finite difference method.
- Design guideline
  - Two heater strips per quadrant
  - Zig-zag pattern to provoke quench in more turns
  - Maximum hot spot temperature < 300 K
  - Controlling total resistance by partially Cu-plating
  - Four power supplies: Two heater strips are connected in series
  - No dump resistor
- Coil geometry taken from ROXIE output
- Field distribution calculated by OPERA 3D
- Total MIITs and max hot spot temperature in consideration of failure cases of QPH power supplies

Two strips per quadrant



## QPH for MBXFS2



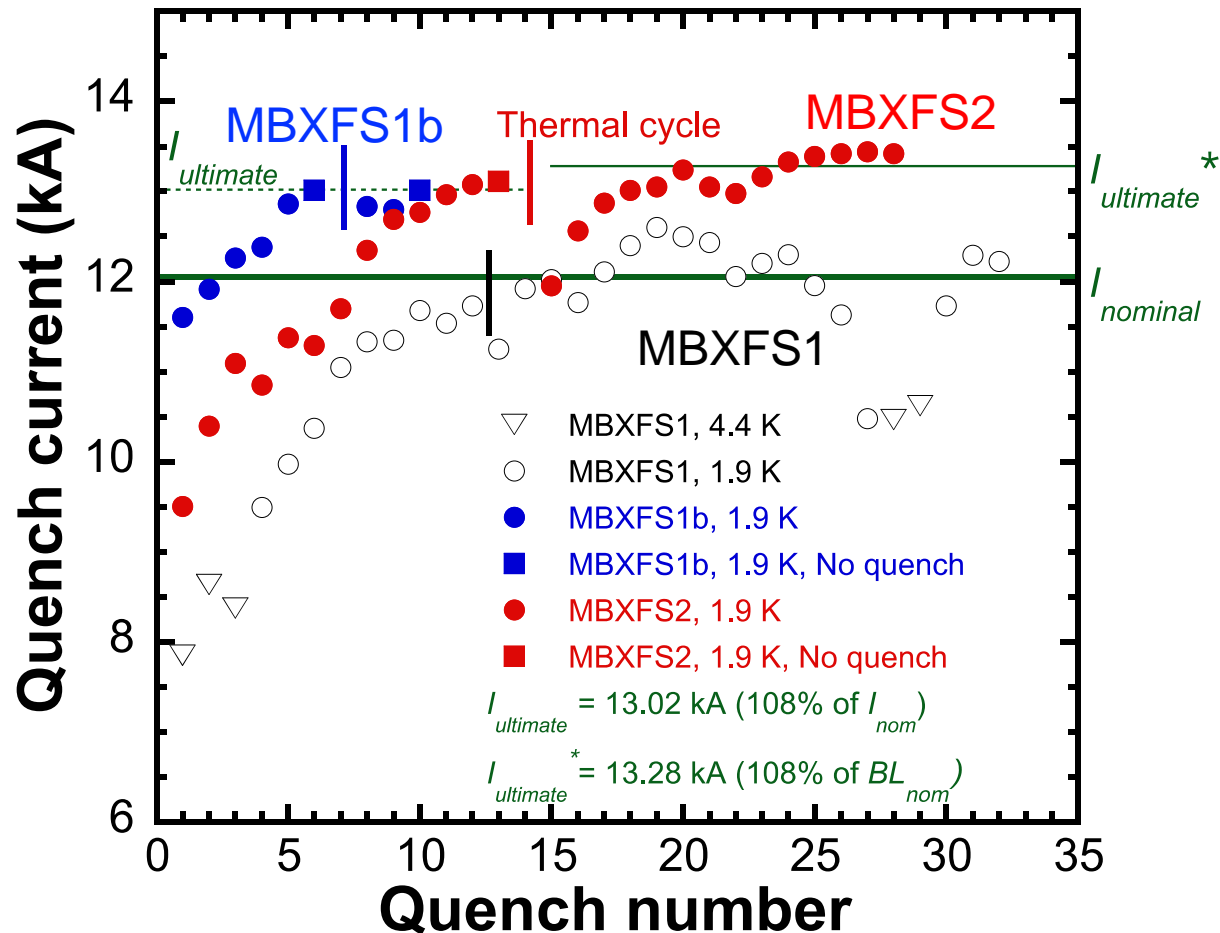
Validity of new QPH was checked in heater test of MBXFS2.

# Test result of MBXFS2

# Test items

- Training performance
- Heater test to validate new QPH
- Magnetic field measurement
- Visual inspection of coils after magnet test

# Training history

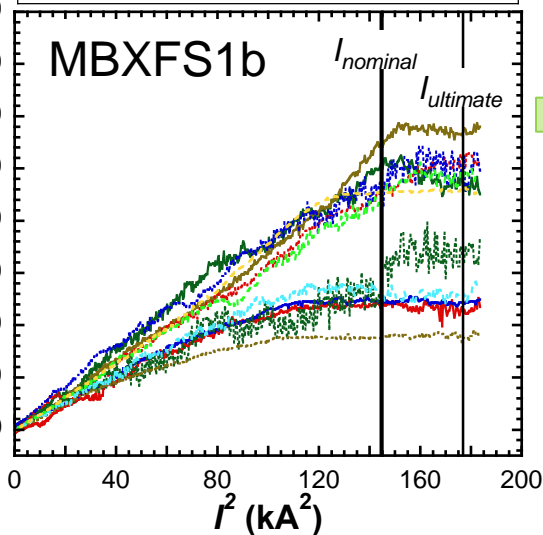


- 8 quenches to the nominal current (12.050 kA)
- Ultimate current was re-defined after the 1st test cycle to be 108% of nominal field integral ( $I_{ultimate}^* = 13.28 \text{ kA}$ ).
- **The ultimate current was achieved in the 2nd cycle.**

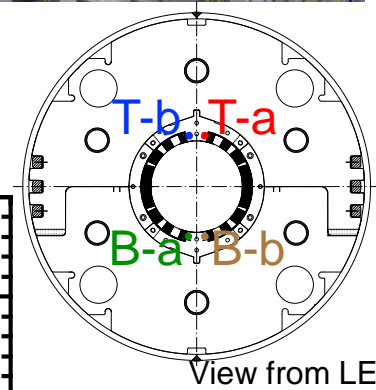
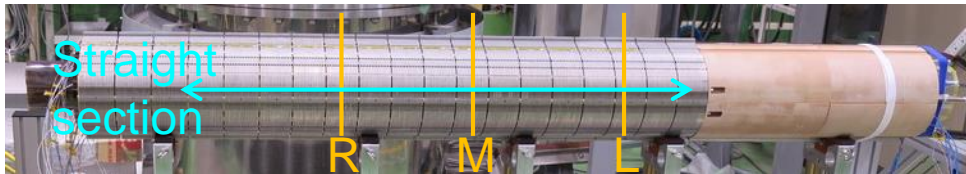
# Coil stress in straight section

LE

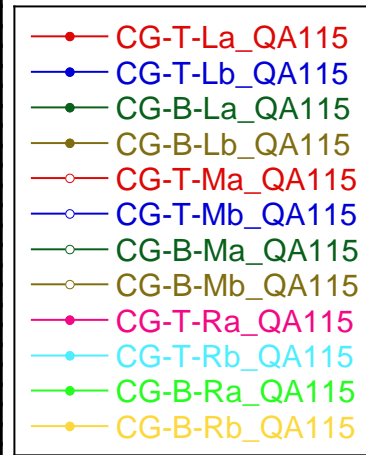
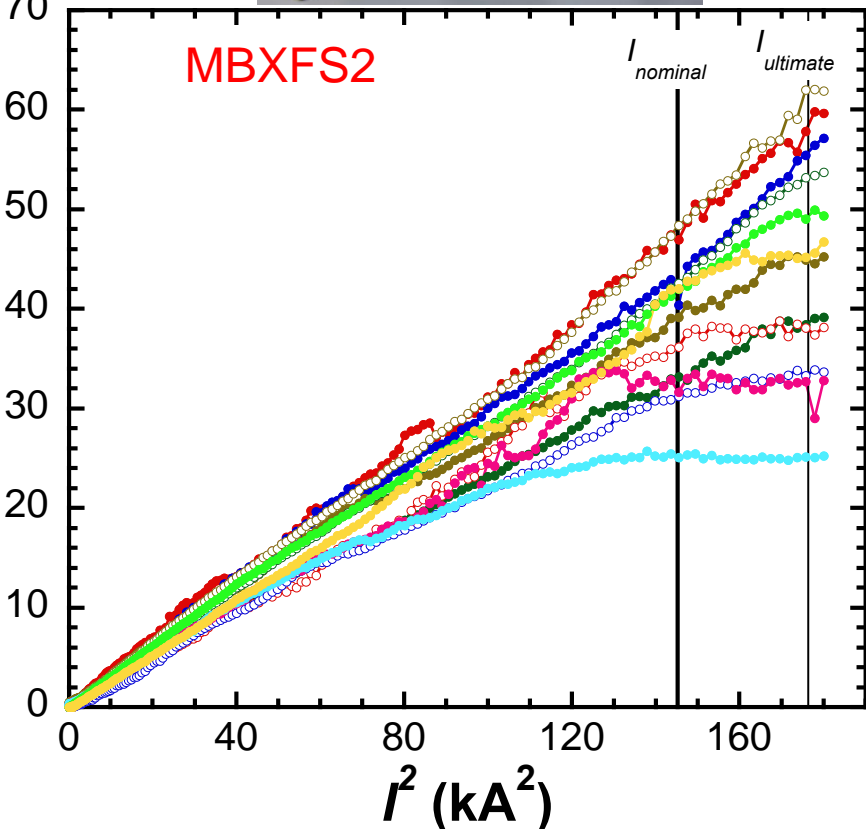
Stress variation,  $D_s$  (MPa)



RE



Variation of azimuthal coil stress (MPa)



Azimuthal coil pre-stress in straight section was confirmed to be sufficient.



# Quench start location

1st cycle

Quench#	Iq (kA)	Quench start location
1	9.504	Top, 1st turn, <b>SS to LE</b>
2	10.399	Bottom, 1st turn, <b>SS to LE</b>
3	11.095	Top, 26-27th turn, <b>SS to LE</b>
4	10.852	Top, 26-27th turn, <b>SS to LE</b>
5	11.376	Bottom, 2nd turn, <b>SS to LE</b>
6	11.292	Top, 2nd turn, <b>SS to LE</b>
7	11.703	Top, 13-14th turn, <b>LE</b>
8	12.348	Top, 26th turn, <b>RE</b>
9	12.69	Top, 5th turn, <b>SS to RE</b>
10	12.771	Top, 7-13th turn
11	12.966	Top, 5th turn, <b>SS to RE</b>
12	13.078	Bottom, 5th turn, <b>SS to RE</b>

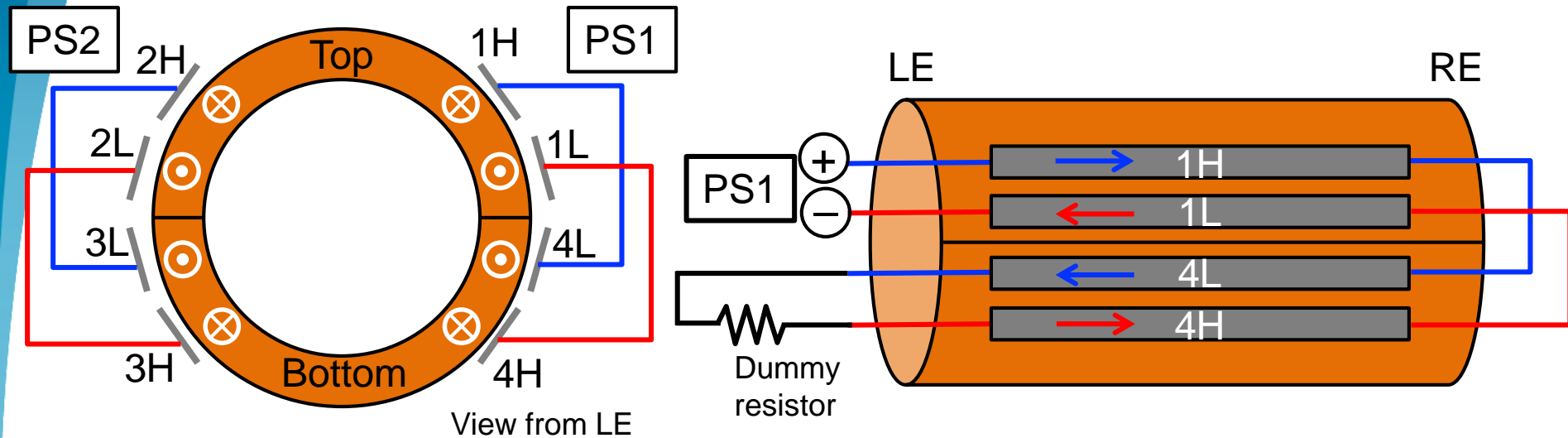
2nd cycle

Quench#	Iq (kA)	Quench start location
13	11.956	Bottom, 2nd-4th turn, <b>SS to LE</b>
14	12.562	Top, 1st turn, <b>SS</b>
15	12.874	Bottom, 13th turn, <b>LE</b>
16	13.011	Bottom, 13th turn, <b>LE</b>
17	13.051	Top, 13th turn, <b>LE</b>
18	13.240	Top, 5th turn, <b>SS</b>
19	13.051	Bottom, 2nd turn, <b>LE</b>
20	12.982	Bottom, 19-26th turn
21	13.161	Bottom, 13th turn, <b>LE</b>
22	13.331	Top, 5th turn, <b>LE</b>
23	13.391	Top, 1st turn, <b>RE</b>
24	13.418	Top, 1st turn, <b>RE</b>
25	13.442	Top, 1st turn, <b>LE</b>
26	13.420	Bottom, Ramp lead

Top coil  
 Bottom coil

Quench start location was concentrated within or close to coil end.

# Heater test with new QPH

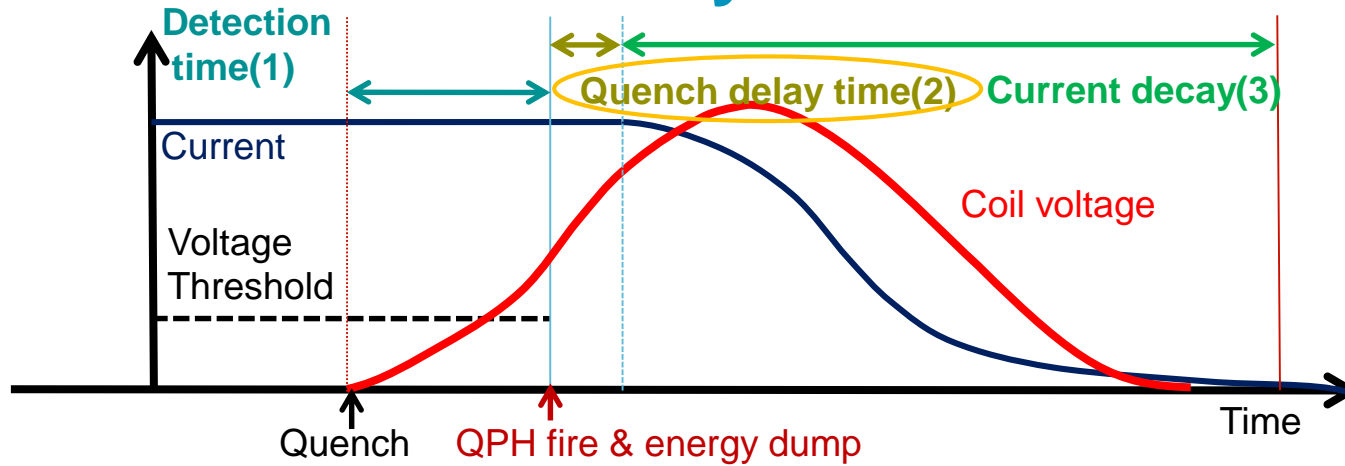


- QPH: 2 strips per each quadrant, 8 strips in total
- 2 strips were electrically shorted at RE.
- Two QPH power supplies were used.
- To deposit the energy density same as 7 m-long QPH for series magnet, dummy resistor was included in the circuit.

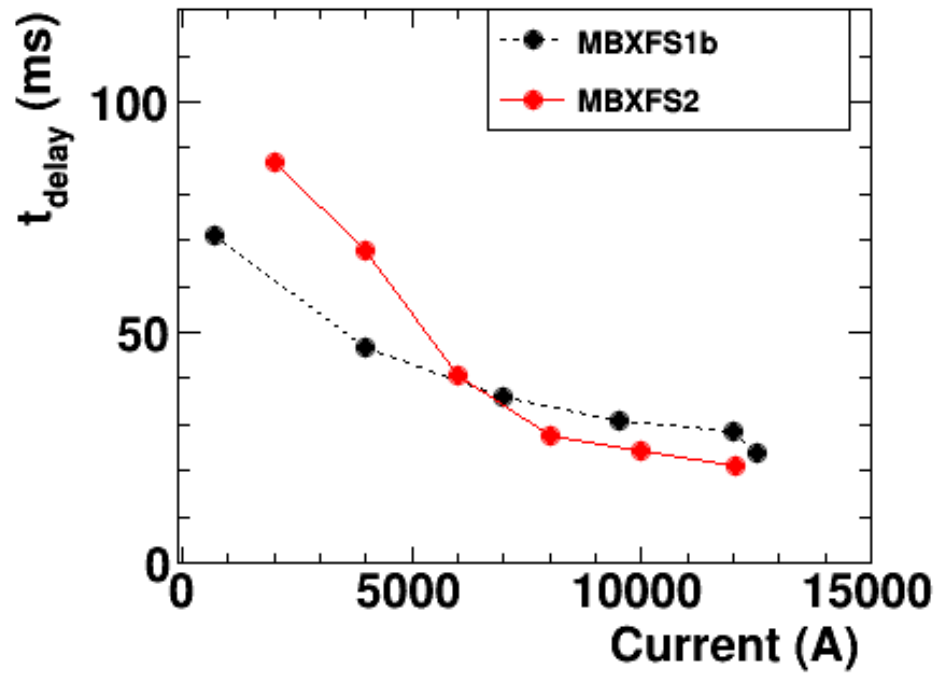
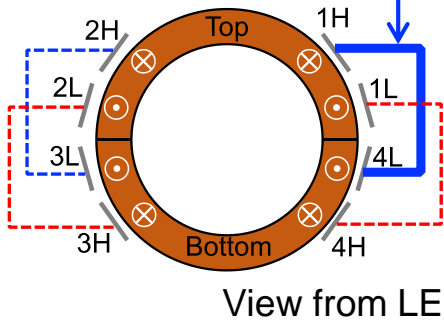
## Test items

- Evaluation of **delay time**
- Full energy dump to evaluate **MIITs during current decay**

# Delay time

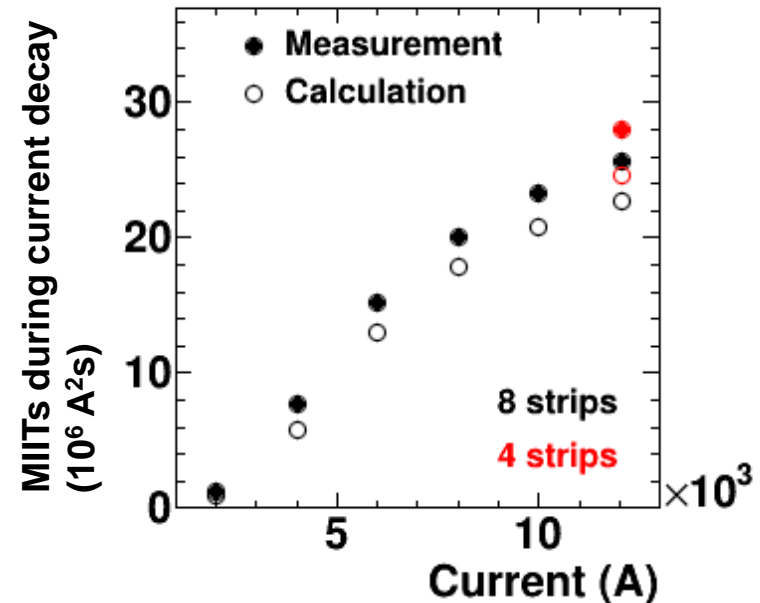
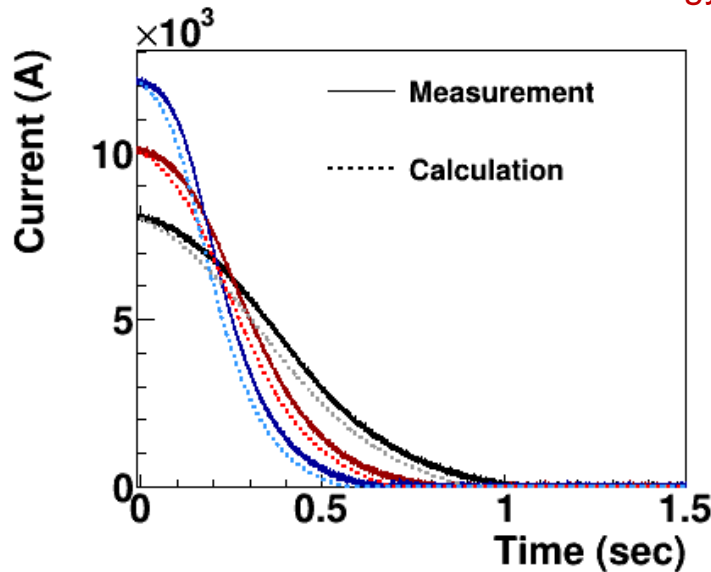
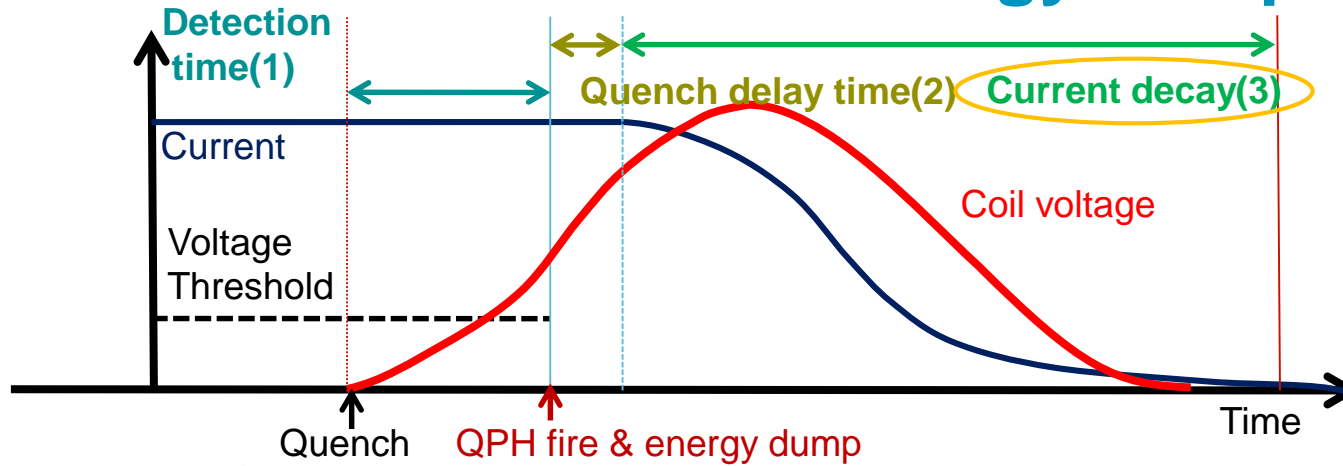


Only this pair of strips was fired



- Delay time was evaluated by firing only one pair of heater strips.
- Shorter delay time was obtained above 7 kA in MBXFS2 than MBXFS1b.

# MIITs evaluation in full energy dump test



- Calculated MIITs during current decay agrees with measured MIITs within  $\Delta\text{MIITs} = 3$ .
- Validity of quench simulation and newly designed QPH was confirmed.

# Magnetic field measurement

## ■ MFM at warm

- Vertical measurement at RT before cool-down and after warm-up
- Both DC loop and Z scan
- Current:  $\pm 5$  A

## ■ MFM at cold

### ■ DC loop at Z=0 mm with the long coil (L=350 mm)

- Current loop : 50A  $\rightarrow$  12.2 kA  $\rightarrow$  50A
- Field angle is corrected at I=12.2 kA

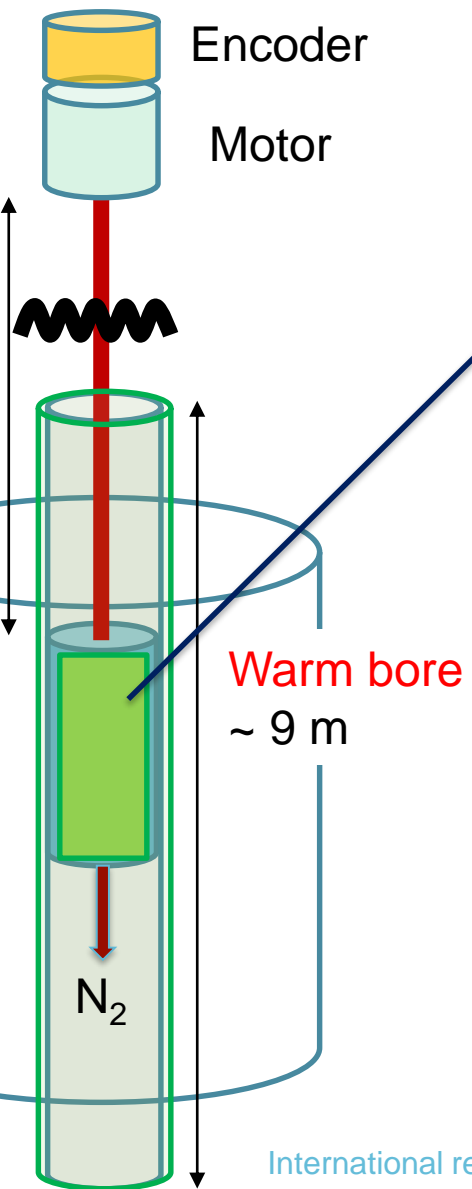
Skew:  $a_n(z = 0, I) = \frac{A_n(z = 0, I)}{B_1(z = 0, I)} \times 10^4$     Normal:  $b_n(z = 0, I) = \frac{B_n(z = 0, I)}{B_1(z = 0, I)} \times 10^4$

### ■ Z scan with the long / short coil (L=350 mm / 80 mm)

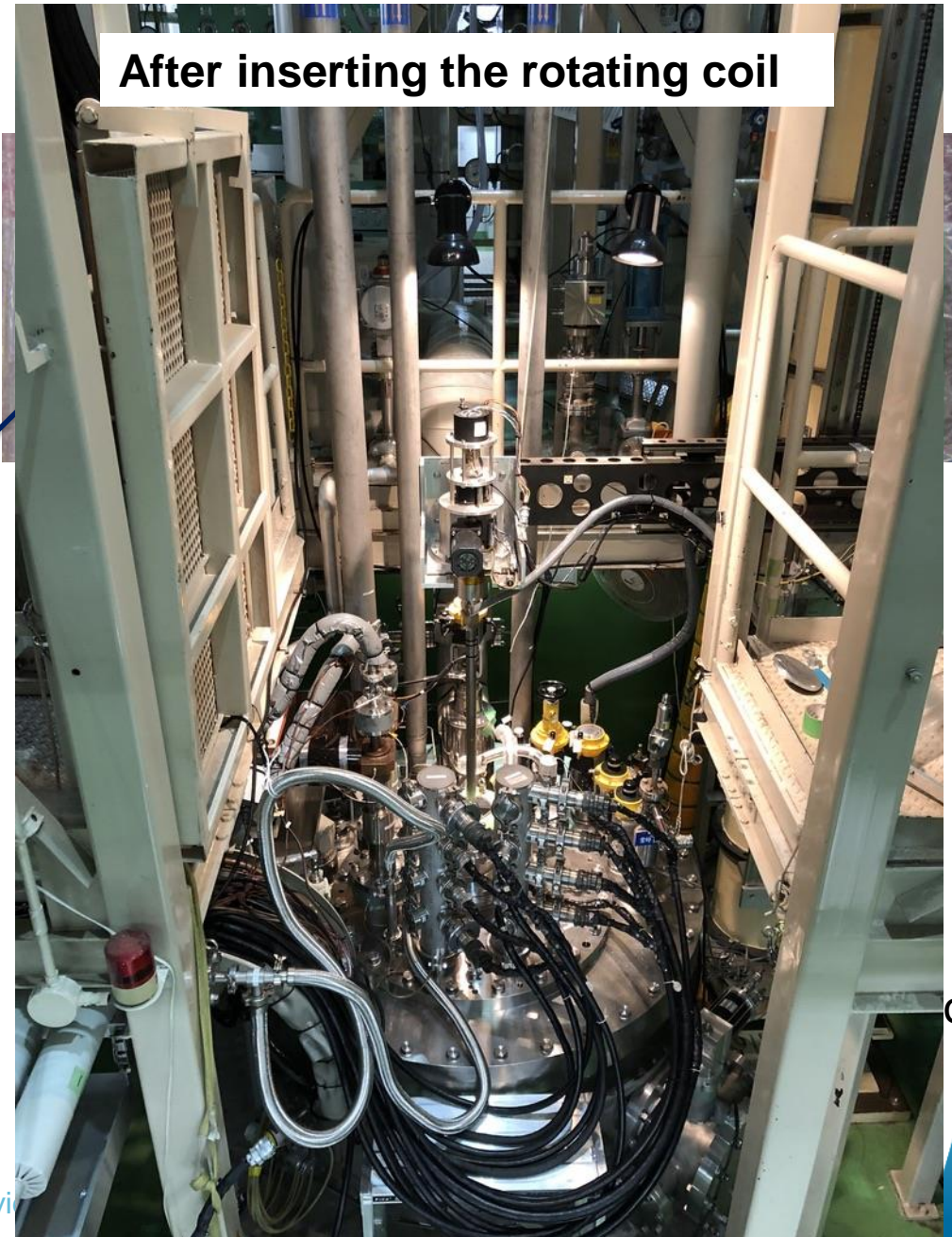
- Field angle is corrected at Z=0 mm for every operating current

Skew:  $a_n(z, I) = \frac{A_n(z, I)}{B_1(z = 0, I)} \times 10^4$     Normal:  $b_n(z, I) = \frac{B_n(z, I)}{B_1(z = 0, I)} \times 10^4$

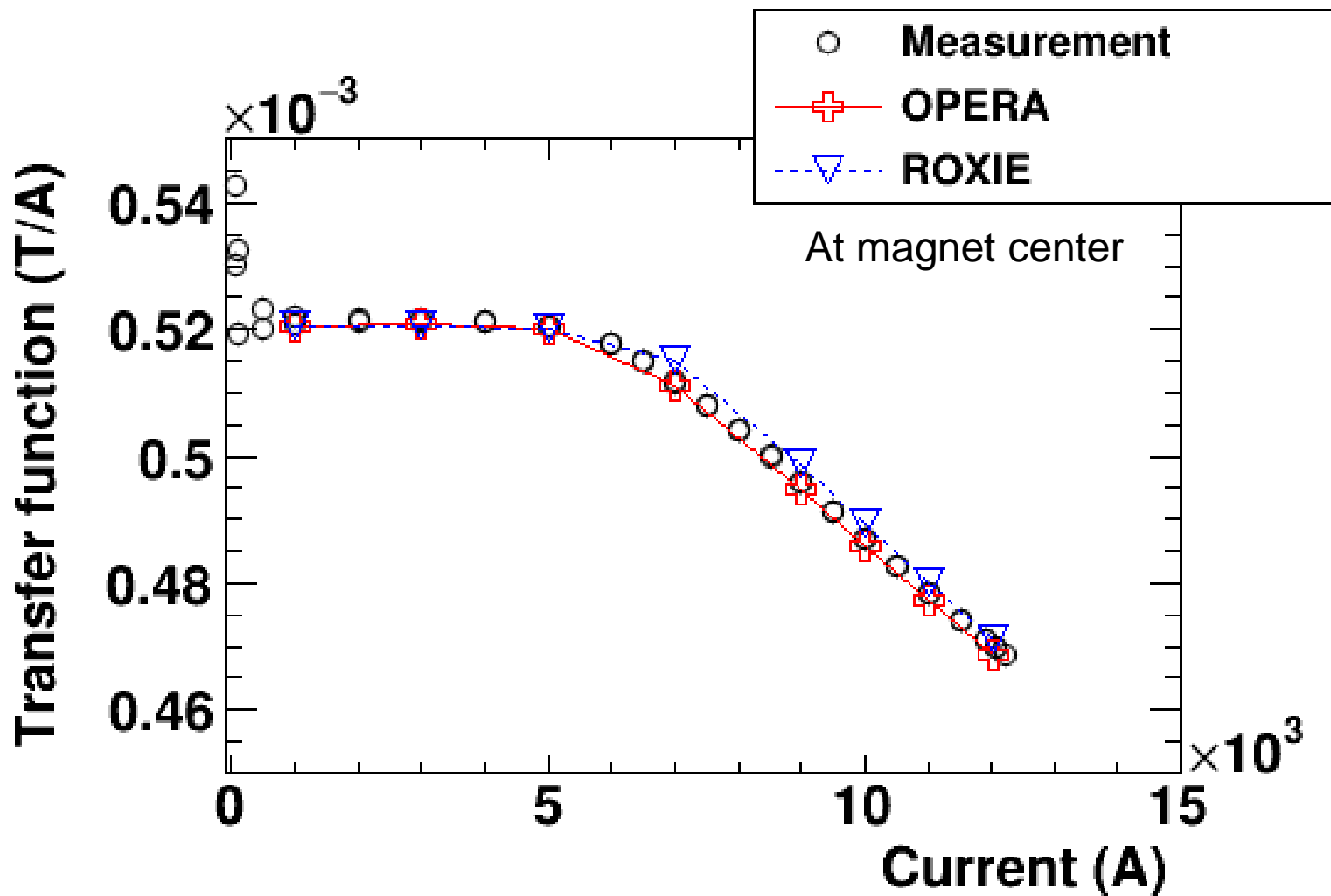
# Rotating (Harmonic) coil system



After inserting the rotating coil

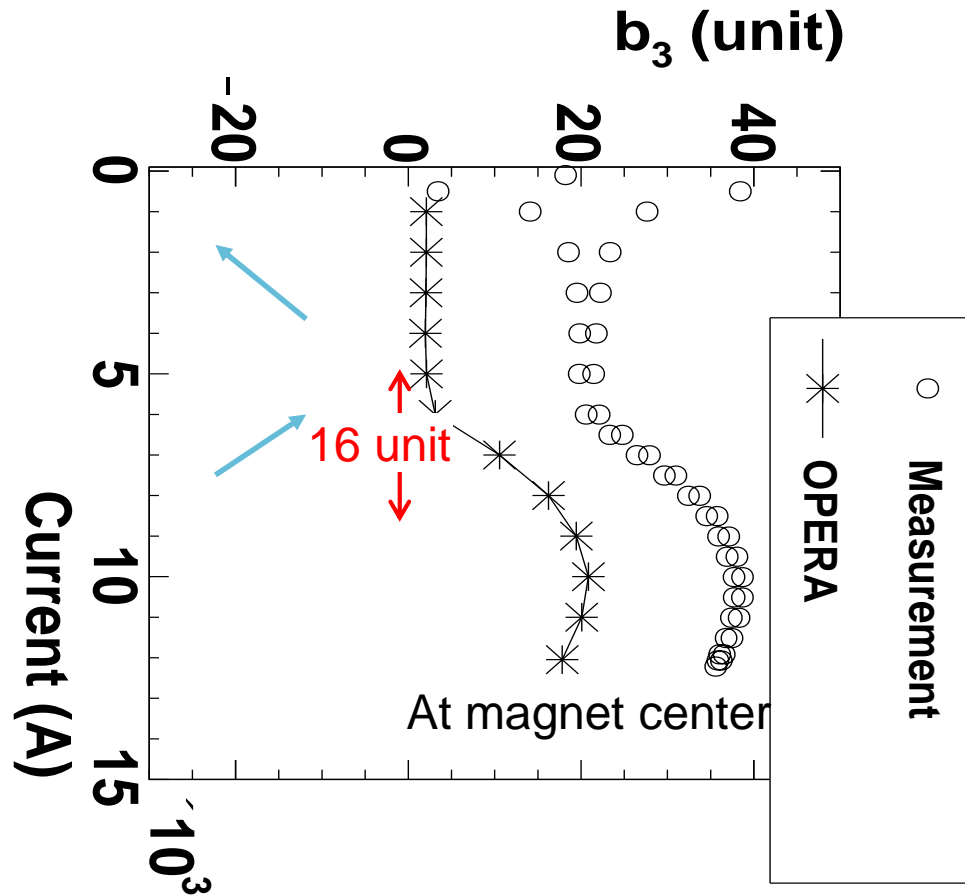


# DC loop - Transfer function-



- Consistent with the two calculations (OPERA, ROXIE)  
Better agreement obtained when compared to OPERA

# DC loop - b3 -

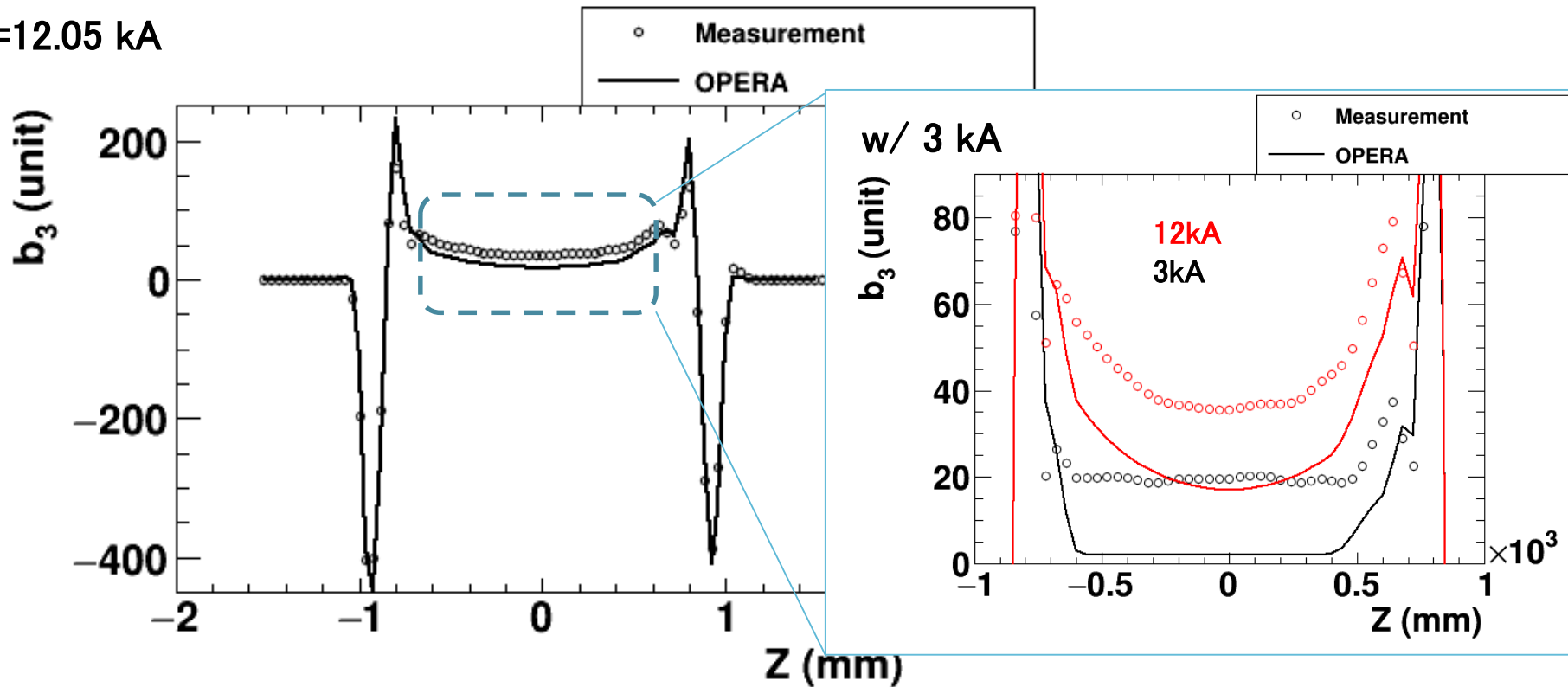


- Difference of  $b_3$  between measurements and calculations by OPERA 3D
  - $\Delta b_3 = +16$  units at 3 kA
  - $\Delta b_3 = +18$  units at 12 kA



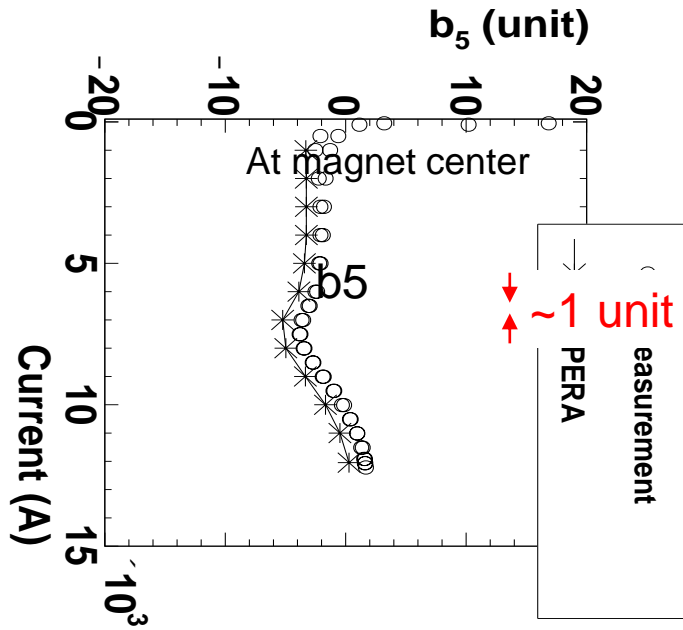
# Z scan of b3

I=12.05 kA

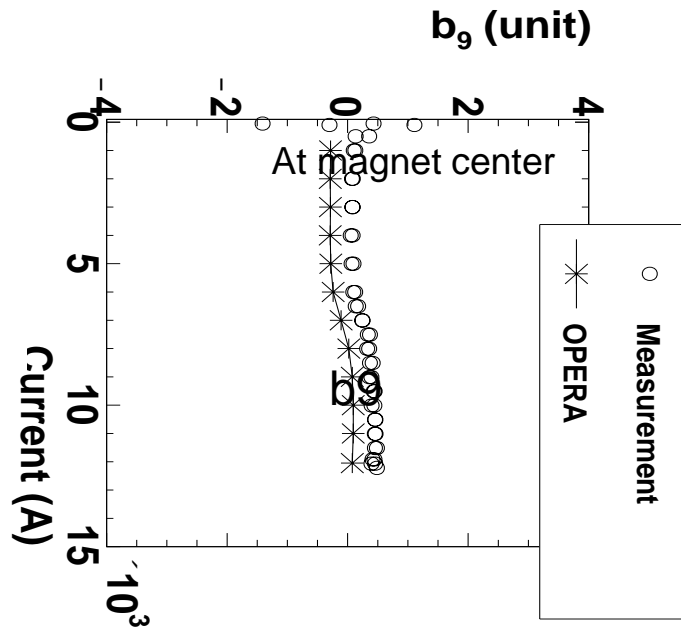
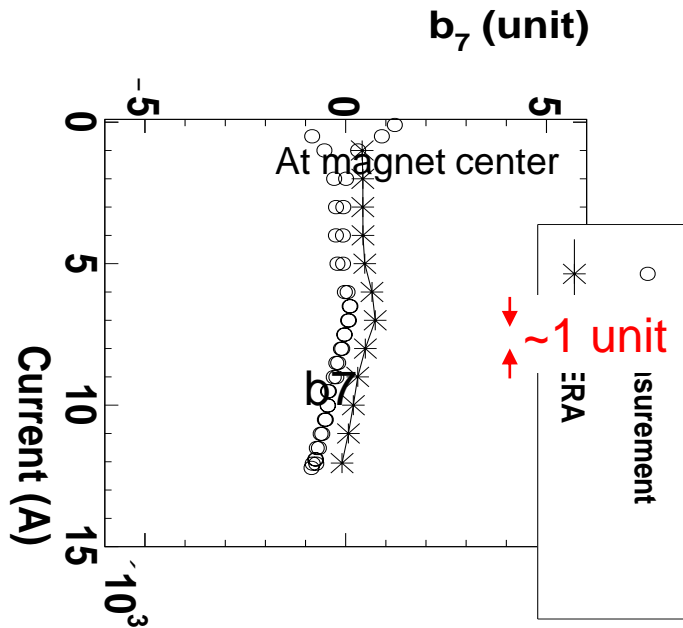


- $b_3$  offset by 16 – 18 units along the straight section
- $b_3$  offset is found even at 3 kA at which iron saturation is marginal  
→ Imperfect coil geometry ?

# DC loop - b5, b7, b9 -



- Measured  $b_5$ - $b_9$  are within 1 unit compared to OPERA 3D calculations.



Measured  
(OPERA 3D)

# Field integral ( $I=12.047\text{kA}$ ) $\bar{b}_n(I) = \frac{\int_{z_1}^{z_2} B_n(I, z) dz}{\int_{-1750}^{1750} B_1(I, z) dz} \times 10^4$

n	RE (-1750 ~ -525)		SS (-525 ~ 525)		LE (525 ~ 1750)		Total (-1750~1750)	
	bn	an	bn	an	bn	an	bn	an
1	1925 (1871)	3.44 (0.03)	6259 (6268)	-1.12 (0.20)	1816 (1862)	<b>-34.07</b> <b>(-15.05)</b>	10000 (10000)	<b>-31.75</b> <b>(-14.83)</b>
2	1.18 (0.00)	-1.05 (-0.01)	-2.52 (-0.01)	0.16 (0.01)	1.03 (0.04)	-3.66 (-0.05)	-0.31 (0.03)	-4.55 (-0.05)
3	-14.11 (-12.27)	-0.45 (0.00)	<b>24.81</b> <b>(13.80)</b>	0.15 (0.11)	-9.74 (-9.94)	7.30 (5.50)	<b>0.95</b> <b>(-8.41)</b>	7.01 (5.66)
4	0.02 (0.00)	-0.30 (0.00)	-0.40 (0.01)	0.16 (0.00)	-0.63 (-0.04)	-0.01 (-0.01)	-1.00 (-0.03)	-0.14 (0.00)
5	-0.40 (-0.89)	-0.02 (0.00)	1.09 (0.23)	-0.14 (-0.10)	<b>2.62</b> <b>(0.79)</b>	-0.66 (-0.48)	<b>3.30</b> <b>(0.13)</b>	-0.82 (-0.58)
6	0.22 (0.00)							-0.05 (0.01)
7	-1.25 (-1.00)							0.40 (0.50)
8	0.29 (0.00)	0.05 (0.00)	-0.15 (0.00)	0.07 (0.00)	0.26 (0.00)	0.02 (0.00)	0.40 (0.00)	0.14 (-0.01)
9	-0.98 (-0.99)	-0.06 (0.00)	0.28 (0.05)	-0.05 (-0.03)	-0.50 (-0.66)	-0.04 (-0.10)	-1.19 (-1.60)	-0.15 (-0.13)
10	0.14 (0.00)	0.01 (0.00)	-0.05 (0.00)	0.01 (0.00)	0.13 (-0.01)	0.01 (0.01)	0.21 (-0.01)	0.03 (0.01)
11	-0.37 (-0.43)	0.01 (0.00)	0.06 (0.10)	0.02 (0.01)	-0.29 (-0.32)	0.03 (0.07)	-0.60 (-0.65)	0.06 (0.08)

**Integral of b3: Large contribution from the straight section**  
**Other multipoles agree with calculations within 1 unit.**

Measured  
(OPERA 3D)

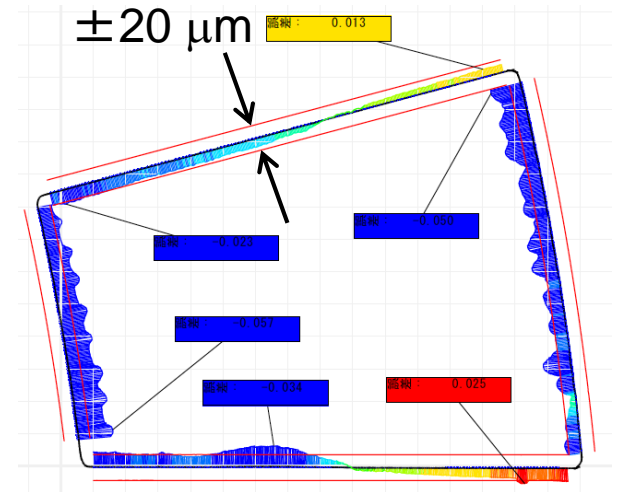
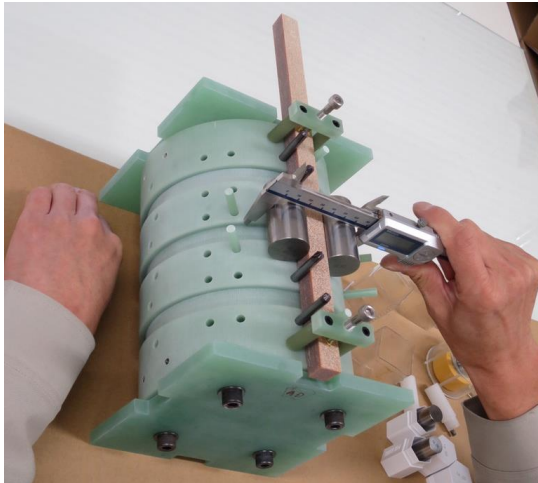
## Field integral (n>12)

n	RE (-1750 ~ -525)		SS (-525 ~ 525)		LE (525 ~ 1750)		Total (-1750~1750)	
	bn	an	bn	an	bn	an	bn	an
12	0.08 (0.00)	0.01 (0.00)	0.23 (0.00)	0.03 (0.00)	0.09 (-0.02)	0.03 (0.00)	0.40 (-0.02)	0.06 (0.01)
13	-0.22 (-0.23)	-0.01 (0.00)	-0.49 (-0.43)	-0.05 (0.00)	-0.15 (-0.16)	-0.01 (-0.02)	-0.86 (-0.82)	-0.07 (-0.02)
14	0.10 (0.00)	-0.01 (0.00)	0.53 (0.00)	0.04 (0.00)	0.10 (0.01)	0.00 (0.00)	0.72 (0.01)	0.03 (0.00)
15	-0.17 (-0.17)	-0.01 (0.00)	-0.80 (-0.72)	-0.07 (0.00)	-0.14 (-0.17)	0.02 (0.00)	-1.11 (-1.05)	-0.06 (0.00)
16	0.04 (0.00)	0.00 (0.00)	0.39 (0.00)	0.05 (0.00)	0.08 (0.00)	-0.02 (0.00)	0.51 (0.00)	0.03 (0.00)
17	-0.06 (-0.07)	-0.01 (0.00)	-0.40 (-0.51)	-0.03 (0.00)	-0.06 (-0.07)	-0.01 (0.00)	-0.52 (-0.64)	-0.05 (0.00)
18	-0.01 (0.00)	0.00 (0.00)	-0.21 (0.00)	-0.03 (0.00)	-0.02 (-0.01)	-0.01 (0.00)	-0.24 (-0.01)	-0.04 (0.00)
19	0.05 (0.03)	0.00 (0.00)	0.23 (0.24)	0.01 (0.00)	0.02 (0.04)	0.00 (0.00)	0.30 (0.31)	0.01 (0.00)
20	0.00 (0.00)	0.00 (0.00)	0.00 (0.00)	0.00 (0.00)	0.00 (0.00)	0.00 (0.00)	0.00 (0.00)	0.00 (0.00)

- For the multipoles (n>12), all the measured results are consistent with the calculations.

# Possible reasons of b3 offset 1

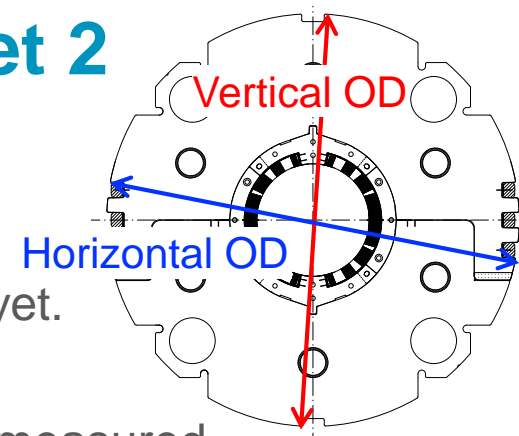
- Dimensions of GFRP wedges
  - Inverted field calculation showed that coil block should move with  $O(0.1 \text{ mm})$  to reproduce  $\Delta b_3=16$  units.
  - Dimensions of wedges were measured using pin gauges and CMM
  - Tolerance of wedges almost within  $\pm 20 \mu\text{m}$  was confirmed.  
→ Out of dimension tolerance of wedges is NOT a reason of b3 offset.



- Unexpected magnetic material
  - We have not found magnetic materials which can shift only b3 by as large as 16 units.

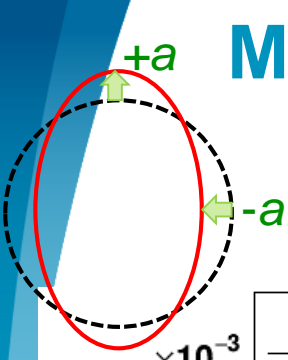
# Possible reasons of b3 offset 2

- Yoked magnet of MBXFS2 showed oval deformation.
  - Vertical OD – horizontal OD = 0.3 mm
  - Coil deformation of MBXFS2 has not been measured yet.
- Dimensions of 200 mm-long mechanical short model was measured
  - Outer diameter of yoked magnet: Vertical OD – Horizontal OD = 0.33 mm  
→ Consistent with measured value for MBXFS2
  - Inner diameter of coil: Vertical ID – Horizontal ID = 0.42 mm  
→ Magnetic field calculation was performed in consideration of coil oval deformation.



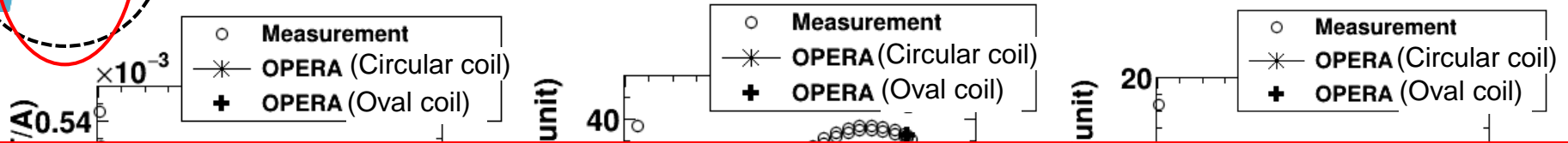
200 mm-long mechanical short model

# Measurements and calculations with oval coils



$a$ : Ovalization factor

$a$ -value was taken to be 0.4 mm.



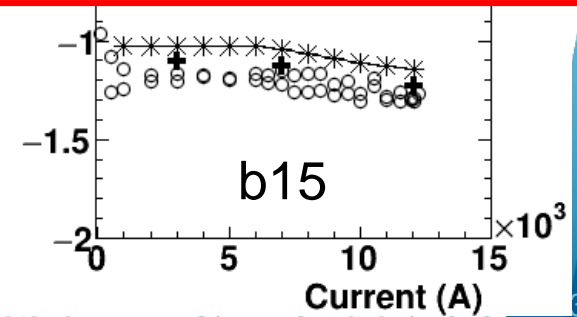
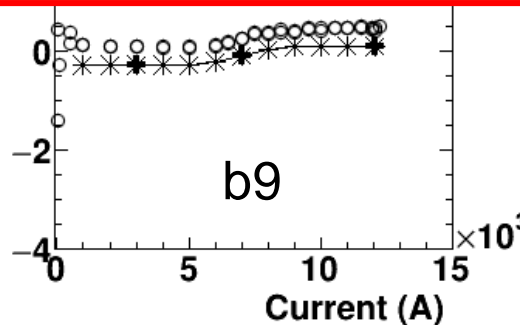
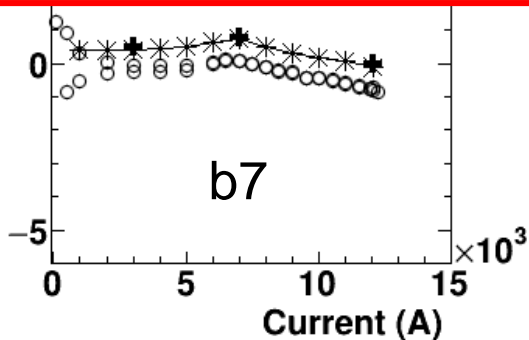
Calculations with  $a=0.4$  mm can reproduce measured b3.

Measured b5, b7, b9 and b15 can also be reproduced within 1 unit.

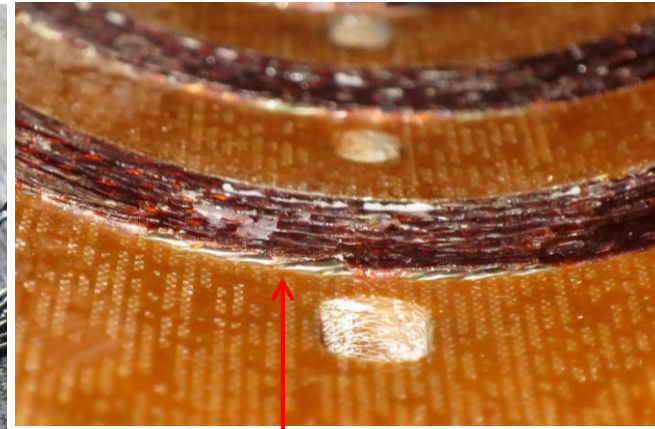
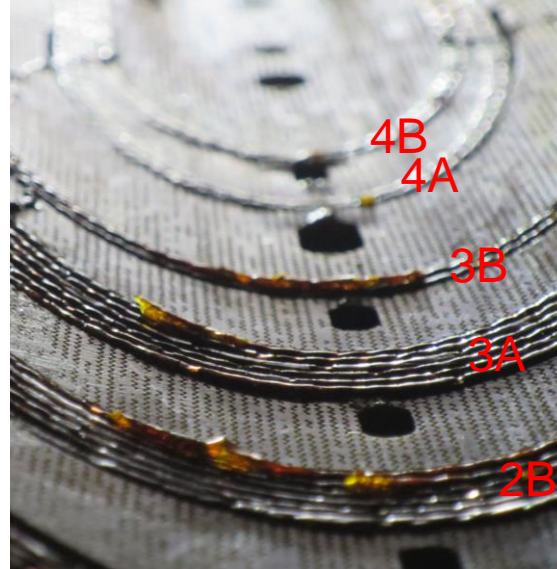
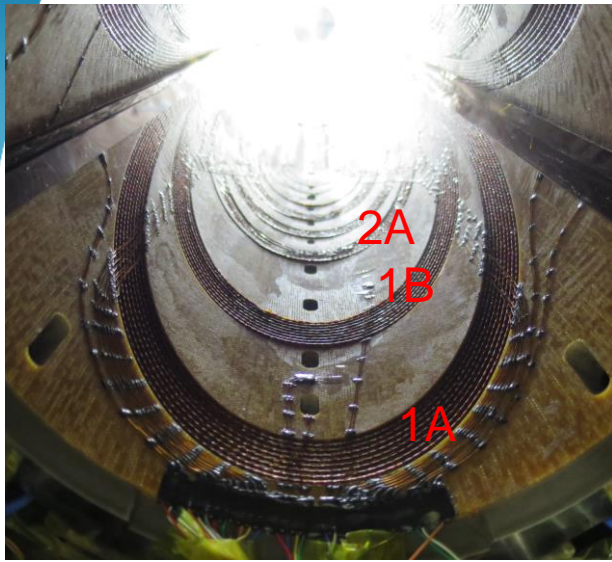
$a = 0.4$  mm  $\rightarrow$  vertical coil ID – horizontal coil ID = 1.6 mm, much larger than measured value of 0.4 mm for mechanical short model

We have a plan to measure coil ID of MBXFS2 using a laser displacement sensor.

We have not fully understood the reason of b3 offset in MBXFS2, but correction will be made in prototype assuming that coil oval deformation is the primary reason.



# Cable displacement at coil end



Breakage of cable insulation only at the interface btw cable and end spacer

Coil end block at which insulation breakage due to cable displacement occurred.

	1A out	1A in	1B out	1B in	2A out	2A in	2B out	2B in	3A out	3A in	3B out	3B in	4A out	4A in	4B out	4B in
Top, LE			X	X	X		X		X		X					
Top, RE				X			X	X	X							
Bottom, LE			X	X			X									
Bottom, RE				X			X									

- Cable displacement at coil end was still observed in MBXFS2, though the displacement is smaller compared to MBXFS1 and 1b.
  - Max displacement: MBXFS1=3.4 mm, MBXFS1b=2.5 mm, **MBXFS2 < ~1 mm**
- Wet-winding enhanced turn-to-turn bonding, but polyimide cable insulation is too weak to confine the cable against Lorentz force. As a result, **breakage of cable insulation** occurred. **Pre-stress at coil end should be further increased.**



# Status of MBXFS3

# Purposes of MBXFS3

- The main purpose of MBXFS3 is reproducibility check.
  - Design of wedge and end spacers are the same as those of MBXFS2.
  - Should be checked if the same b3 offset as MBXFS2 is observed
- Countermeasure to cable displacement at coil end
  - Pre-stress at coil end will be increased by inserting shims into MP.
  - Pressing test using curing press with a 2 m-long coil to determine shim thickness
  - Axial pre-load can be further increased.



# Status and schedule

- Coil winding and curing were completed.
- Instrumentation and coil size measurement are ongoing.
- After yoking, warm magnetic field measurement will be conducted. The results will be fed back to design of prototype magnet.

	2019									
	Jan	Feb	Mar	Apr	May	Jun	Jul	Aug	Sep	Oct
<b>Fabrication</b>										
Coil fabrication	■	■								
Coil size masurement		■	■							
Instrumentation			■	■	■					
QPH, insulation wrapping				■						
Collaring				■	■					
Yoking					■	■				
<b>Warm MFM</b>					■					
Shell welding						■				
End ring welding							■			
Axia pre-loading							■			
Splice work								■		
<b>Magnet test</b>										
Preparation							■	■		
Magnet test									■	■

Bid opening of prototype magnet

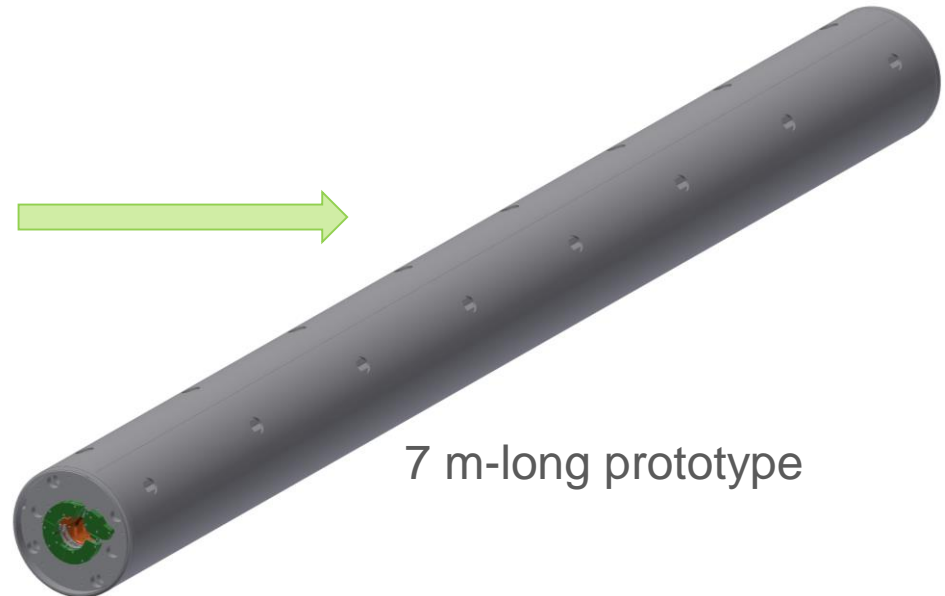
# Prospect for prototype

# From model magnet to prototype

- 7 m-long prototype will be manufactured by a company after technology transfer from KEK. Fabrication process is basically the same as model magnets.
- Major part of magnet design will not be changed except for the following two points.
  - **Modification of magnet cross-section to correct b3 offset**
    - MBXFS3 has the same cross-section as MBXFS2.
    - **Modification will be applied to prototype.**
  - **Increase in coil pre-stress at coil end**
    - **Countermeasure to cable displacement at coil end will be taken in MBXFS3.**



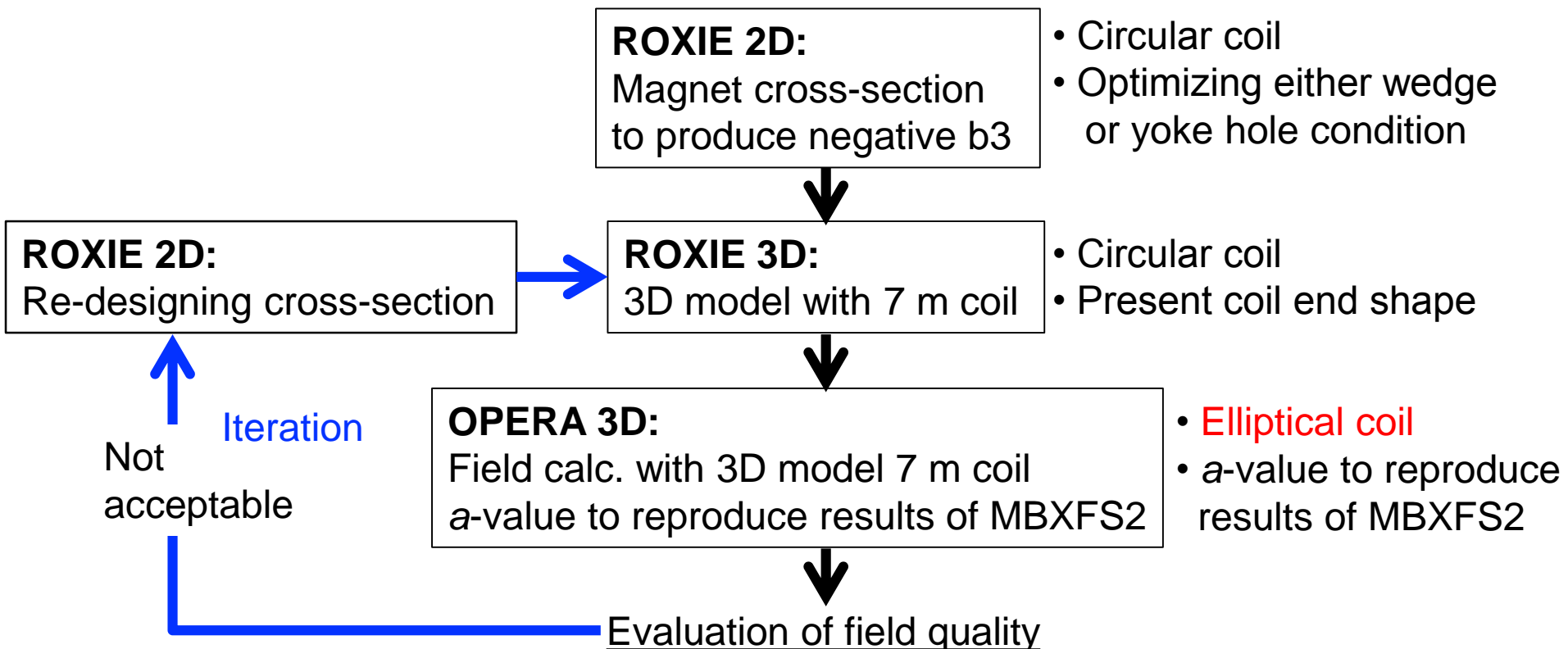
2 m-long model magnet



7 m-long prototype

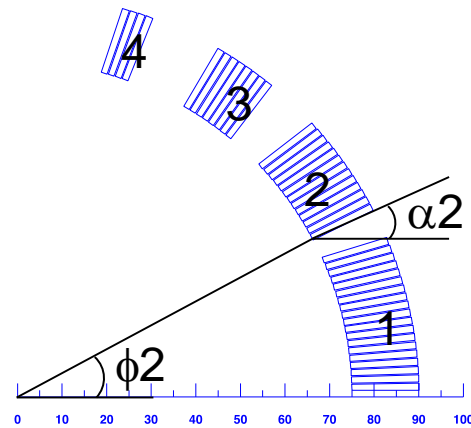
# Magnetic design of 7 m-long prototype

- Strategy to correct b3 offset
  - Assumption: b3 offset is caused only by coil oval deformation.
  - Other higher order multipoles will not be further corrected.
  - Coil end shape will not be changed.
  - Two options to cancel positive integrated b3. Correction by re-designing either wedges or yoke holes is still under discussion.
- The result of warm MFM after yoking for MBXFS3 is possibly fed back.



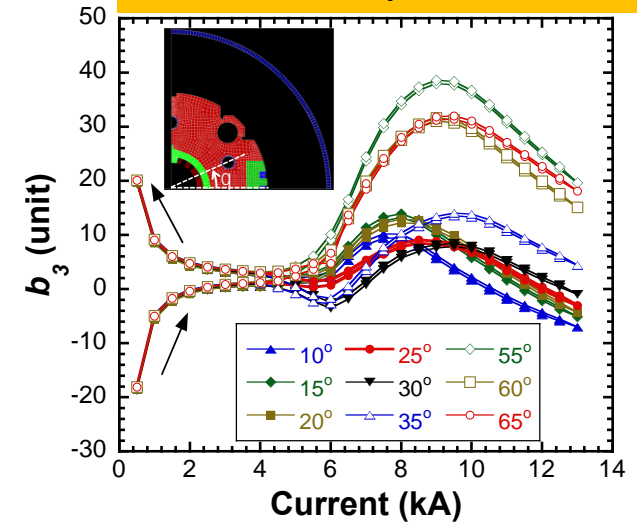
# Preliminary study for b3 correction

## Coil block re-arrangement

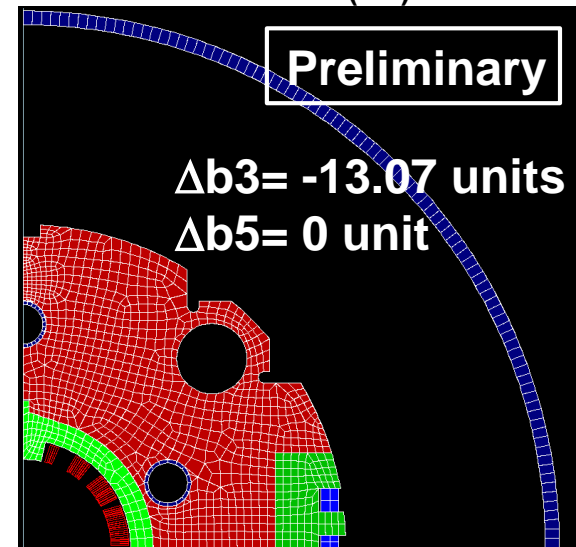


I=12.047 kA

## Yoke hole optimization



	MBXFS2	$\Delta b_3 = -16$ units $\Delta b_{n+1} = 0$ unit	$\Delta\phi, \Delta\alpha$ (deg)
$\phi_1$	1.1346	<b>1.239</b>	+0.104° (+137 $\mu\text{m}$ )
$\phi_2$	27.8721	<b>28.0885</b>	+0.216° (+283 $\mu\text{m}$ )
$\phi_3$	50.2969	<b>50.5061</b>	+0.209° (+274 $\mu\text{m}$ )
$\phi_4$	70.6992	<b>70.8005</b>	+0.101° (+133 $\mu\text{m}$ )
$\alpha_2$	26.0000	<b>26.1154</b>	+0.115°
$\alpha_3$	52.4212	<b>52.455</b>	+0.033°
$\alpha_4$	68.0015	<b>68.0619</b>	+0.060°



- b3 in SS should have a negative value to compensate positive b3 offset observed in MBXFS2.
- There are two options such as coil block re-arrangement or change in yoke hole.
- Which option we should select will be decided by considering pros and cons.

# Mechanical design of 7 m-long prototype

- Target pre-stress
  - Azimuthal pre-stress in SS: 115 MPa (same as MBXFS2, MBXFS3)
    - GFRP wedges will be oversized from the final dimension which is determined by ROXIE 2D.
  - Axial pre-load: **to be determined based on the results of MBXFS3**
- Pre-stress at coil end
  - **Shim thickness determined by MBXFS3 will be added to end saddle.**
- Mechanical short model will be assembled with cut-outs of 7 m-long practice coil to evaluate azimuthal coil pre-stress which is critical to training performance.



# Summary

- Two model magnets and one re-assembled model have been fabricated and tested at KEK.
  - Acceptable training performance
  - Two remaining issues such as b3 offset and cable displacement at coil end should be addressed.
- The third model magnet is being assembled.
  - The main purpose is reproducibility check.
  - Reproducibility of b3 offset should be checked.
  - Countermeasure to cable displacement by enhancing mechanical support of cable at coil end will be applied.
- Strategy for prototype design
  - Correction of b3 considering coil oval deformation



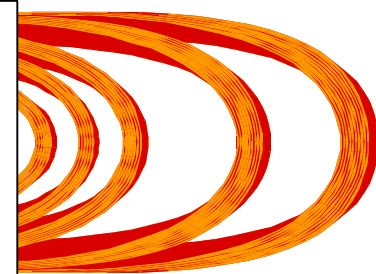
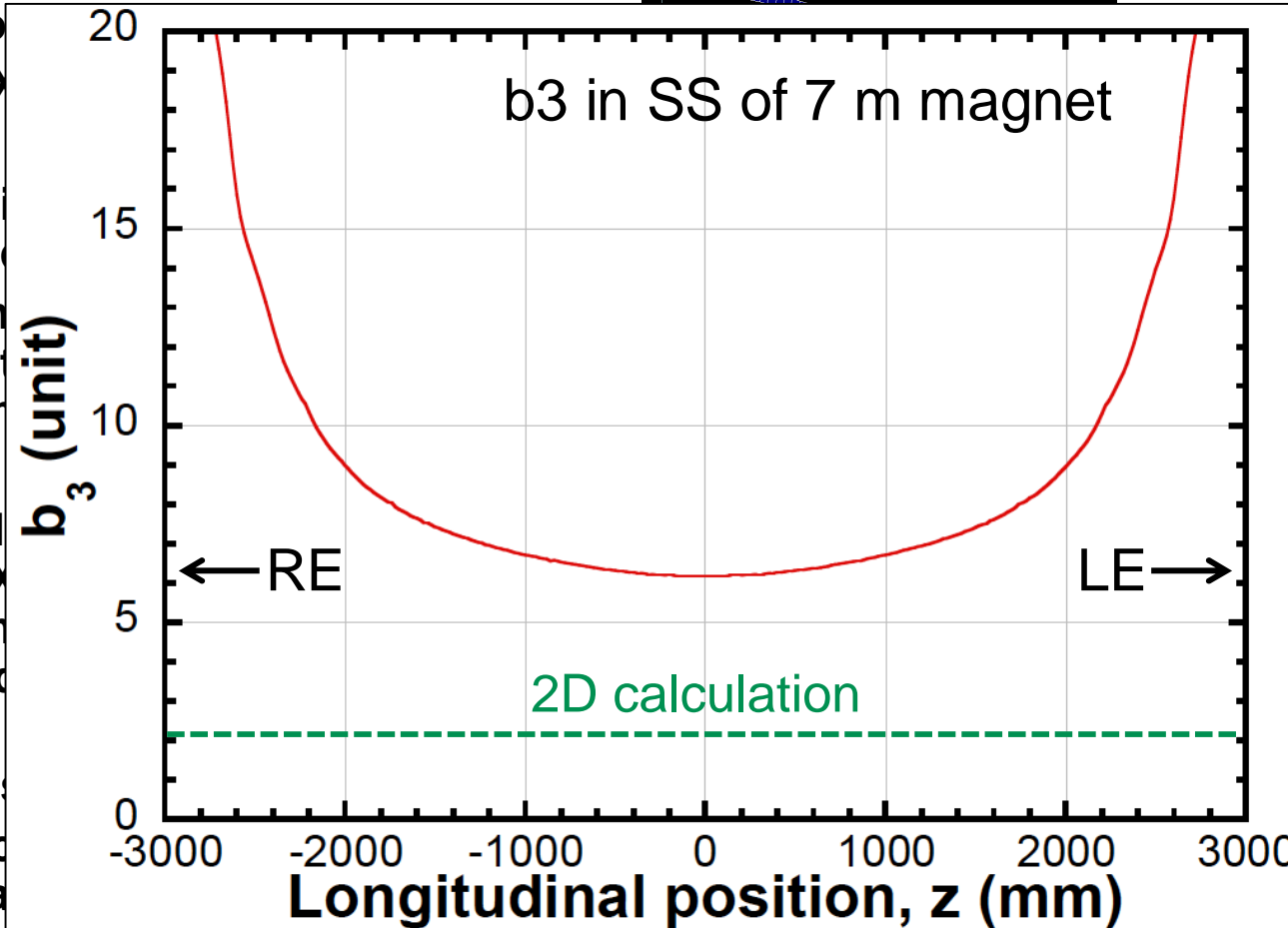
# Appendix

# Appendix

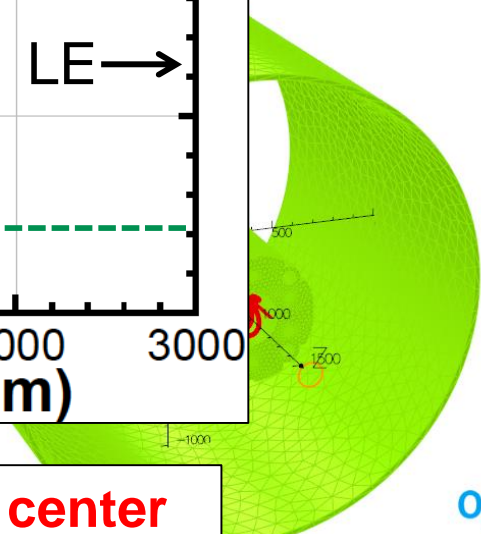
## D1 magnet for HL-LHC

# Design overview: Magnetic design

- Field coil
- 2D (ROX)
  - coil
  - mini
  - effe
  - all n
  - con
  - nom
- 3D :
  - Coil
  - ROX
  - com
  - proc
  - 2-m
  - end
  - Disc
  - mea



End model (XIE 3D)



Model (OPERA 3D)

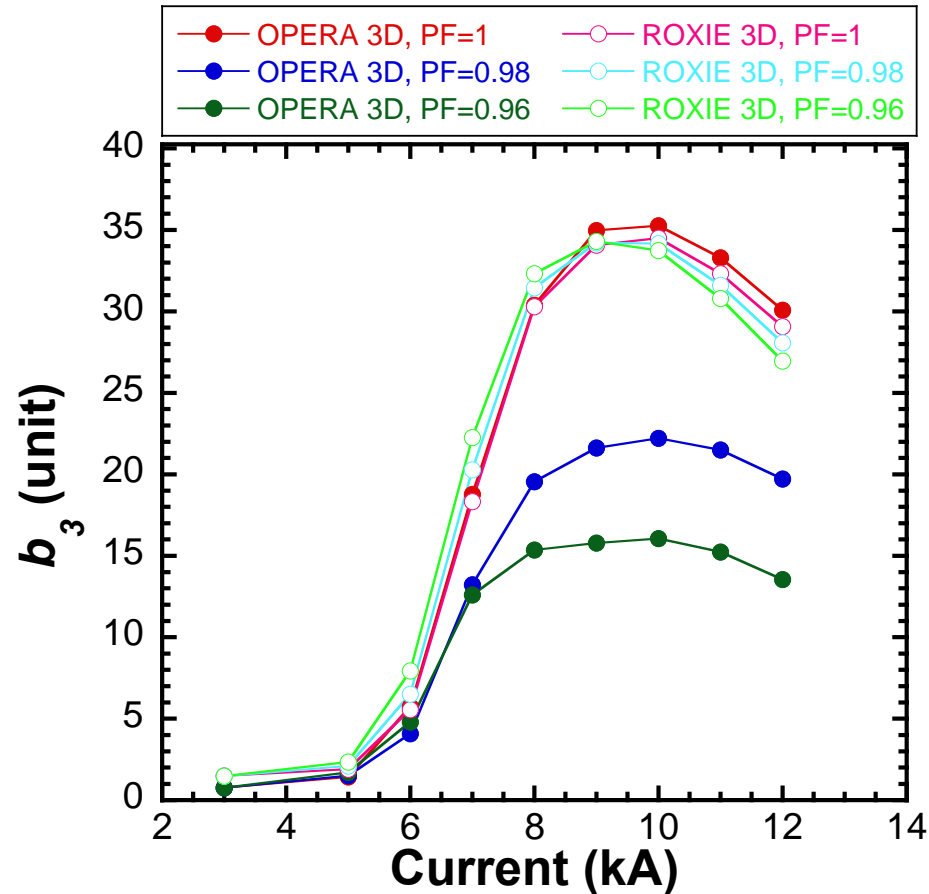
→ Switched to OPERA 3D

which  
meas

**Note: field quality even at the magnet center strongly influenced by the coil end.**



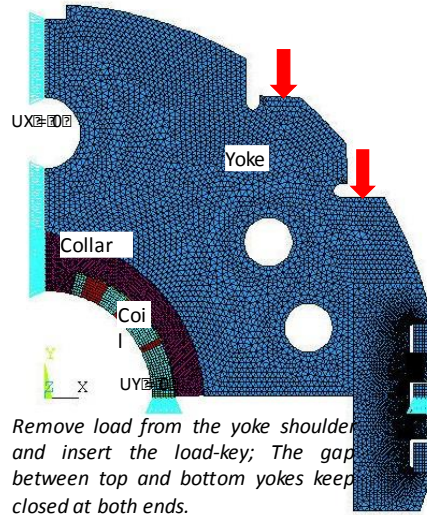
# Comparison of ROXIE 3D and OPERA 3D



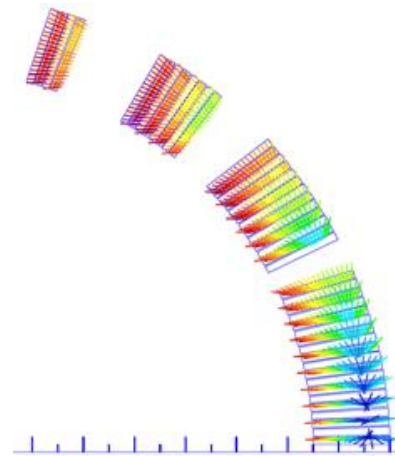
- At  $I > 5$  kA at which iron saturation is remarkable,  $b_3$  calculated by OPERA 3D is strongly dependent on packing factor of iron yoke.
- In ROXIE 3D, effect of yoke packing factor is marginal.

# Design overview: Mechanical design

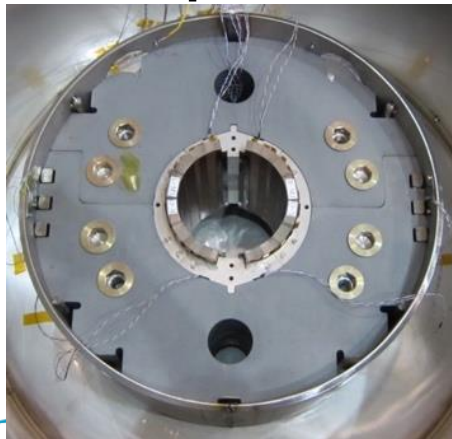
- 2D FEM Analysis (ANSYS)**
  - Fabrication, cooling and excitation (110%)
  - Pre-stress applied in yoking
  - Target azimuthal pre-stress: **115 MPa**
- 200 mm long mechanical model**
  - Validation of mechanical design.
  - Check of assembly tooling and procedures.



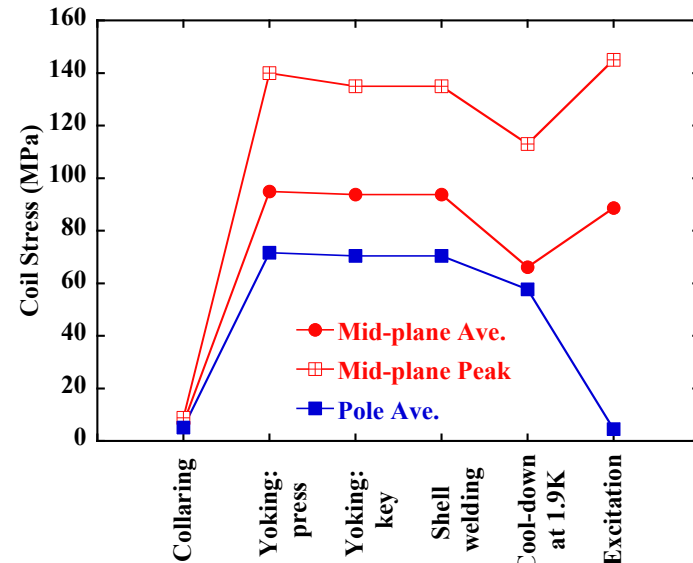
2D Model for ANSYS



E.M. Force on coil



200-mm mechanical model for structural validation

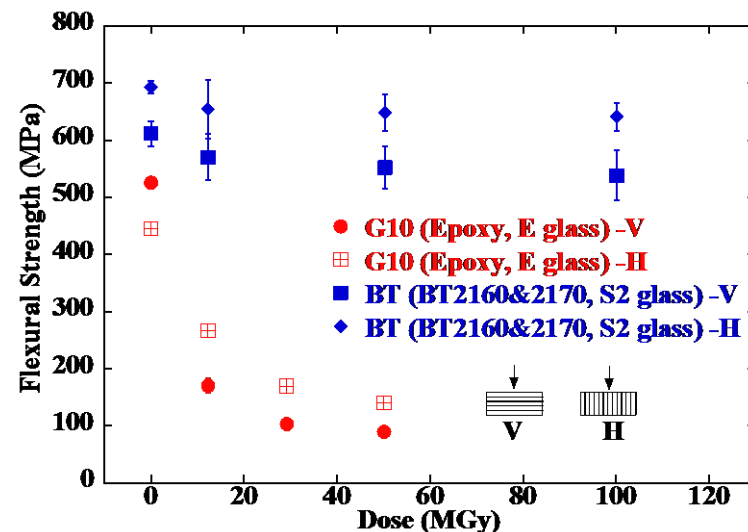


Coil stress calculated by ANSYS

# Materials for Radiation Resistant Coil

## Radiation resistant GFRP

- Bismaleimide-Triazine (BT) resin + boron-free S2 glass fibers
- Flexural strength is not degraded at least up to 100 MGy of  $\gamma$ -ray irradiation
- Application to accelerator magnets for the first time



Pole shim and wedges

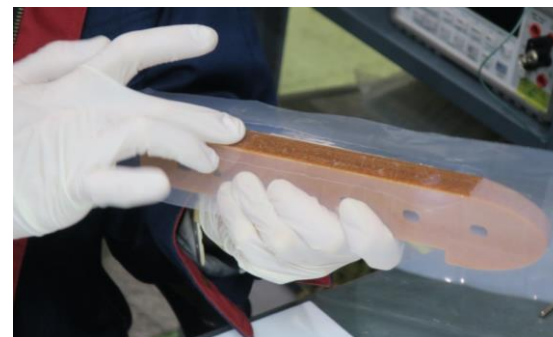


End spacers



## Radiation resistant adhesive

EC-1HB-F7P (Epoxy B + CE + 7wt% Silica filler) was selected from acceptable bonding strength with highest viscosity





# Appendix

## Design update from MBXFS1/1b to MBXFS2

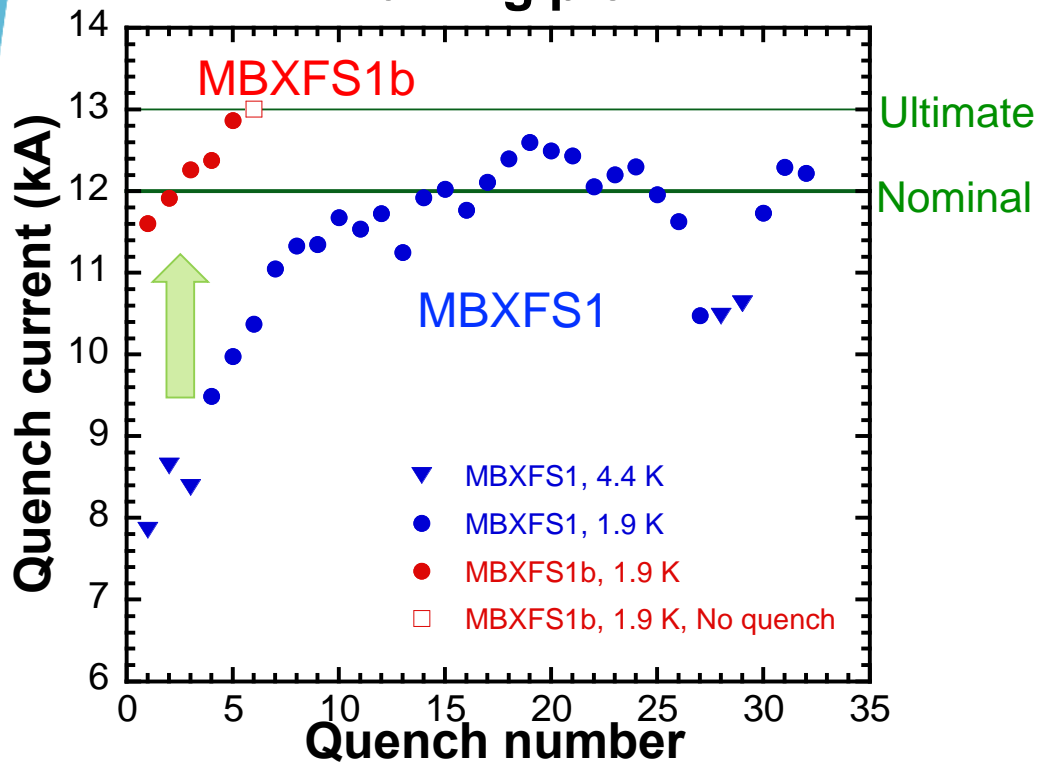
# Training performance of MBXFS1/1b

Previous work

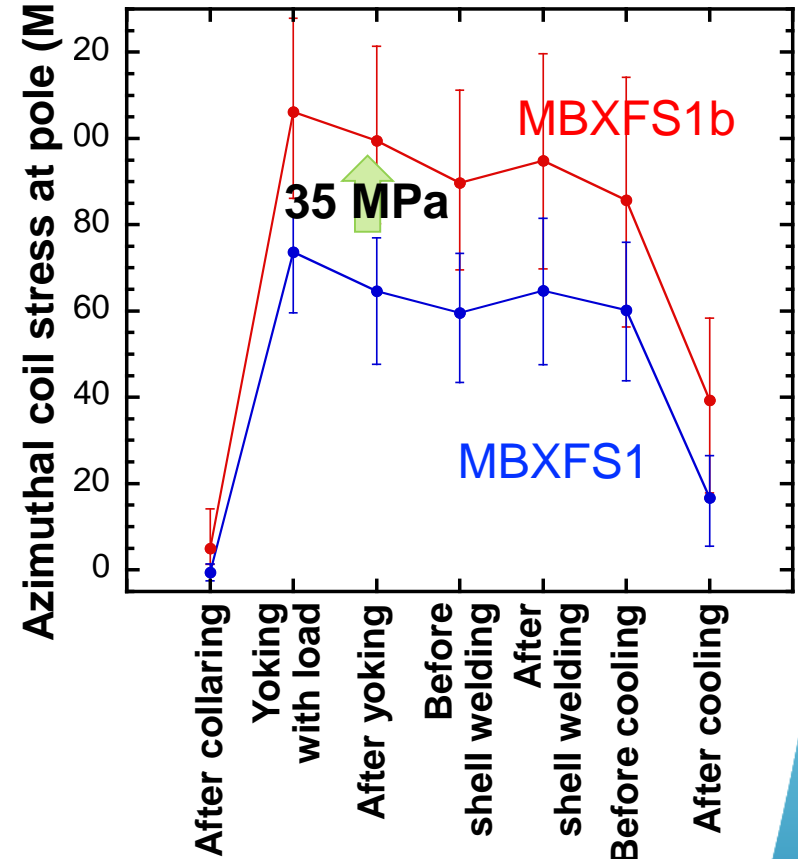
MBXFS1: First model magnet

MBXFS1b: Re-assembled first model magnet  
with enhanced coil pre-stress

## Training plot

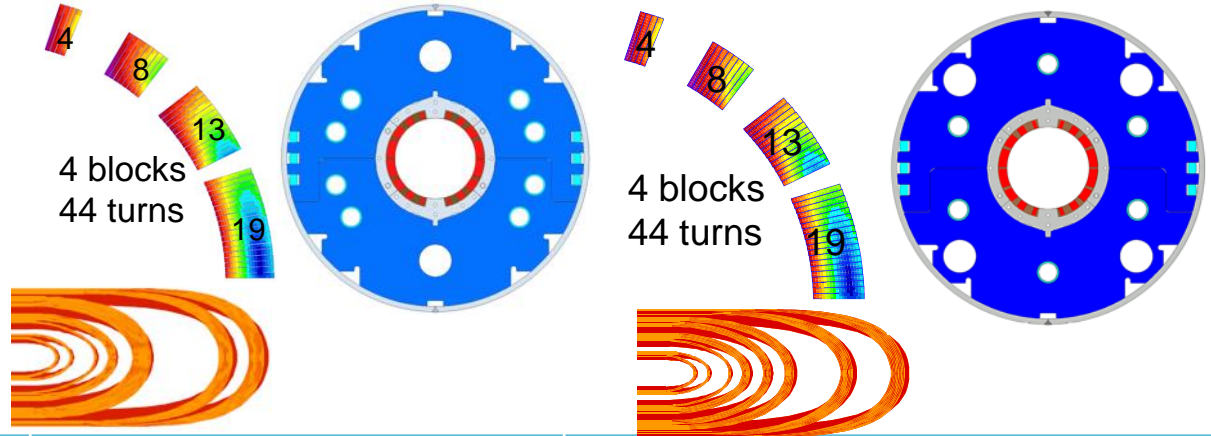


## Azimuthal coil stress at pole (MPa)



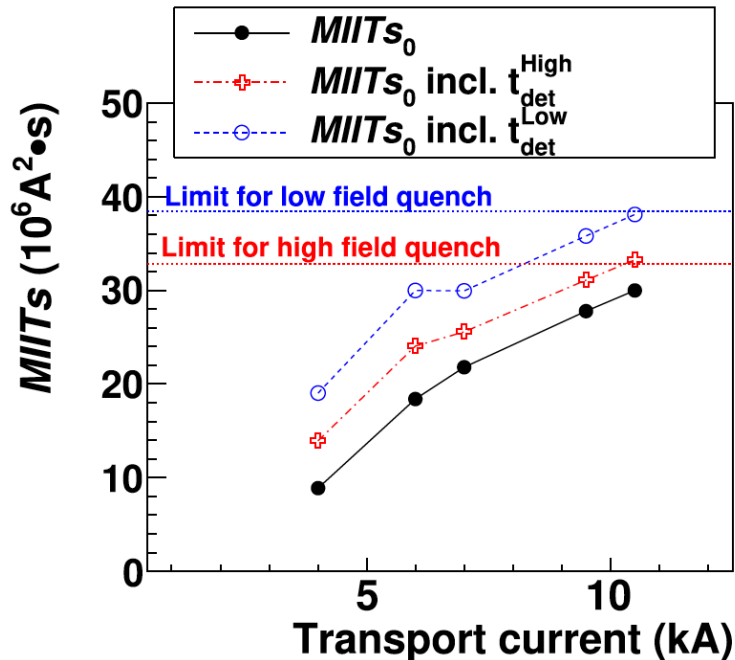
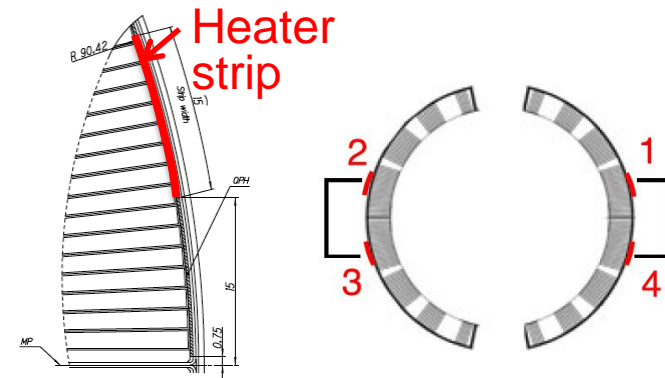
- Pre-stress control is a key factor for good training performance in D1 magnet.

# Design Parameters: 1st vs 2nd Models



Item		MBXFS1, 1b	MBXFS2
Target pre-stress / load	lateral	#1: 80 Mpa, #1b: 110 MPa	115 MPa
	axial	Tightening torque of 12 Nm for four M12 bullets	Tightening torque of 20 Nm for four M12 bullets
Coil	2D	4 blocks (4+8+13+19)	
	Coil end	7 blocks	8 blocks
	Resin	100 % CE (BT-2160RX)	Epoxy + CE (EC-1HB w/ filler)
	length	525,1100,375mm	561.2,1025.5,413.3mm
QPH	straight	zigzag	
Yoke	2 HX holes	4 HX holes	
Cold tube Support	No	Yes	
Nominal Current	12.000 kA	12.047 kA	
Main Field	5.573	5.569	
Coil Peak Field	6.56 T	6.58 T	
Load line ratio	76.3%	76.7%	
Coil Mech. Length (full-scale)	6518 mm	6580 mm	

# Tentative QPH implemented into MBXFS1/1b



- Tentative QPH implemented into MBXFS1/1b could not protect coil at nominal current. New QPH was designed for MBXFS2.

# Quench simulation: Heat balance equation among 'nodes'

$$S_{i,j,k}^p \Delta V_{i,j,k} \frac{T_{i,j,k}^{p+1} - T_{i,j,k}^p}{\Delta t} = q_{i,j,k}^{\text{joule},p} + q_{i,j,k}^{\text{qph},p} + \left[ \left( \frac{T_{i-1,j,k}^p - T_{i,j,k}^p}{R_{i-1 \rightarrow i}^p} \frac{T_{i+1,j,k}^p - T_{i,j,k}^p}{R_{i+1 \rightarrow i}^p} \right) + \left( \frac{T_{i,j-1,k}^p - T_{i,j,k}^p}{R_{j-1 \rightarrow j}^p} + \frac{T_{i,j+1,k}^p - T_{i,j,k}^p}{R_{j+1 \rightarrow j}^p} \right) + \left( \frac{T_{i,j,k-1}^p - T_{i,j,k}^p}{R_{k-1 \rightarrow k}^p} + \frac{T_{i,j,k+1}^p - T_{i,j,k}^p}{R_{k+1 \rightarrow k}^p} \right) \right]$$

$S_{i,j,k}$ : Volumetric specific heat (J/m<sup>3</sup>/K)

$\Delta V_{i,j,k}$ : Volume (m<sup>3</sup>)

$q_{i,j,k}^{\text{joule}}$ : Joule heat (J)

$q_{i,j,k}^{\text{qph}}$ : Heat input from QPH (J)

$R$ : Thermal resistance (m/W)

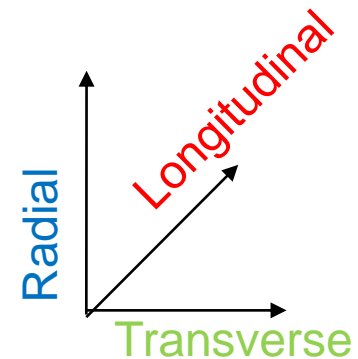
Index  $p$ : time evolution

## In case of D1 magnet:

- $i-1$  ( $i+1$ )  $\rightarrow$   $i$  : Longitudinal direction (**current direction**)
- $j-1$  ( $j+1$ )  $\rightarrow$   $j$  : Transverse direction (**turn-to-turn propagation**)
- $k-1$  ( $k+1$ )  $\rightarrow$   $k$  : Radial direction (**layer-to-layer propagation**)

### **Strategy on the simulation: as realistic as possible**

- Geometry : position, contact material
- Magnetic field
- Coil inductance etc.

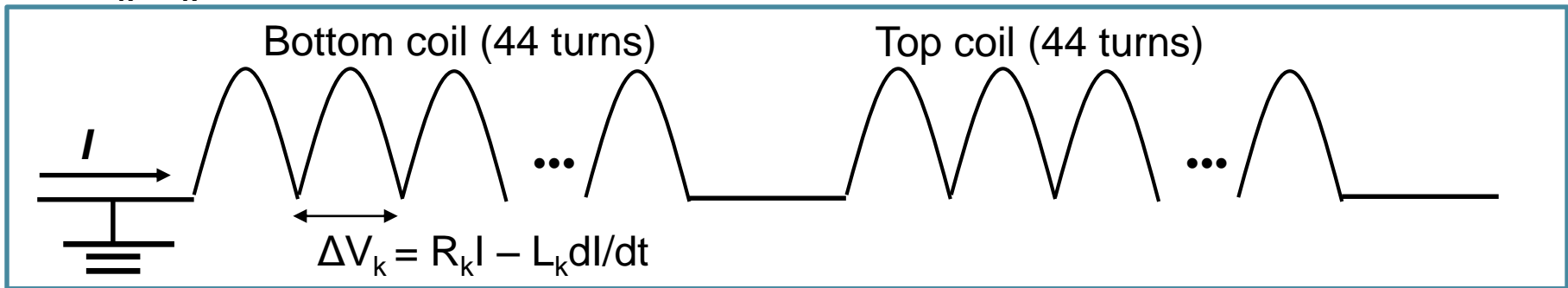


Current

Kento Suzuki, D1 magnet review 2017

# Estimation of the maximum voltage to ground for the 7m-long magnet

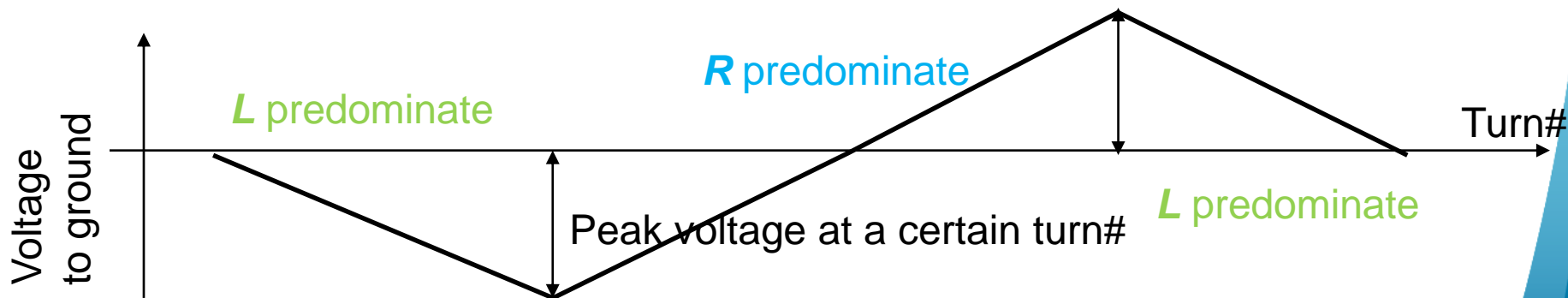
Resistance and mutual inductance are computed for each turn  
 ( $R_k, L_k$ :  $k$ =turn#, 88 turns in total)



Then sum the voltage drops ( $\Delta V_k$ ) until  $X$  turns :

$$V_{\text{to ground}}(X) = \sum_{k=1}^{k=X} \Delta V_k$$

index  $k$  : turn# (1-88)



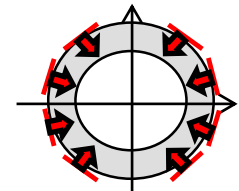
We can seek the maximum  $V$  by sweeping  $X$  for each time step

We define the highest  $V_{\text{to ground}}(X)$  as the maximum voltage to ground at quench

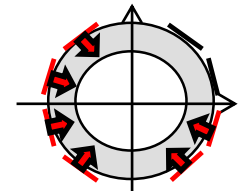
# Calculated total MIITs

Failure cases

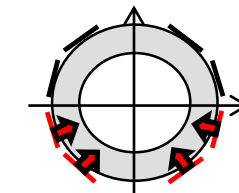
	MIITs (after shutting of the current)	Expected total MIITs (incl. detection time and simulation uncertainty: $\Delta$ MIITs=3)	
		HF quench (5T) - limit: <b>32.1</b> -	LF quench (1T) - limit: <b>36.9</b>
<b>Nominal ( I = 12047A)</b>			
Success	23.5	<b>29.6 (249 K)</b>	<b>35.0 (259 K)</b>
Failure case1	25.1	<b>31.2 (281 K)</b>	<b>36.6 (293 K)</b>
Failure case2	28.2	<b>34.3 (357 K)</b>	<b>39.8 (375 K)</b>
Failure case3	27.3	<b>33.4 (333 K)</b>	<b>38.9 (350 K)</b>
<b>Ultimate ( I = 13280A)</b>			
Success	24.3	<b>30.4 (264 K)</b>	<b>35.8 (275 K)</b>
Failure case1	26.0	<b>32.1 (300 K)</b>	<b>37.5 (314 K)</b>
Failure case2	29.2	<b>35.3 (384 K)</b>	<b>40.7 (399 K)</b>
Failure case3	28.2	<b>34.3 (357 K)</b>	<b>39.7 (372 K)</b>



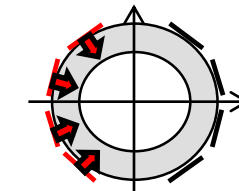
Success



case1



case2



case3

Acceptable

Not acceptable

( ): Hotspot temperature

- Magnet can protect if all four power supplies work successfully.
- Even if one power supply fails to be operated, magnet can be protected.
- Failure of more than two power supplies can lead to magnet damage.

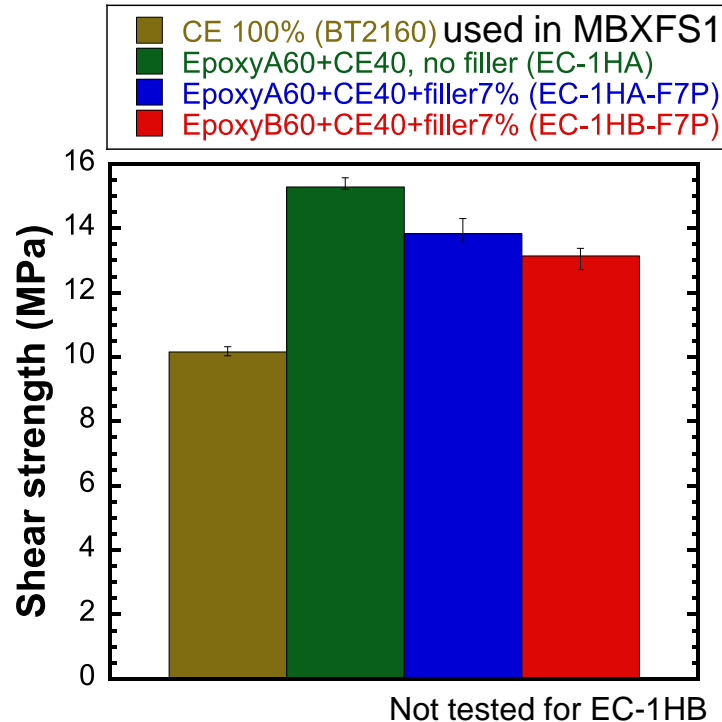
# Appendix

## Fabrication of MBXFS2

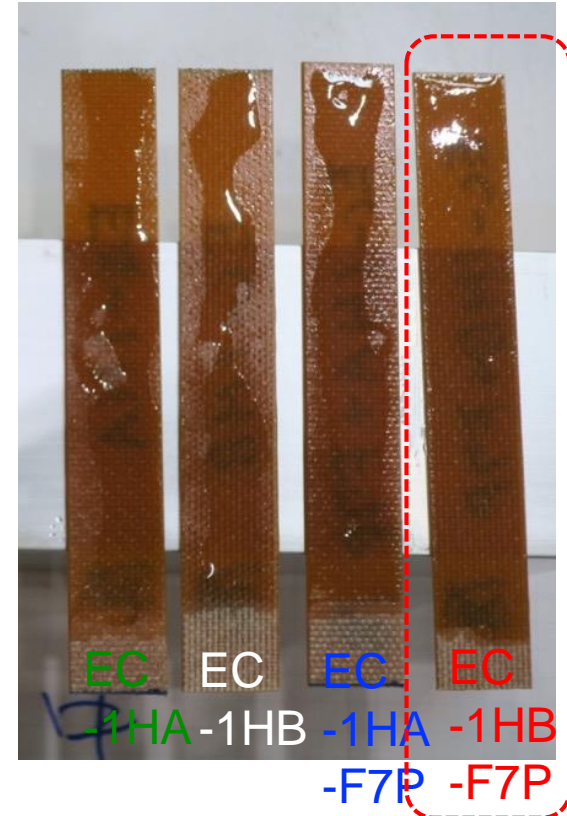


# Wet-winding with epoxy-blended CE resin (A countermeasure against coil end deformation)

## Shear strength



## Painting test



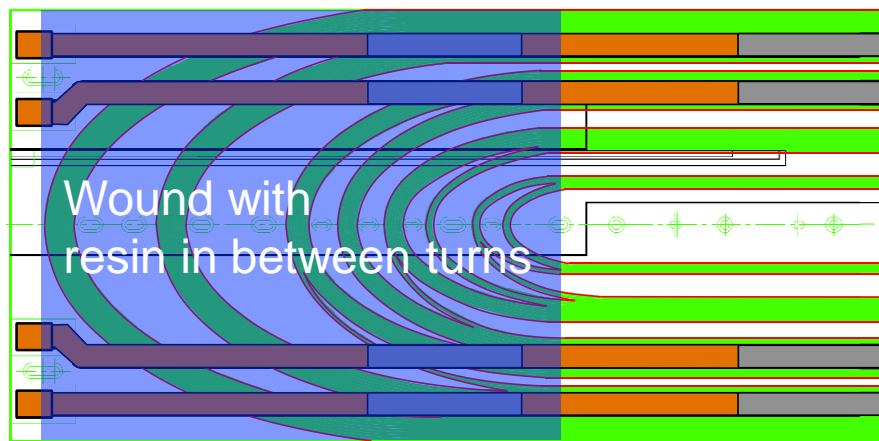
- Four kinds of epoxy-blended CE resins provided from ARISAWA were tested
  - Epoxy : CE = 60 : 40 for all resins
  - Viscosity: lower in epoxy A, higher in epoxy B
  - W or W/O filler (to control viscosity)
- EC-1HB-F7P (Epoxy B + CE + 7wt% Silica filler) was selected from acceptable bonding strength with highest viscosity

# Wet-winding

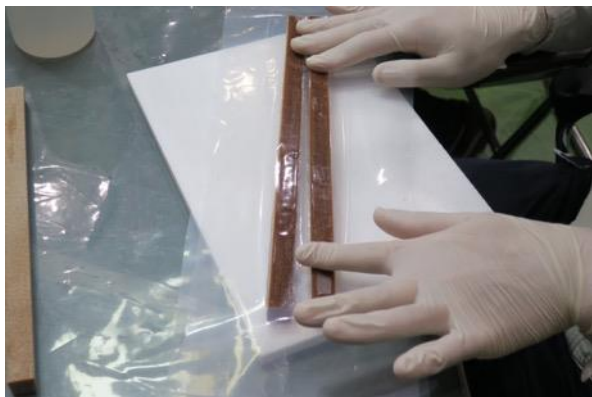
## Cable surface



Coil S2-2, S2-3 used for assembly



## Wedges

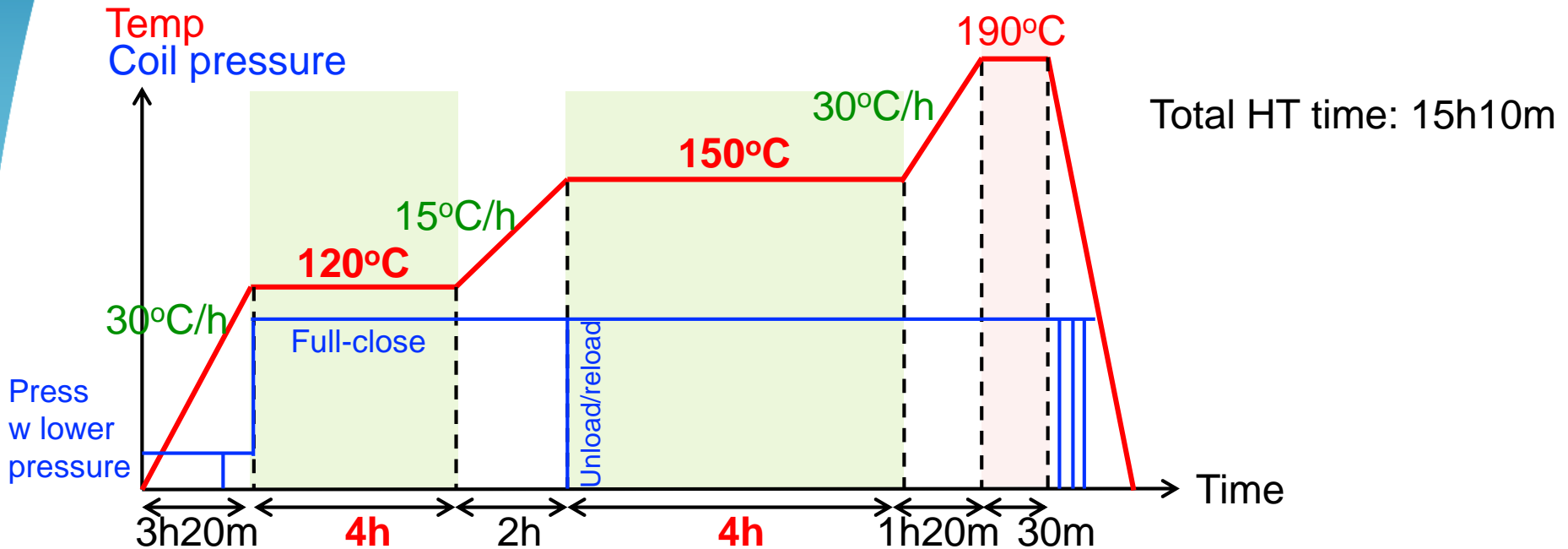


## End spacers



- Minimum amount of resin possible was painted on wedges, end spacers and cable surface to easily release a coil from curing mold and keep the coil surface smooth.

# New curing condition for Coil S2-2 and S2-3



- Curing condition for epoxy-blended cyanate ester: 120°C x 4h + 150°C x 4h
- Self-fusing of polyimide insulation: 190°C x 0.5h
- Coil pressure: lower at RT, while **full-closing at 120°C**

# Coil after curing



- Smooth and clean coil surface after curing
- No detachment of end saddle

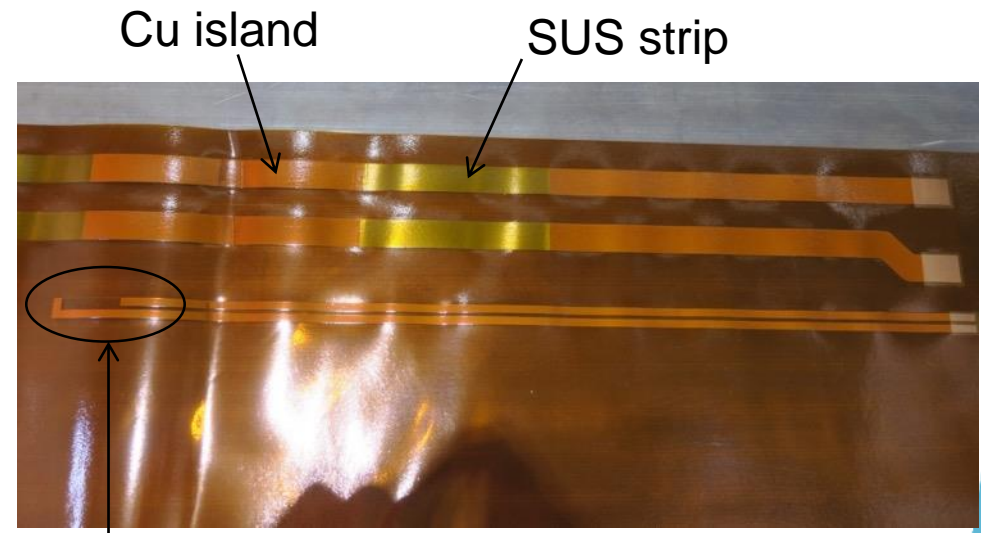
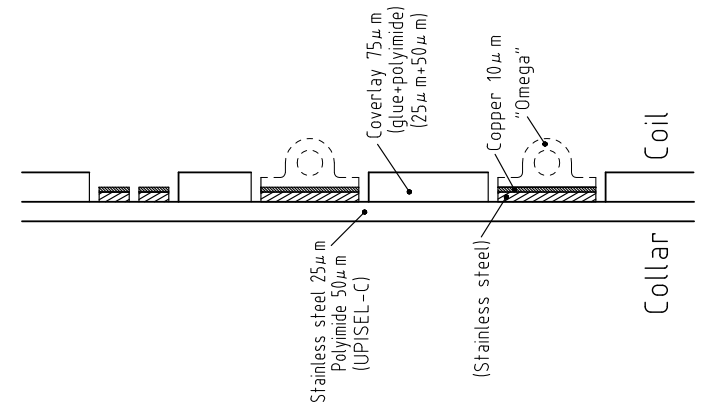
→ Wet-winding was successful

# QPH provided from CERN



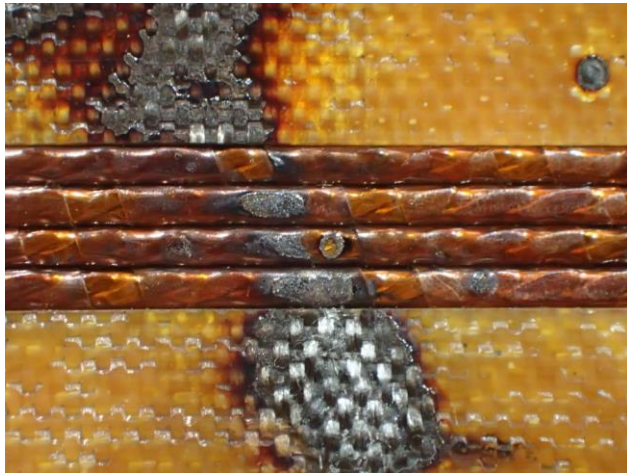
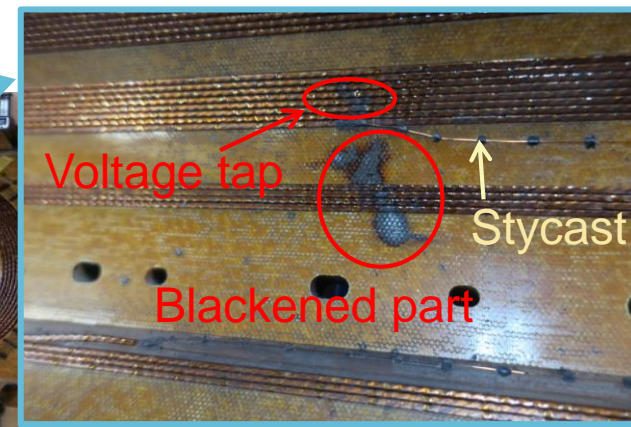
Thanks to Christian Scheuerlein,  
Rui de Oliveira, Andrea Musso

# QPH

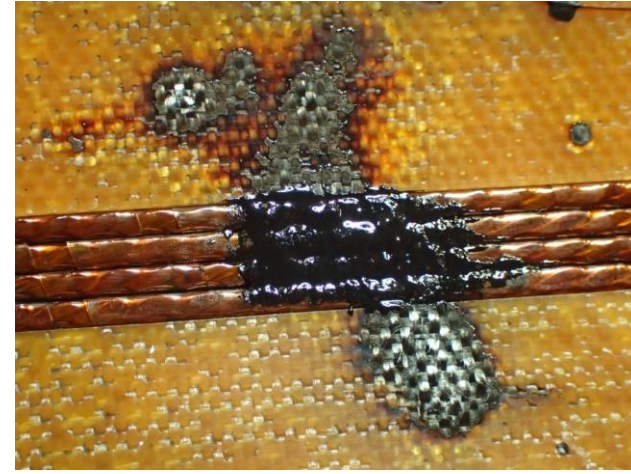


Spot heater

- Two heater strips per quadrant
- Meandering patterns with 25  $\mu$ m SUS strips and 10  $\mu$ m Cu islands
- QPH sheets for MBXFS2 were provided from CERN.

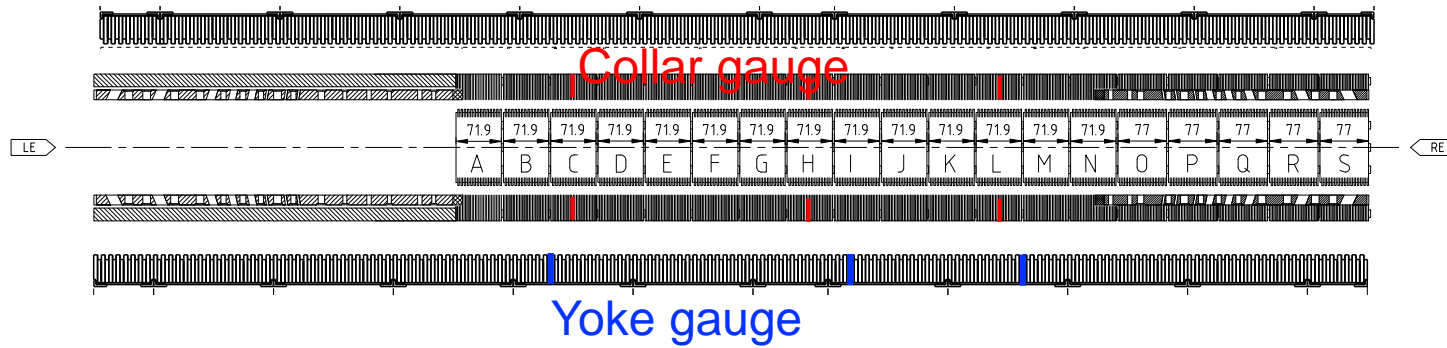


Repair

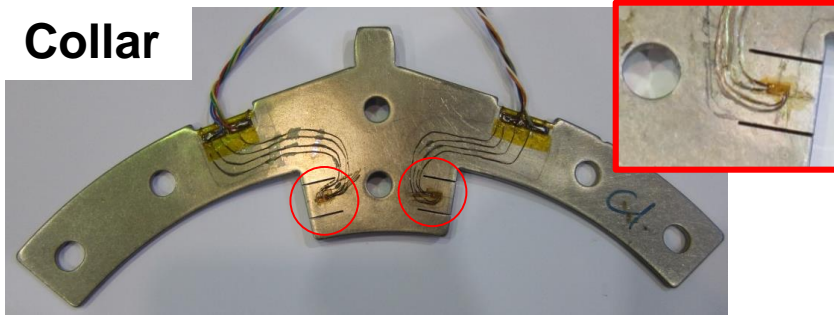


- Coil S2-3 after instrumentation was partly blackened due to insulation test in an incorrect manner by a worker from an outside company.
- After this incident, electrical inspection was performed. As long as we checked coil resistance, inductance and waveform of surge test up to 1 kV, electrical soundness seems to be no problem.
- After discussion with CERN, we reinforced cable insulation with Stycast and decided to use this coil for MBXFS2.

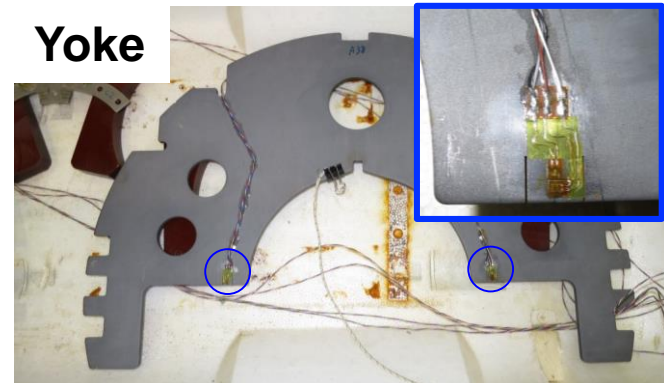
# Strain gauges implemented into MBXFS2



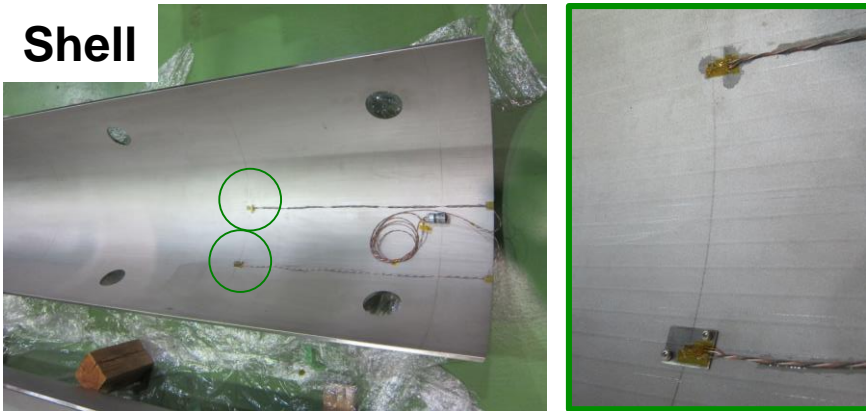
**Collar**



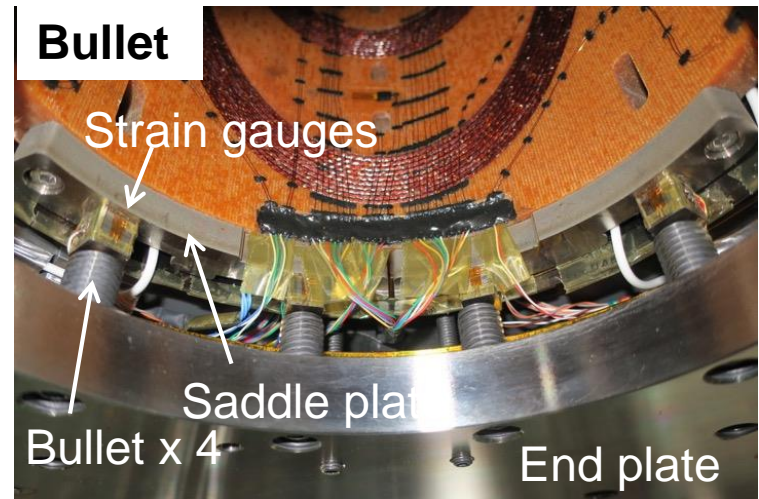
**Yoke**



**Shell**



**Bullet**

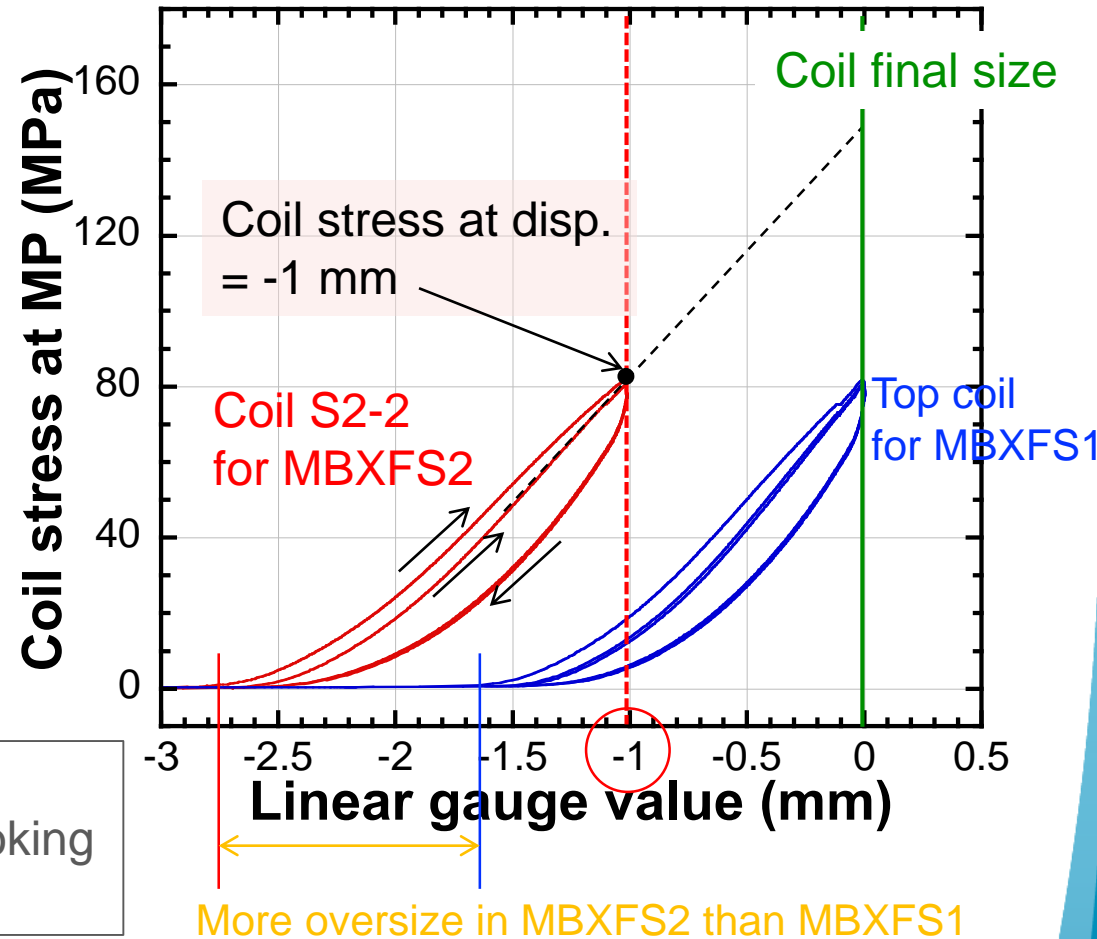


# Coil size measurement



Purposes of coil size measurement

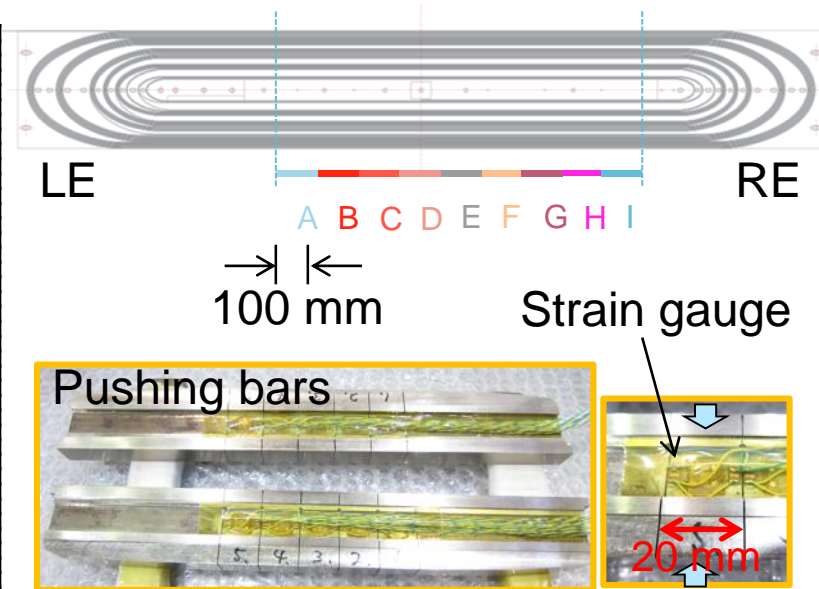
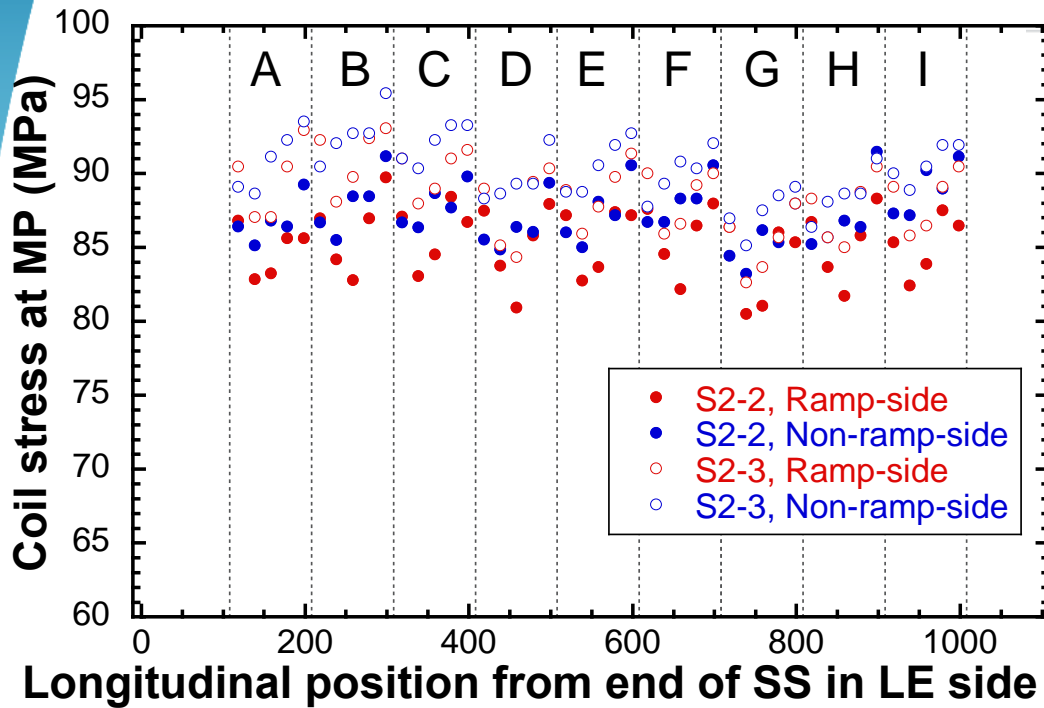
- Prediction of coil pre-stress after yoking
- Homogeneity of coil size over 2 m



- Due to limited load capacity of hydraulic press of 60 ton, coils for MBXFS2 with larger size than MBXFS1 could not be compressed to the final size after yoking.
- Coil stress at MP at the displacement of -1 mm was evaluated and its homogeneity over SS was checked.

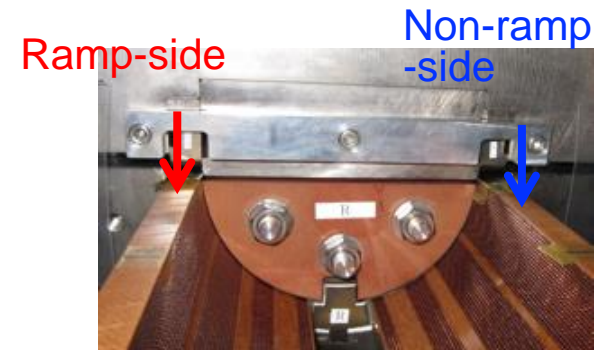


# Variation of coil stress at displacement of -1 mm



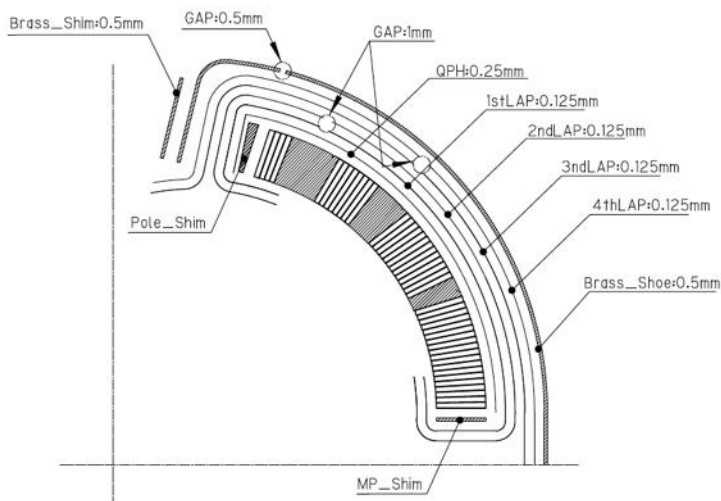
Average coil stress at each quadrant (MPa)

	Ramp-side	Non-ramp-side
Coil S2-2	$85 \pm 2$	$87 \pm 2$
Coil S2-3	$89 \pm 2$	$90 \pm 3$



- Measured only for SS
- Longitudinal distribution of coil stress seems to be OK.

# QPH and insulation wrapping



- QPH (0.15 mmt)+ dummy sheets (0.10 mmt)
- Ground insulation: 0.125 mmt x 4 layers
- Brass shim, brass shoe: 0.5 mm

Bare coil



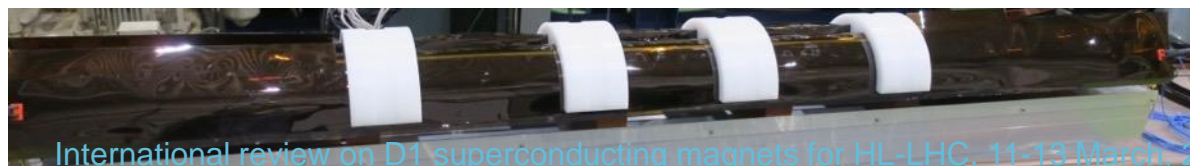
QPH



QPH dummy  
for thickness  
compensation

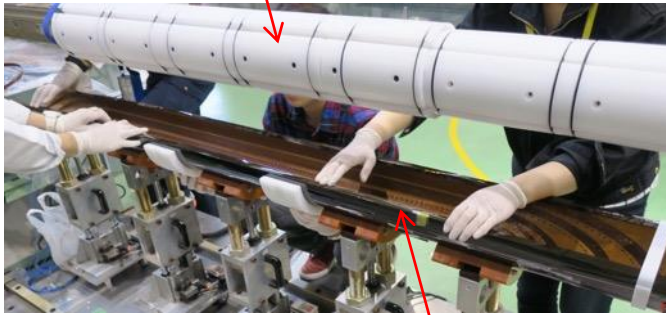


1st, 2nd layer  
of ground insulation



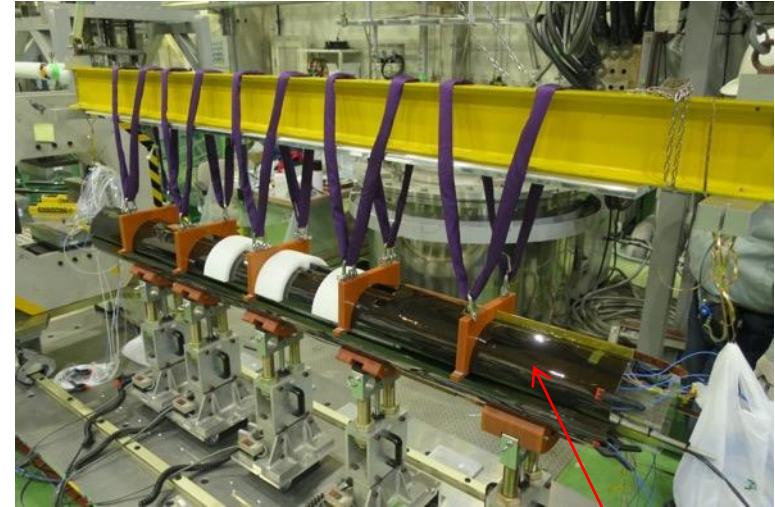
# Insulation wrapping and brass shoe assembly

Collapsible collaring mandrel



Top/Bottom coil assembly

Bottom coil

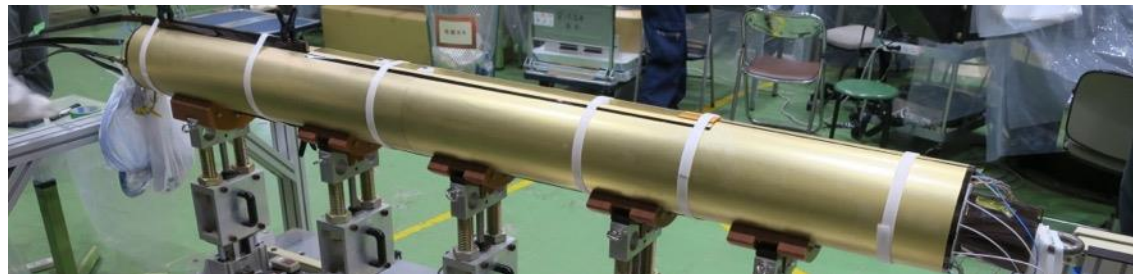


Top coil

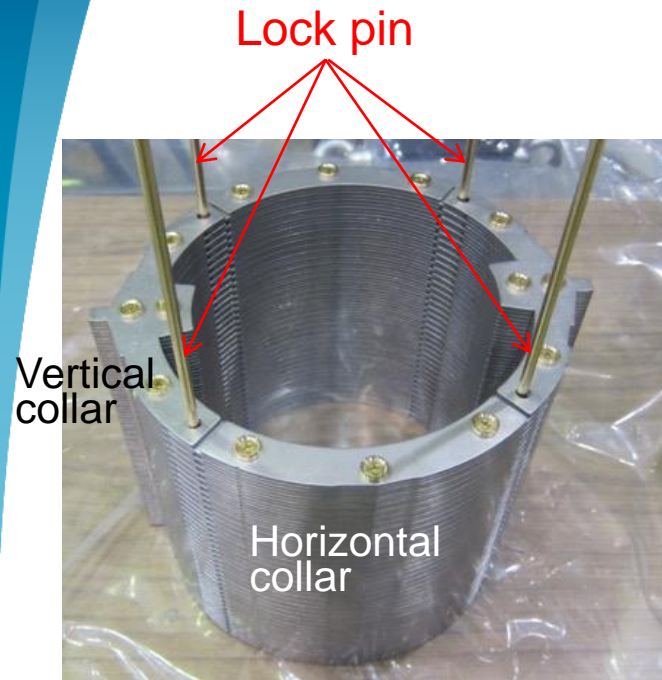
3rd, 4th layer of ground insulation



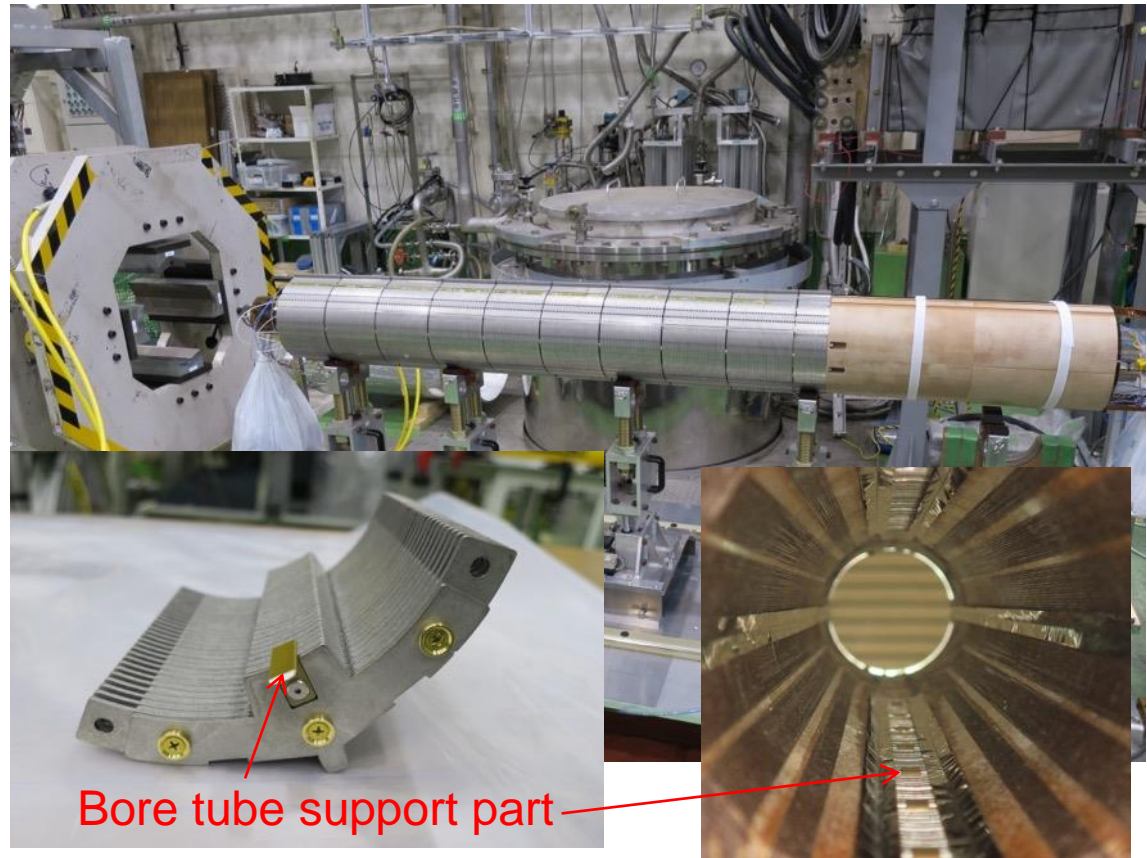
Brass shim, brass shoe



# Collaring with four-split collar



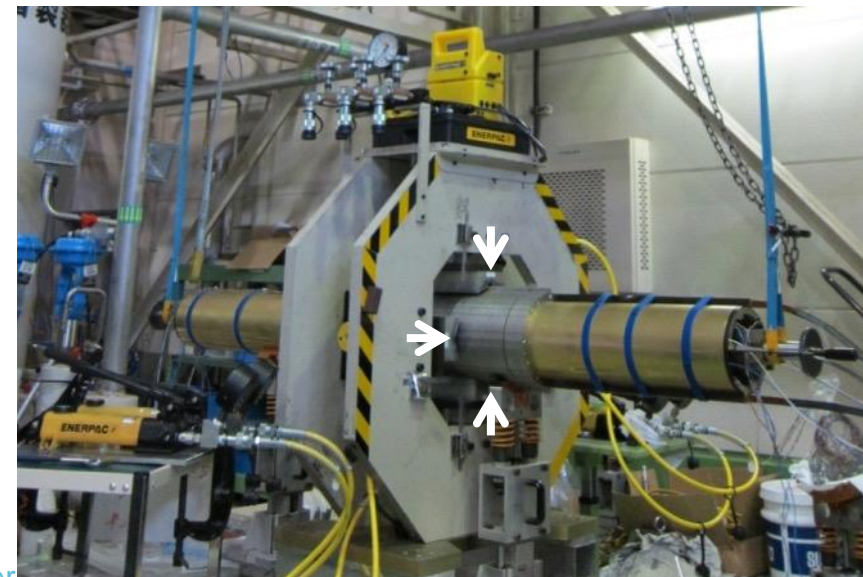
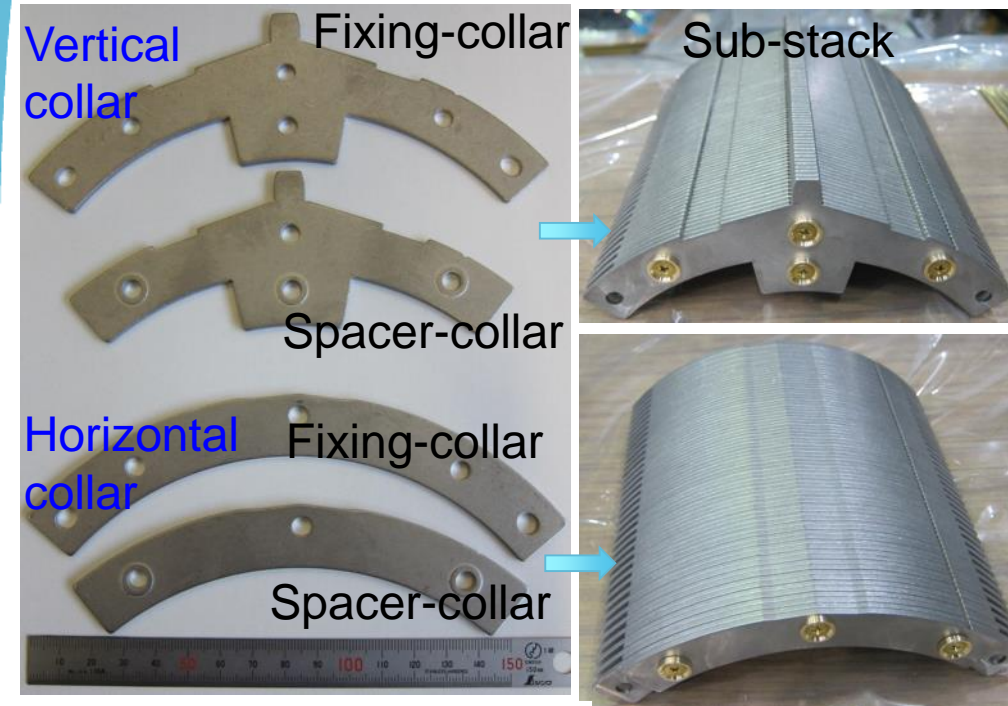
Four-split collar



- Collars fabricated by fine-blanking
- Four-split collars are linked with “lock pins”.
- T-shaped brass parts with polyimide coating were introduced to support beam tube
- **Large impact of larger coil oversize on collaring**
  - Only thinner lock pins could be inserted due to limited load capacity ( $\phi 5.7 \rightarrow \phi 5.2$ )  $\rightarrow$  Larger collared coil diameter

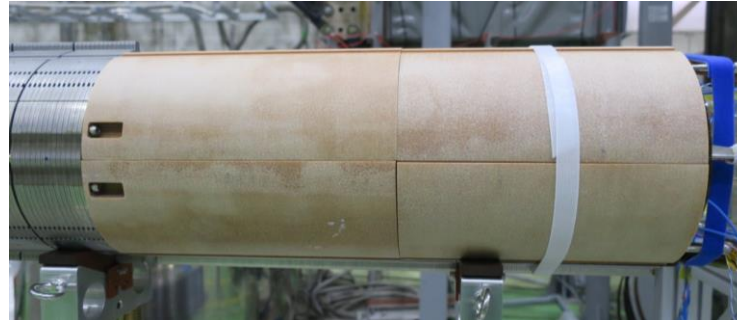
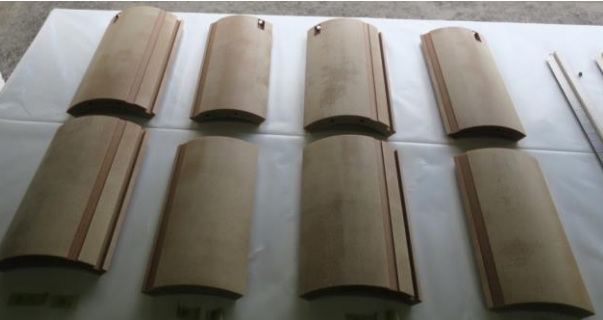
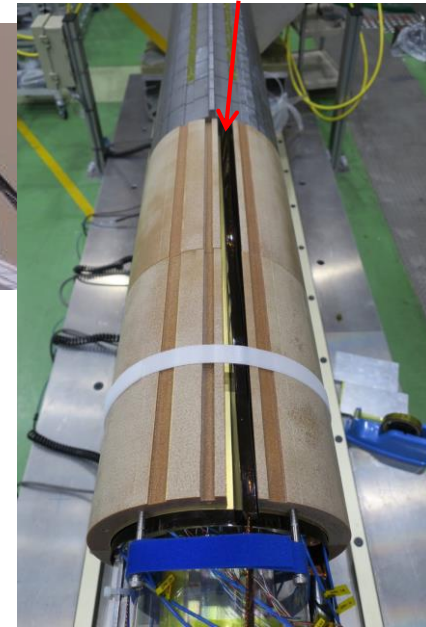
# Collar

- Collar plates were fabricated by fine-blanking.
- Good size accuracy in the critical parts:  $\pm 10 \mu\text{m}$
- Four-way split collar even for a dipole
- Alternate lamination of Fixing- and Spacer-collar (t2.3 mm, t2.6 mm)
- Embossing to control PF to be 96%

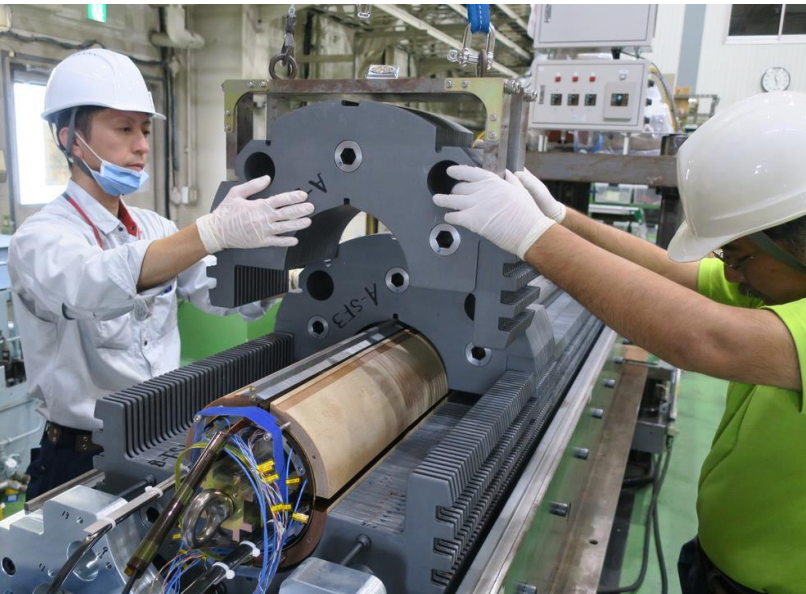


Collar plates fabricated by fine-blanking

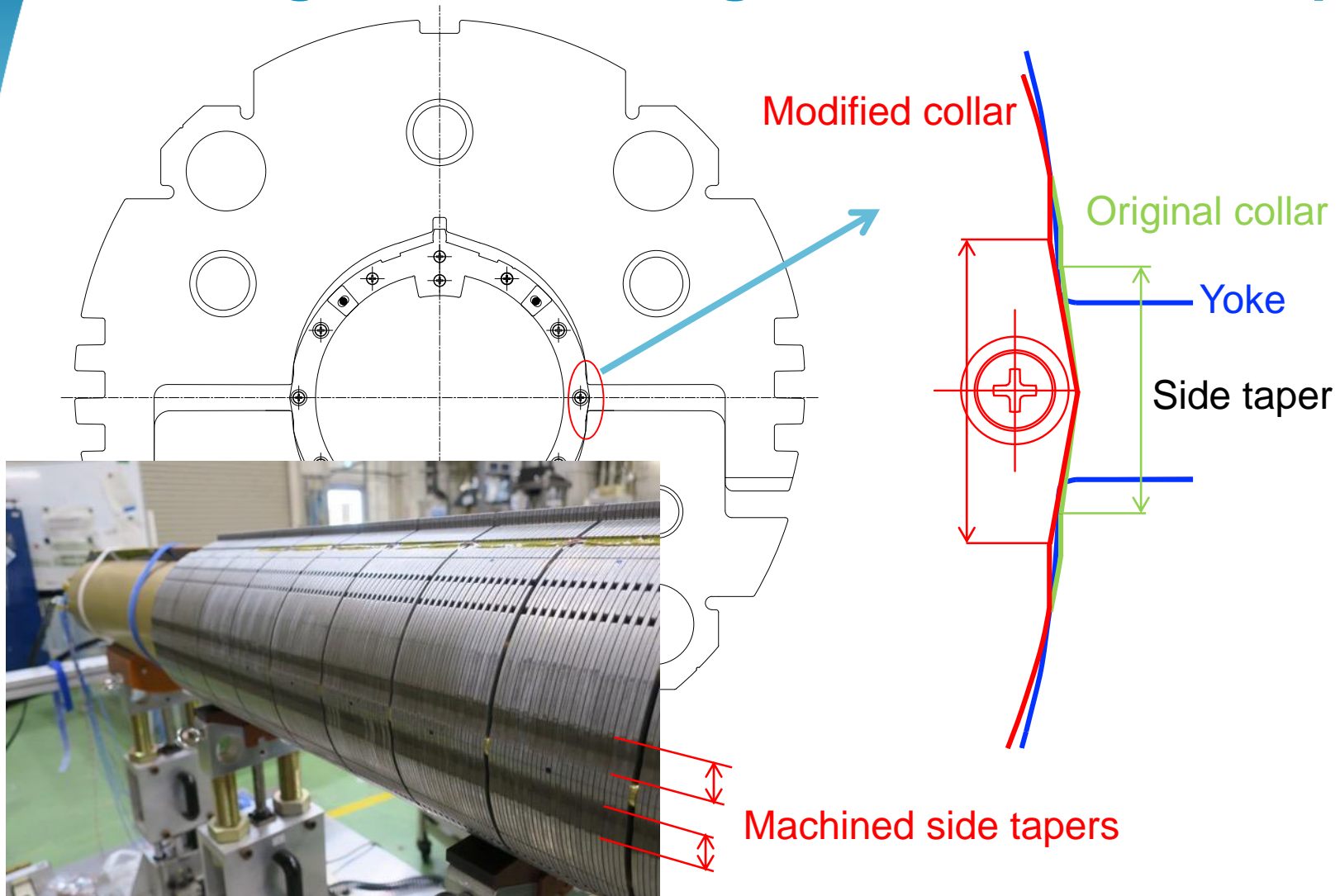
# GFRP collar at LE



- GFRP collar made of BT resin and S2 fiber holds ramp lead.
- Longitudinally two-split, azimuthally four-split structure



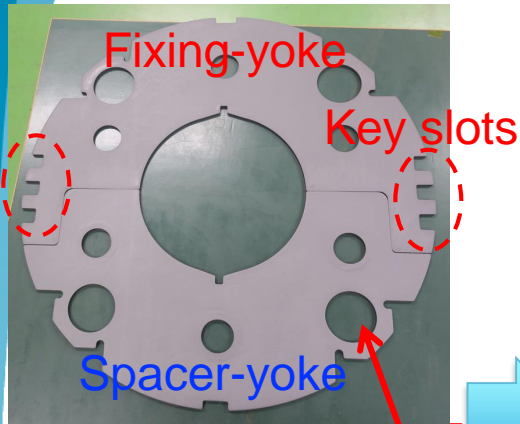
# Enlarged Coil: Change of side collar shape



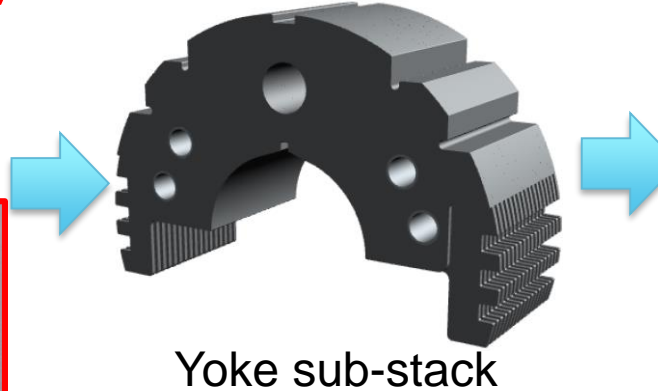
- To cope with a larger collared coil, **side taper in horizontal collar was extended by wire-cutting.**

# Yoke

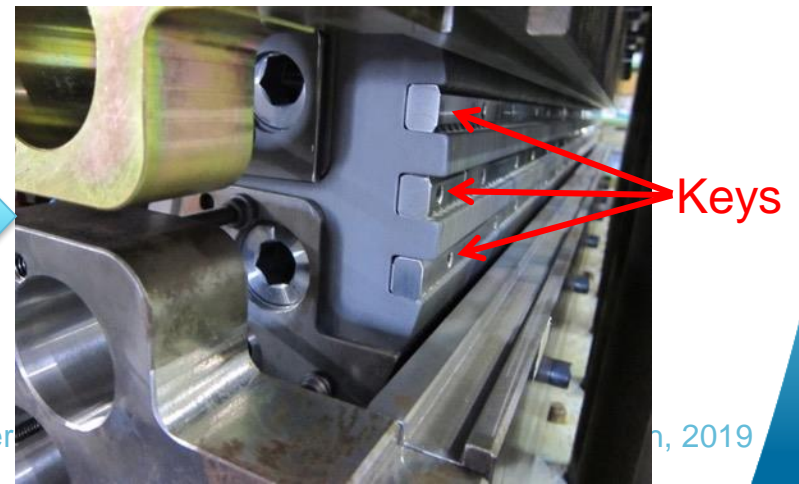
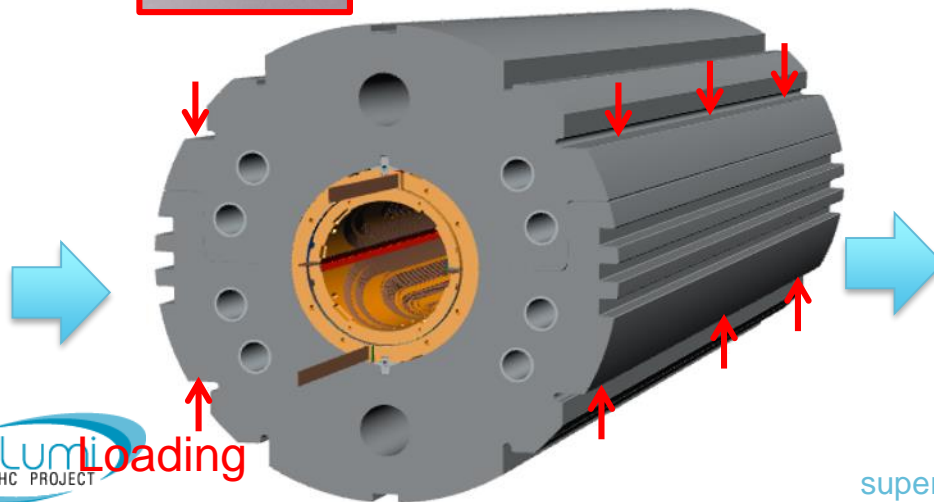
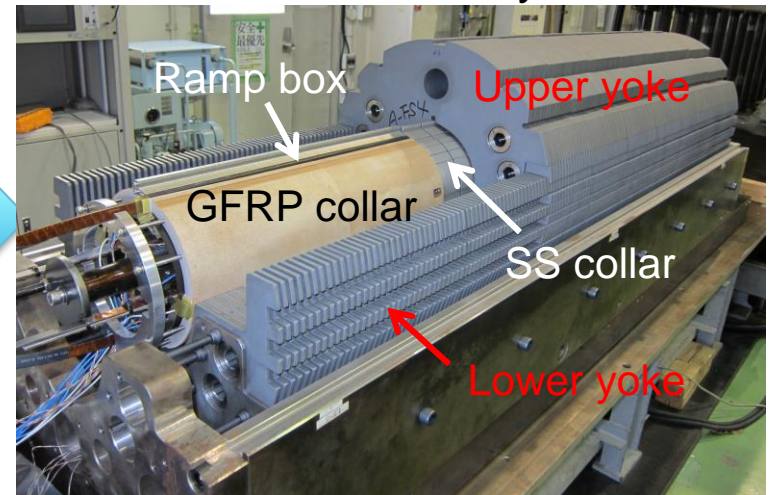
- Yoke plates were fabricated by fine-blanking.
- Alternate lamination of Fixing- and Spacer-yoke (t5.6 mm, t6 mm)
- Embossing in S-yoke to control yoke packing factor to be 98%



0.2 mm-high embossing

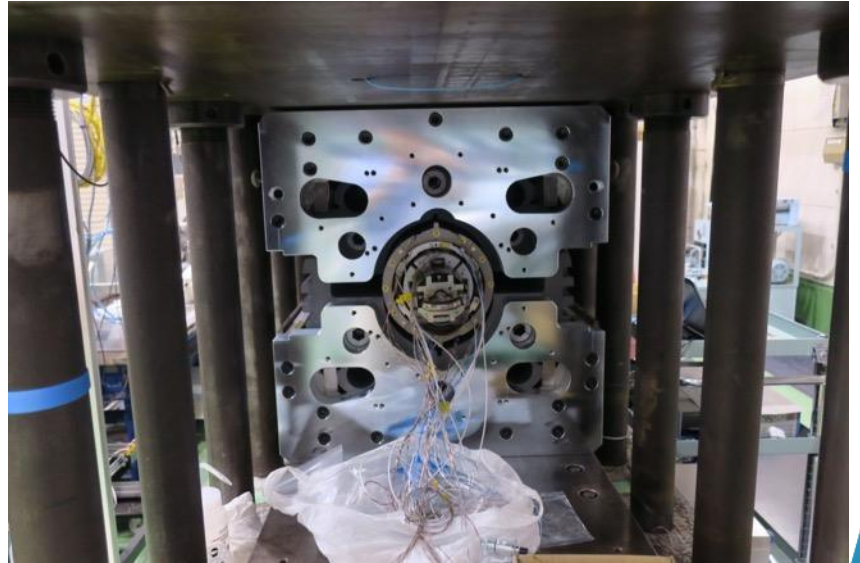


## Yoke assembly

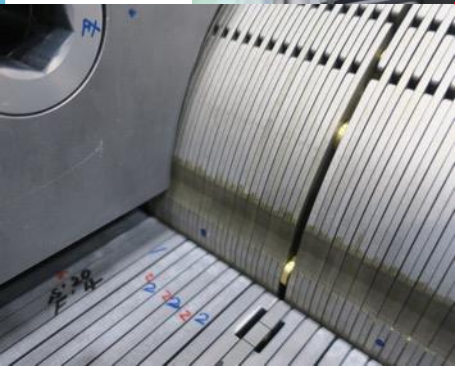
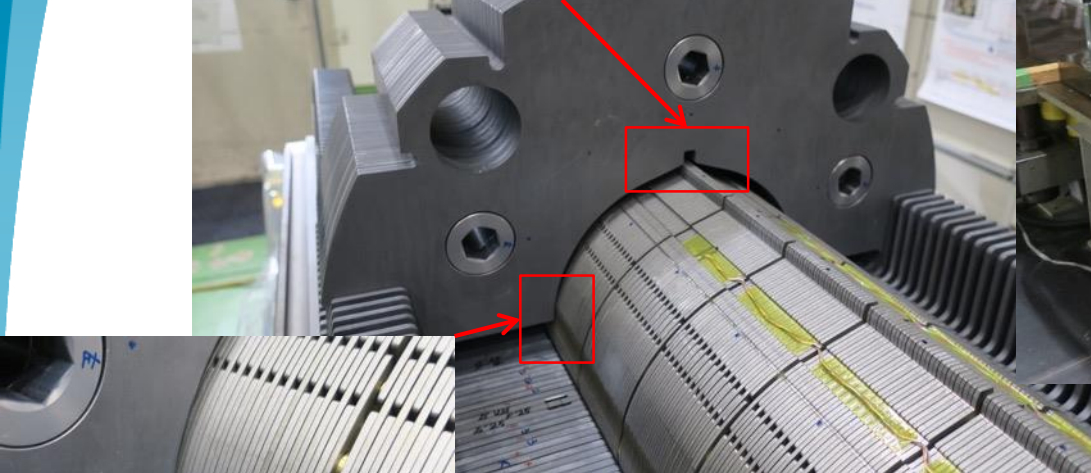
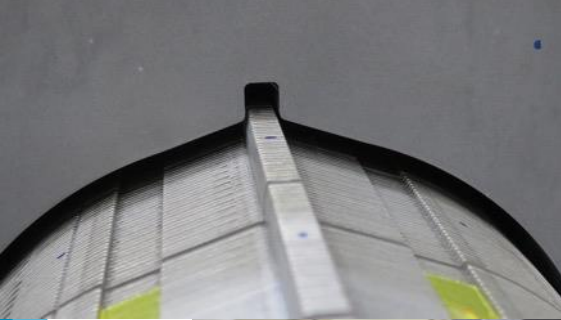




# Preparation for yoking

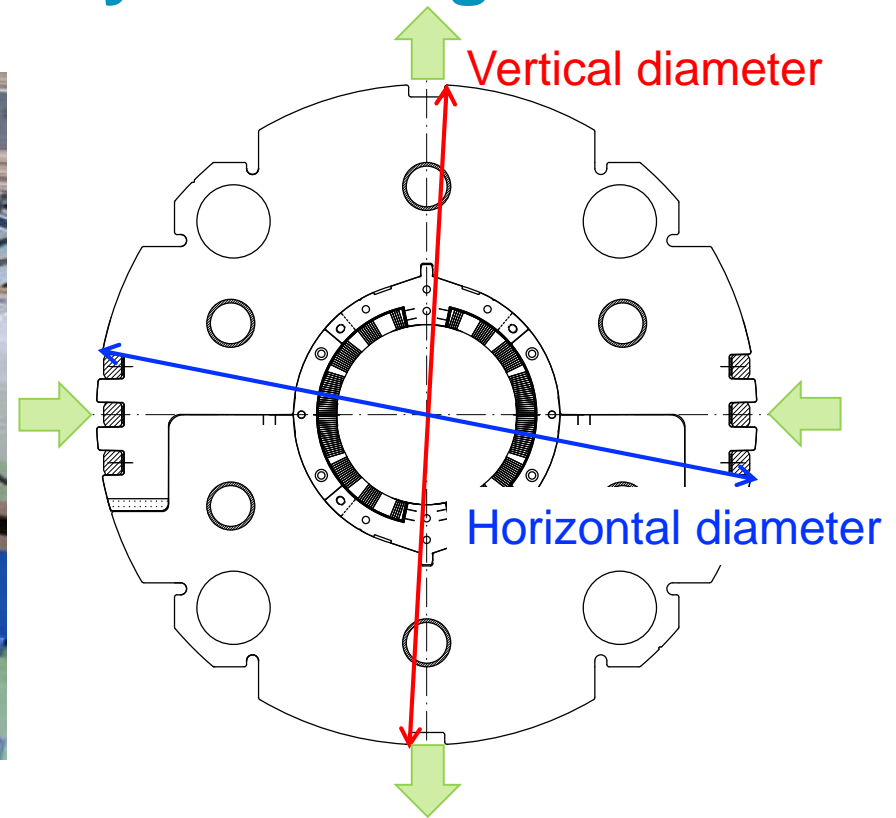
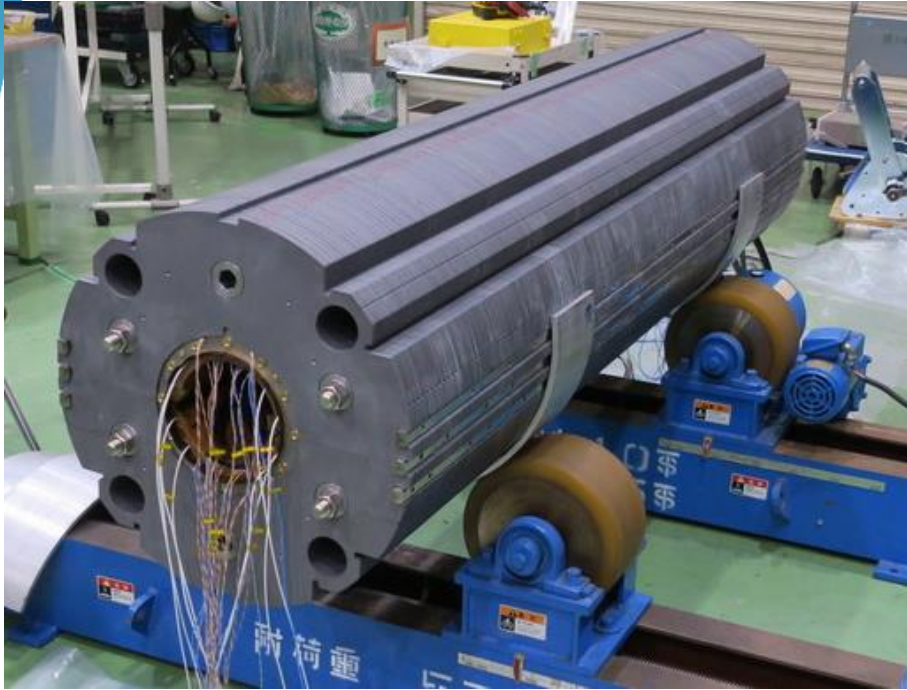


# Yoking



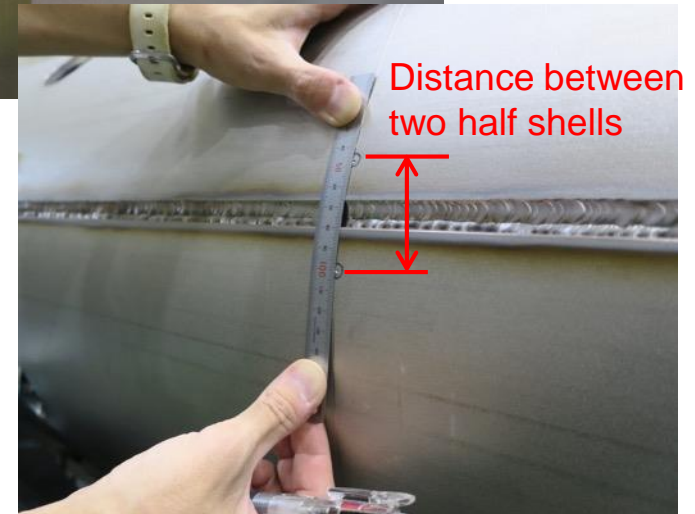
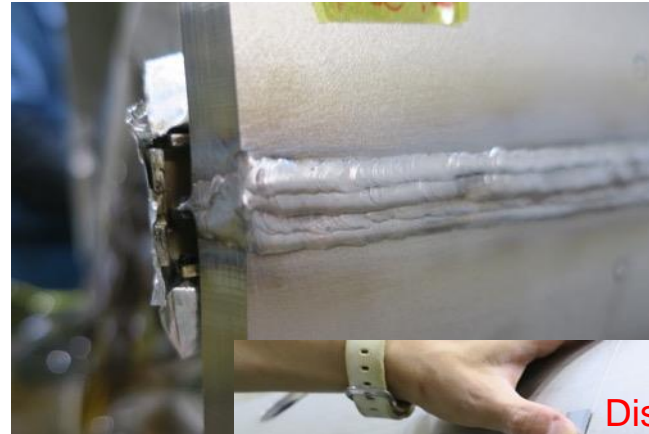
- Modified side collar functioned as expected. Collared coil was properly aligned with respect to yoke.
- Yoking press and key insertion were successful.
- Collapsible collaring mandrel was removed.

# Oval deformation of yoked magnet



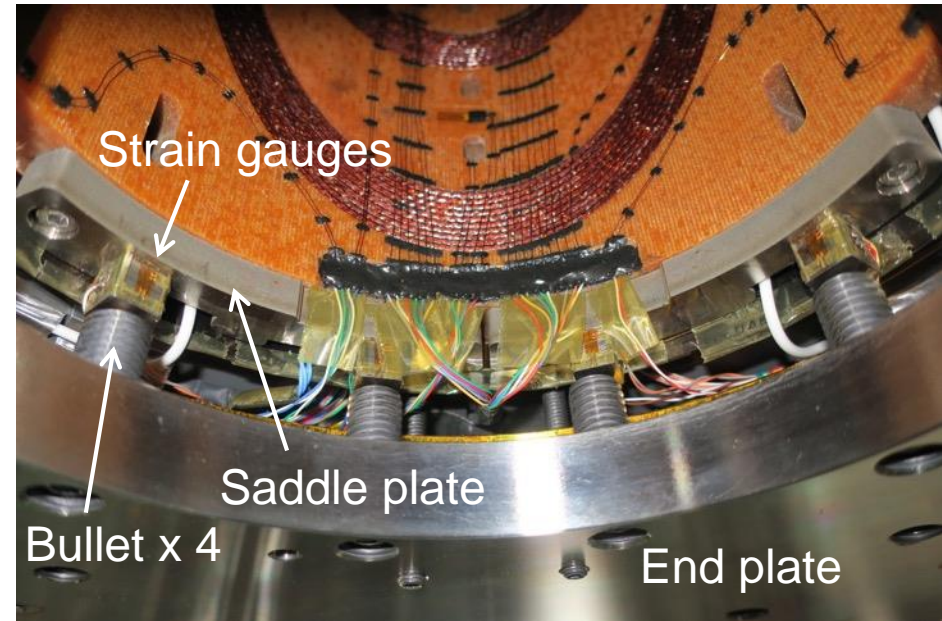
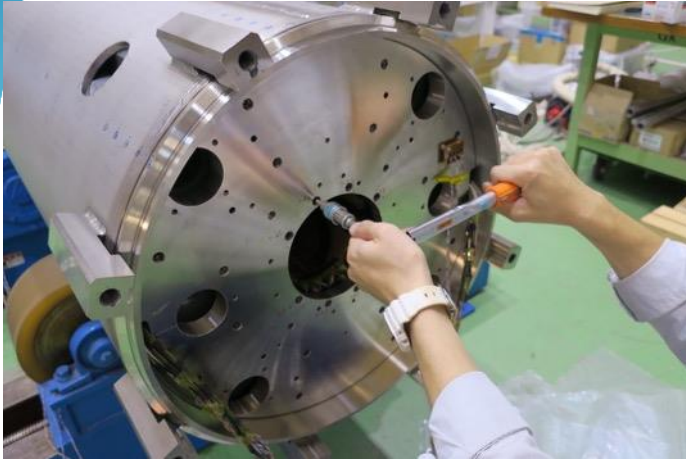
- Outer diameter of yoked magnet was measured using outside micrometer.
- **Oval deformation: 0.3 mm larger vertical diameter** than horizontal diameter
- Influence of oval deformation on field quality is discussed later.

# Shell welding



- Two half shells were manually welded from both sides with 11 passes.
- Azimuthal tensile strain by welding in **MBXFS1b of 0.26%** should be decreased.
- **0.5 mm longer** circumferential length of half shells in MBXFS2  
→ Azimuthal strain could be decreased to **0.17%**.

# Axial pre-load



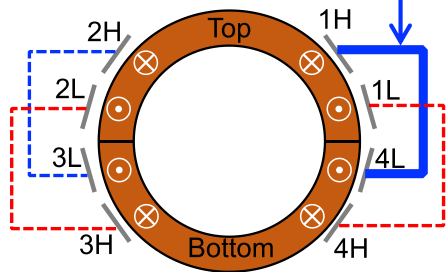
- Axial pre-load was applied with four bullets per coil after end-ring welding
- Material of bullets and saddle plate was replaced from SUS304L to Ti6Al4V to prevent significant plastic deformation
- Tightening torque of M12 bullets:
  - MBXFS1b: 12 Nm >> 53 kN per coil
  - **MBXFS2: 20 Nm >> 88 kN (S.G. meas. 30~43 kN per coil)**

# Appendix

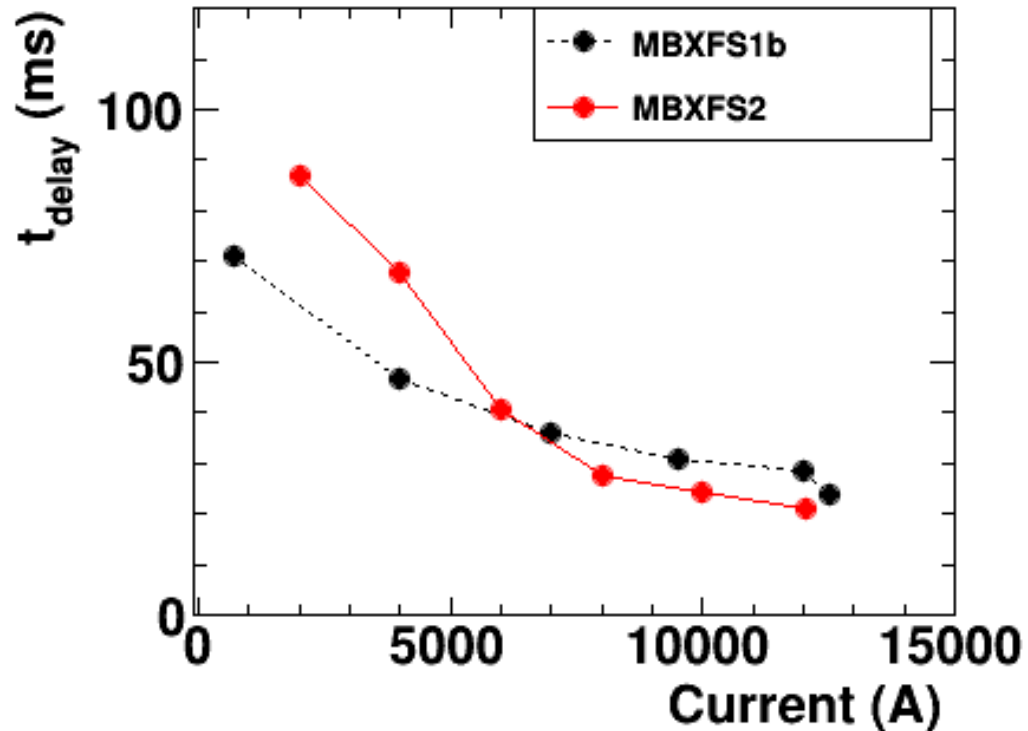
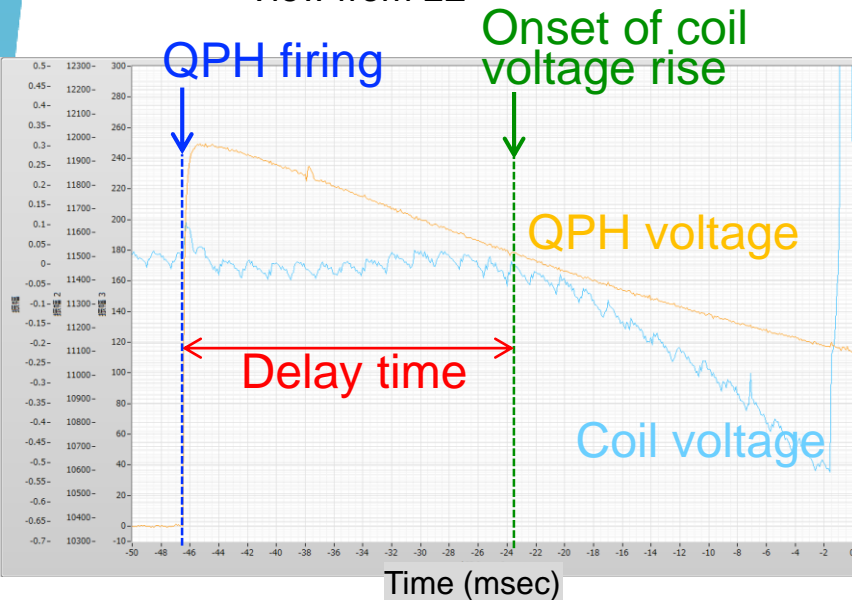
## Test result of MBXFS2

# Delay time

Only this pair of strips was fired



View from LE



- Delay time was evaluated by firing only one pair of heater strips with a 50 mΩ dump resistor.
- Delay time was defined as  $\Delta t = t_{\text{onset of voltage rise}} - t_{\text{QPH firing}}$
- Shorter delay time was obtained above 7 kA in MBXFS2 than MBXFS1b.

# Quench start location

## MBXFS1

	CB1	CB2	CB3	CB4	Splice
Top	0	8	4	0	1
Bottom	3	14	3	1	0
Both	0	2	0	0	0

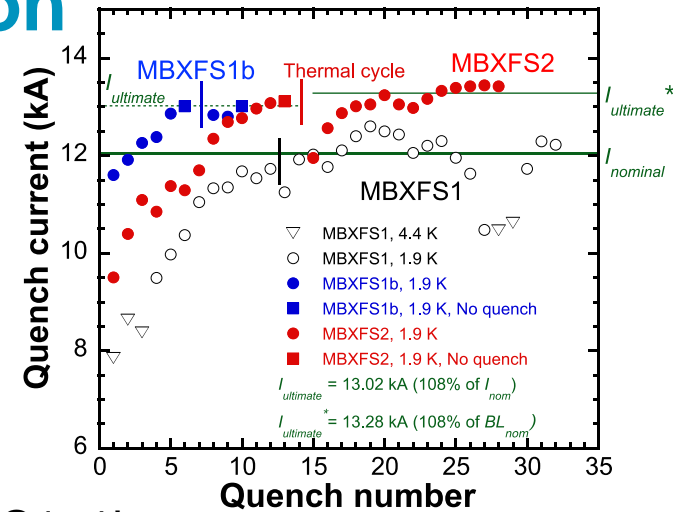
## MBXFS1b

	CB1	CB2	CB3	CB4
Top	5	0	5	0
Bottom	2	2	6	0

## MBXFS2

	CB1	CB2	CB3	CB4
Top	2	1	7	7
Bottom	1	3	4	5

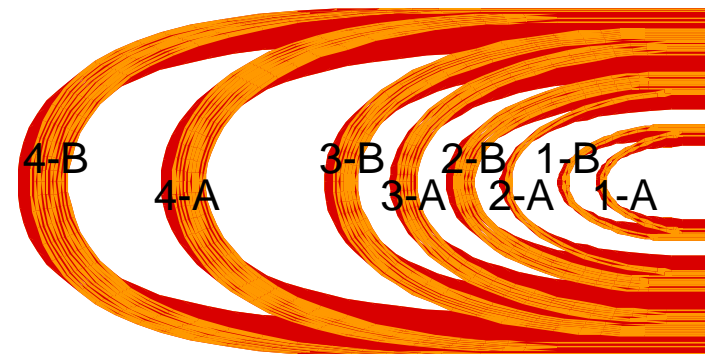
- Compared to MBXFS1/1b, quench started more frequently at high field regions (CB3 and CB4) in MBXFS2.



## MBXFS1, 1b

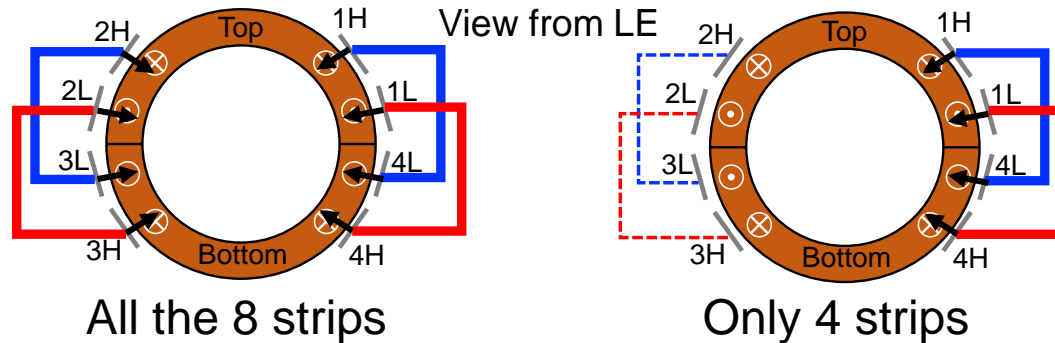
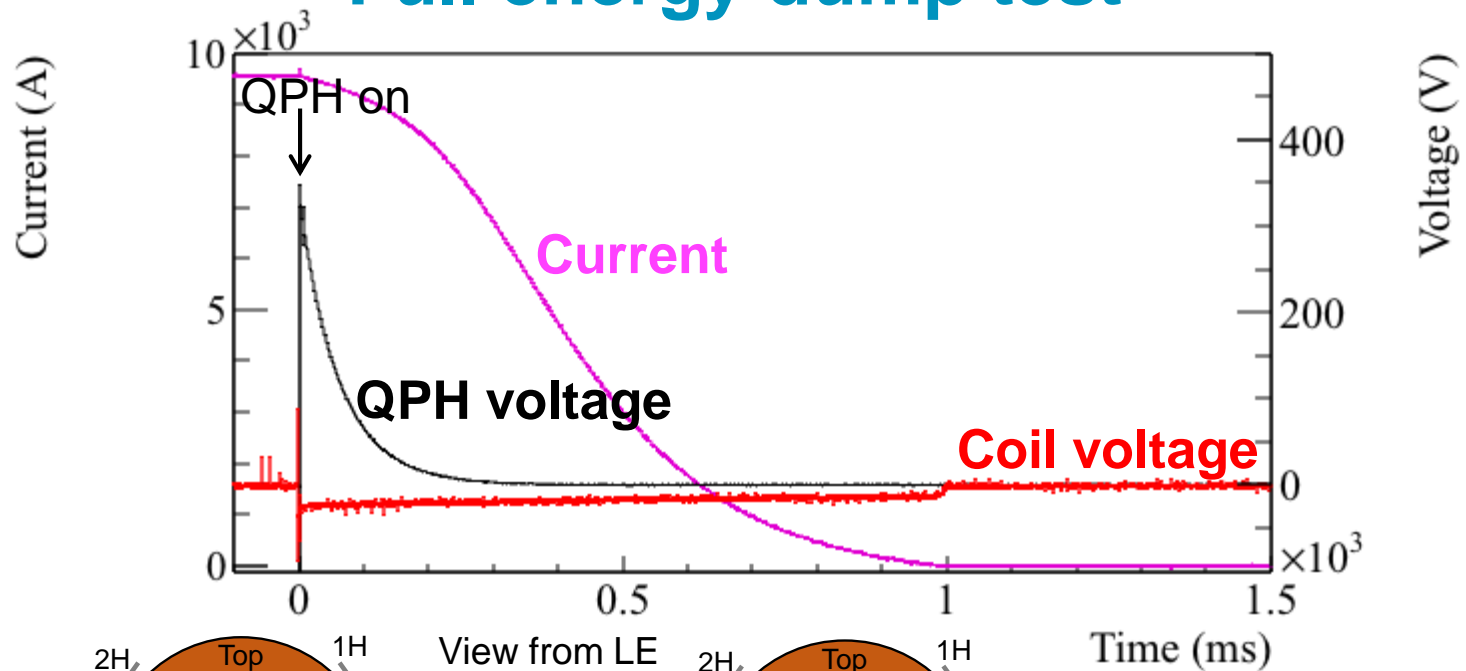


## MBXFS2





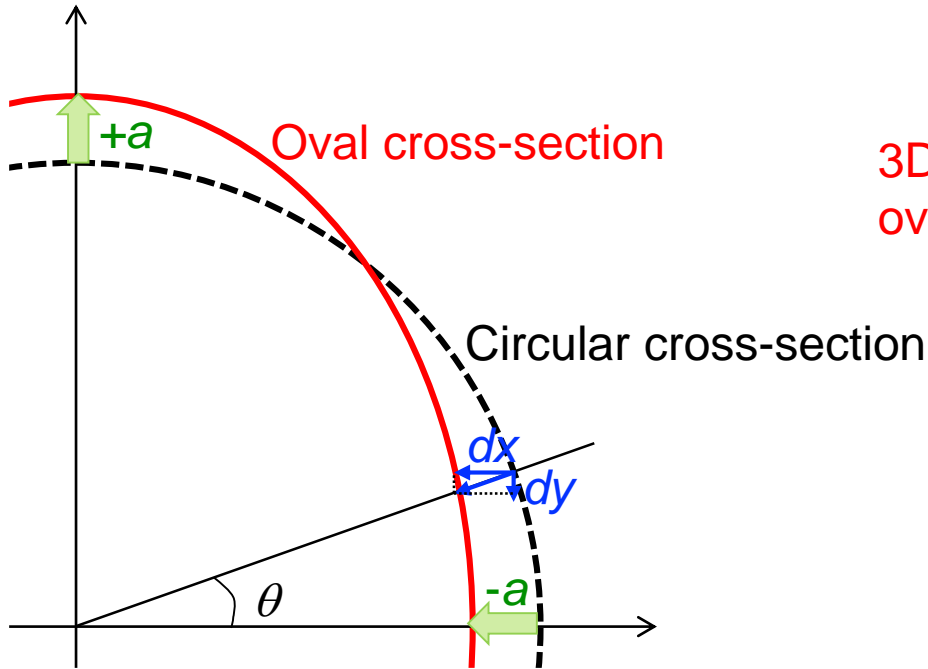
# Full energy dump test



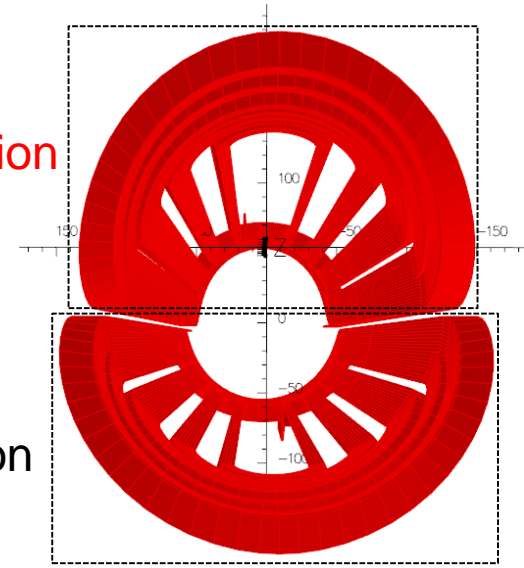
- Full energy dump test was conducted without a dump resistor.
- Two cases in which 8 or 4 heater strips are fired
- MIITs was estimated by taking the integral of the magnet current from  $t_{\text{QPHon}}$  (time at which QPH is fired)

$$\text{MIITs}^1 = \int_{t_{\text{QPHon}}}^{\infty} I^2 dt$$

# Field calculation with coils with oval deformation



3D model with oval cross-section



Circular cross-section

- 3D field calculation with coils deformed in an oval shape was done using OPERA 3D.
- Cable was displaced from the original position along the following equation.

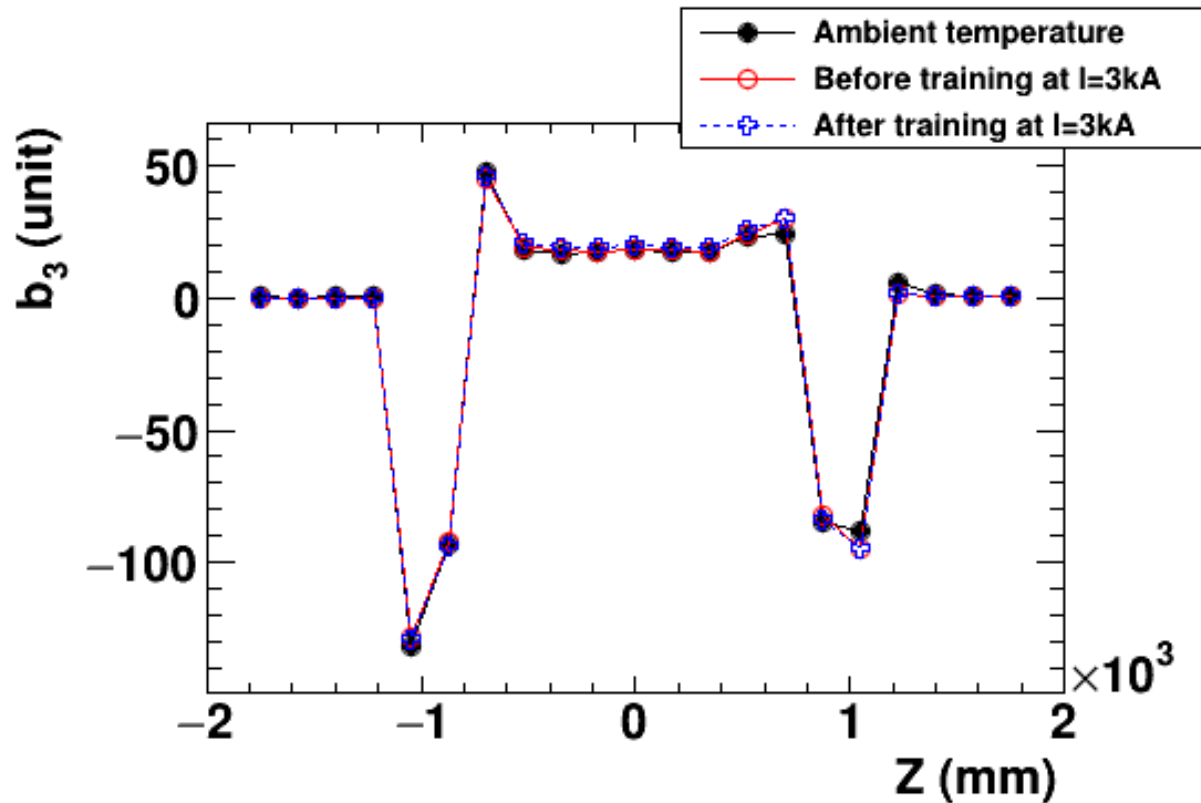
$$dx = -a \cos(2\theta) \cos\theta$$

$$dy = -a \cos(2\theta) \sin\theta$$

$a$ :  $1/4 \times$  (vertical coil ID – horizontal coil ID)

- We assumed b3 offset is caused only by coil oval deformation. The adjustable parameter,  $a$ , was determined to reproduce measured field quality for MBXFS2.

## b3 before and after cooling-down



- Warm magnetic field measurement was performed at  $I = 5$  A before the 1st test cycle.  $b_3$  offset by 18 unit is already observed.

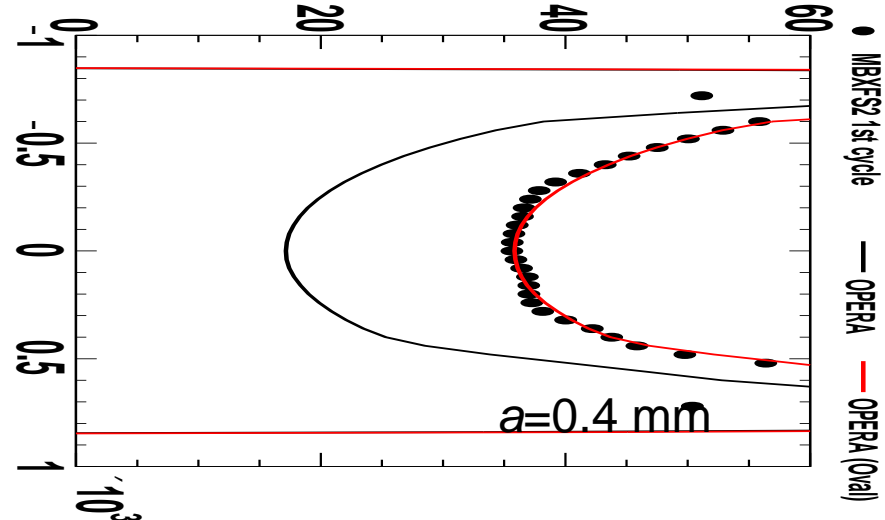
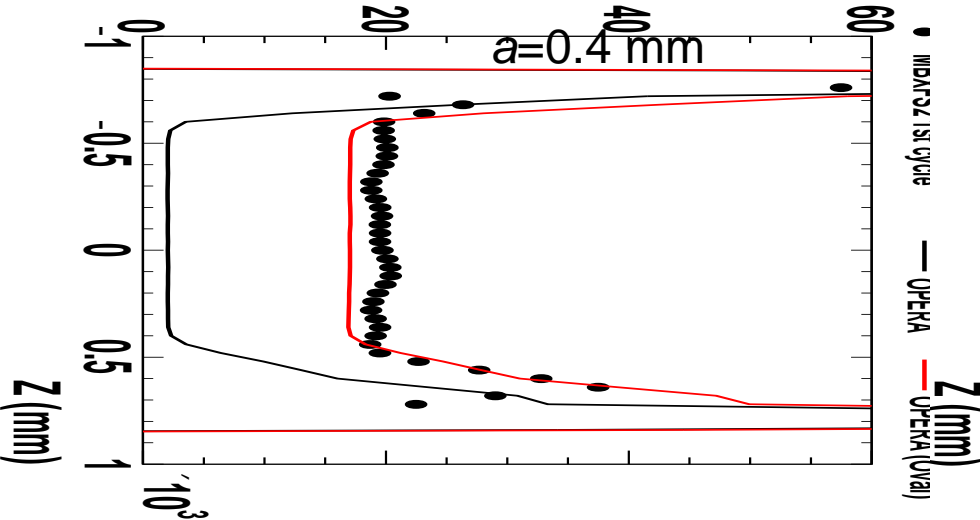
# b3 in straight section

$I=3$  kA

$b_3$  (unit)

$I=12.05$  kA

$b_3$  (unit)



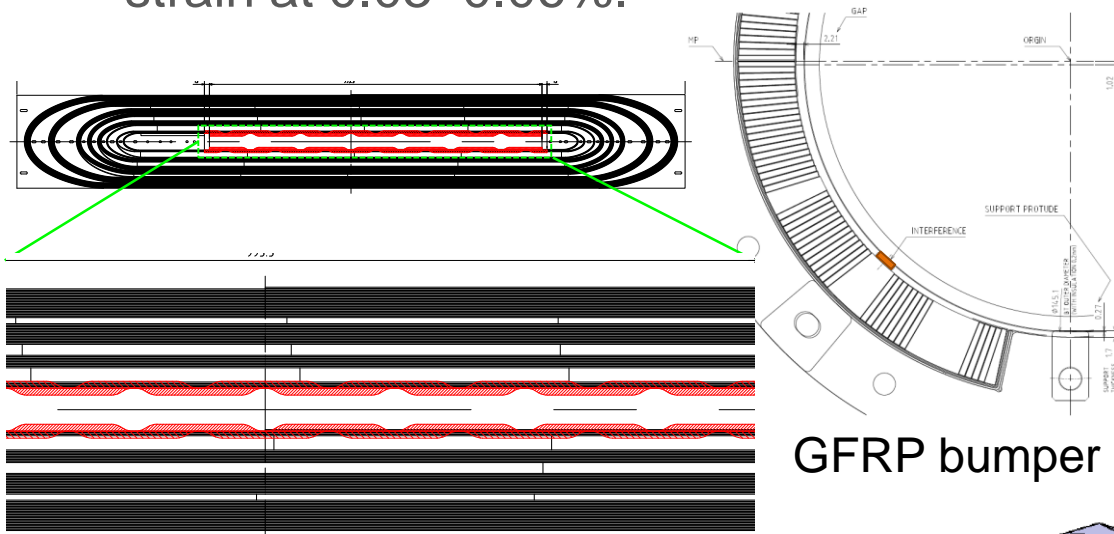
- Axial distribution of  $b_3$  can also be reproduced by calculation with oval coil with  $a=0.4$  mm.

# Appendix

## Status of MBXFS3

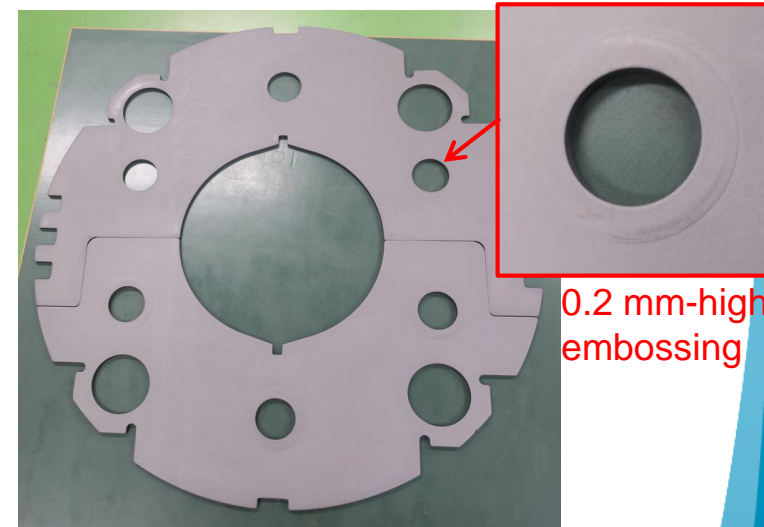
# Other modifications in MBXFS3

- Introducing wavy shape into flap of ground insulation for He gas passage at quench
- GFRP bumpers implemented into coil wedges as a beam tube support
- Yoke was fully fabricated by fine-blanking including making holes and embossing.
- Circumference of a half shell will be increased to control tensile welding strain at 0.03–0.06%.



Wavy-shaped insulation

GFRP bumper



S-yoke fully fabricated by fine-blanking

# Shim thickness for coil end

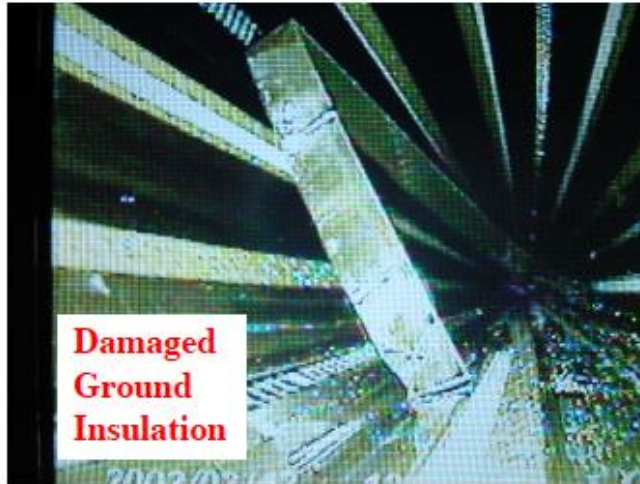


Shim insertion

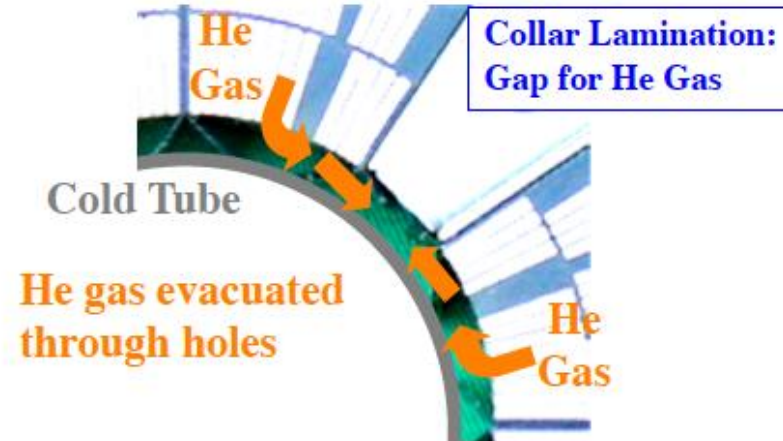
- Young's modulus of a coil at coil end is dependent on the longitudinal position. The end of end saddle is the most rigid, at which a coil is made of 100% GFRP (27 GPa).
- We are attempting to evaluate local modulus by coil size measurement.

# Insulation damage in MQXA

## Problem II : Ground Insulation Peel-off



Inside of MQXA02 after cold test



## Action!! : Implementation of Holes in Ground Insulation

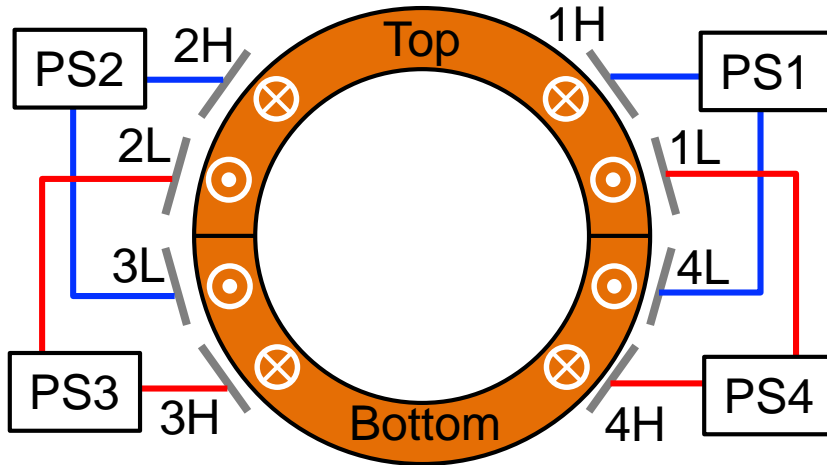
- No further problem after modification.
- New insulation scheme fulfill the electrical insulation specification.
- All magnets passed the electrical insulation tests.





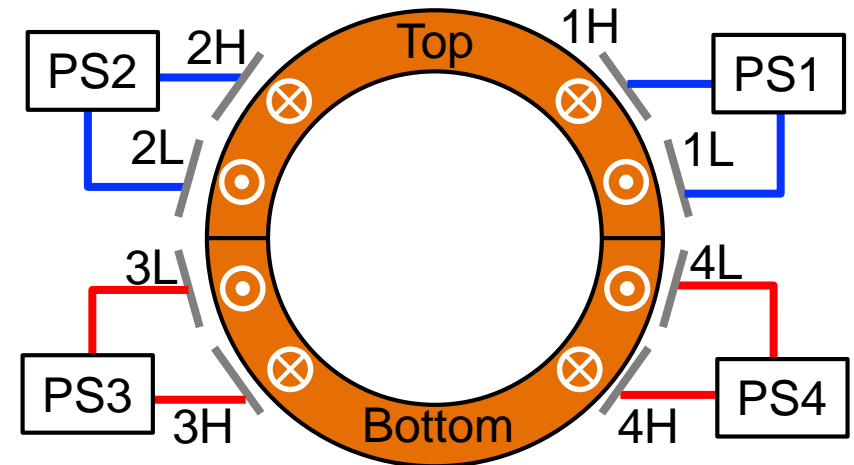
# QPH wiring for prototype (under discussion)

Plan A

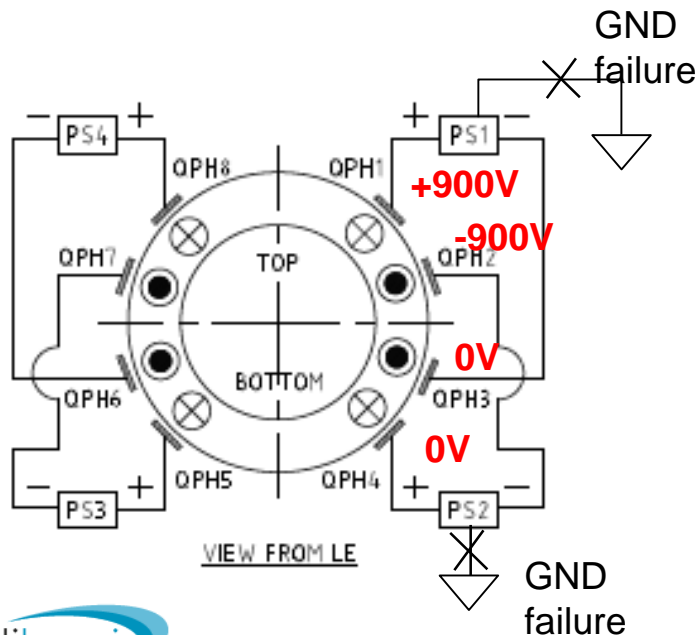


View from LE

Plan B

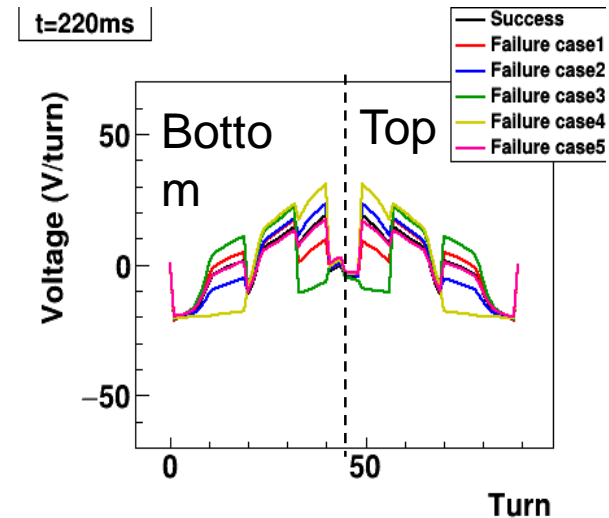
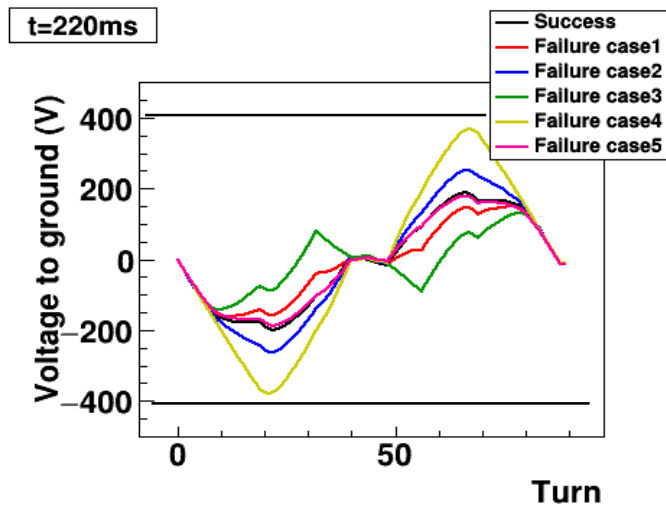
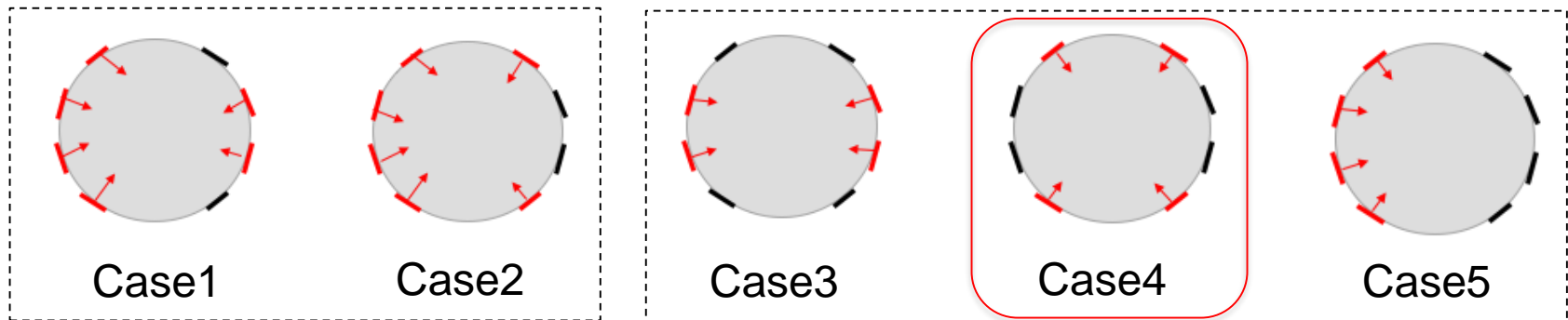


View from LE



- Four QPH power supplies
- Polarity was determined to produce quadrupole field by QPH current
- Plan A can always deposit energy to both coils, but voltage between adjacent strips can reach 1.8 kV at maximum.
- In the failure cases of power supplies, QPH in only one coil is fired in plan B.

# Coil voltage (QPH wiring in plan A)



- The worst scenario is '**case 4**' where the voltage reaches **~400 V** at maximum → Determined test voltage
- The 'maximum inter-turn voltage' using our simulation, which showed **30 V/turn** → Ringing voltage:  $30 \times 44 \text{ turns} = 1.3 \text{ kV}$

# Test voltage

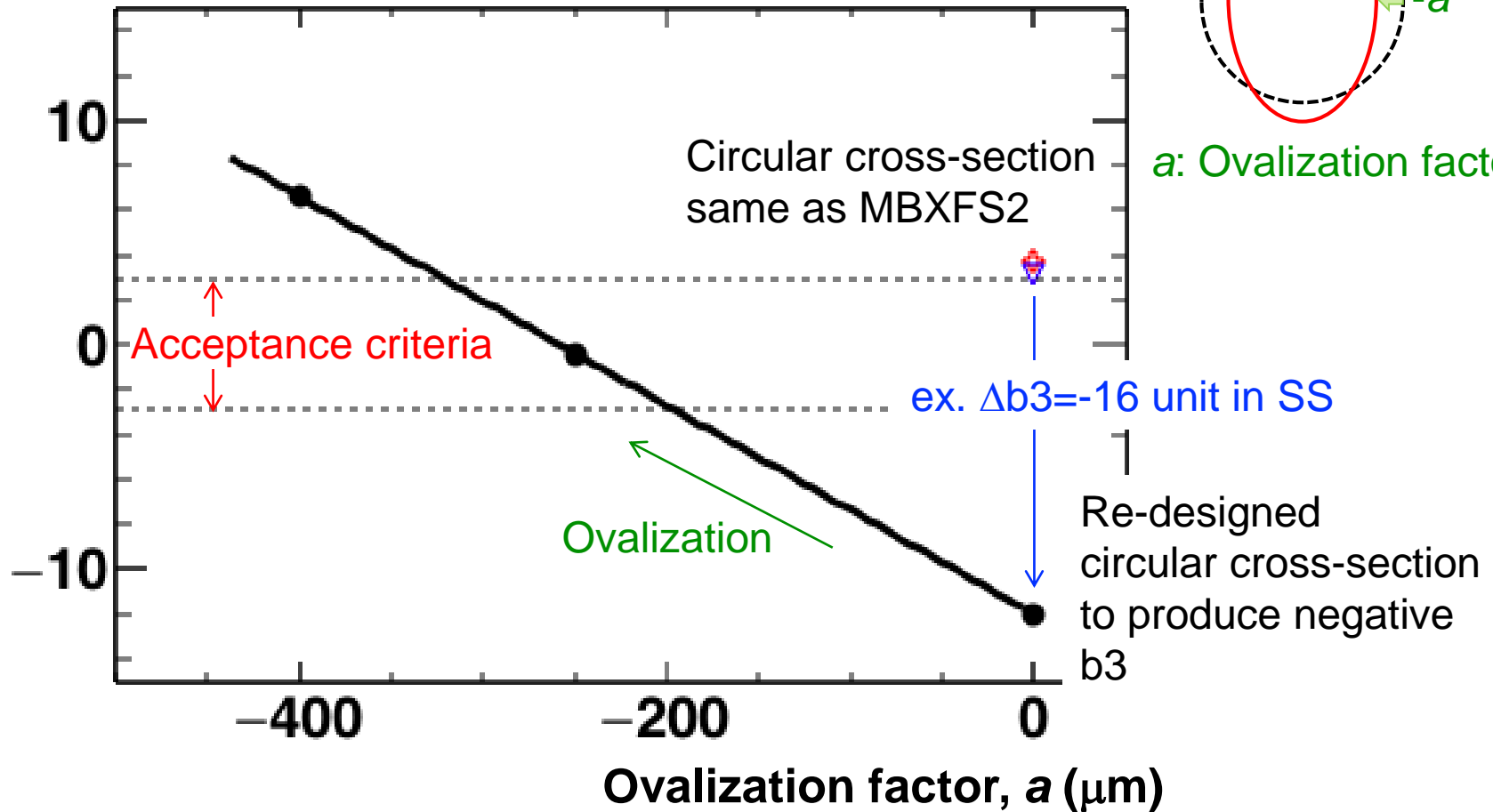
Maximum expected coil voltage at quench (V)	To ground	<b>400</b>
	To heater	900
Maximum design withstand coil voltage at nominal operating conditions (V)	To ground	1300
	To heater	2300
Minimum design withstand coil voltage at warm (V)	To ground	2600
	To heater	4600
Test voltage to ground for installed system at nominal operating conditions (V)		480
Test voltage to ground for installed system at warm (V)		260
Test voltage to heater for installed systems at nominal operating conditions (V)		1080
Test voltage to heater for installed systems at warm (V)		460
Maximum leakage current (uA)		10
Test voltage duration (s)		30

# Appendix

## Prospect for prototype

# How to correct b3 offset

$b_3$  integral



- If we can measure  $a$ -value in a model magnet, appropriate  $\Delta b_3$  in SS can be estimated.